# Development of High-Sensitivity, Wide-Dynamic-Range and Selectable-Regions Fiber-Optic Sensing System Based on Optical Pulse Correlation Measurement

徐勋建

Xunjian Xu

A dissertation submitted to
Kochi University of Technology
in partial fulfillment of the requirements
for the degree of

Doctor of Philosophy

Graduate School of Engineering
Kochi University of Technology
Kochi, Japan

September 2010

# Abstract

To develop a high-sensitivity, wide-dynamic-range and selectable-regions fiber optic sensing system, this dissertation investigates a concept of optical pulse correlation sensing system configuration, and develops a simple high sensitivity and wide dynamic range pulse correlation sensing system, a selectable regions distributed pulse correlation sensing system, and a long-distance remote monitoring pulse correlation sensing system.

Optical pulse correlation sensor has been proposed and developed for past few years as a simple, useful and high resolution sensing mechanism for temperature, stress or strain measurement. Because of the high time resolution performance of this optical pulse correlation sensing system, this sensor concept can be used on many practical applications, such as wide-range ocean temperature monitoring, civil structure monitoring and long distance remote monitoring.

For industrial practical applications of ocean temperature monitoring, high-sensitivity and wide-dynamic-range fiber optic sensing system based on pulse correlation are investigated which is combined with short and long monitoring fibers by a time-division multiplexing (TDM) technique. For practical application of civil structure monitoring, a compact and simple cascadable multi-regions distributed fiber optic sensing system based on pulse correlation is propose and demonstrate. The system uses inline-multiple monitoring fibers connected by wavelength partial reflectors or intensity partial reflectors for cascadable multi-regions responses sampling. For long-distance remote monitoring, a novel reflectometry that detects the reflection point by measuring the optical pulse correlation using the overlap of reference and reflected pulses was investigated. This pulse-correlation-based reflectometry can detect the reflectometry pulse with high time resolution better than 0.02 ps. Moreover, a multi-region fiber sensing system with 30 km remote distance with high resolution are achieved, which can measure 4 με strain or 0.1 °C environmental changes per 1 meter sensing fiber can detect with more than 6 of separated regions within 10 Km tele-monitoring. Using the pulse feedback and moving average technology, the noise factors of this system are

suppressed.

The introduction of this dissertation is presented in Chapter 1. The concepts of optical pulse correlation sensing system are presented in Chapter 2. For industrial practical applications of ocean temperature monitoring, by combining long and short sensing fibers, a high-sensitive and dynamic-range fiber optic sensing system based on pulse correlation is presented in Chapter 3. For practical application such as civil structure monitoring, by employing wavelength multiplexing or time multiplexing techniques, a regional selectable distributed fiber optic sensing system based on pulse correlation is presented in Chapter 4. For long distance remote sensing application, a long-distance remote fiber optic sensing system based on pulse correlation is required and presented in Chapter 5. The Summaries of the main results in this work are presented in Chapter 6.

The main results in this work. The first main result is that using the TDM technique to combine long and short sensing fiber, the pulse-correlation-based fiber optic sensing system successfully reaches to a high-sensitivity temperature measurement of 0.001 °C/mV and wide dynamic range depended on the length of sensing fiber. The second main result is that using wavelength multiplexing or time multiplexing techniques, this system can successfully measure multi-regional strain or temperature. The max number of cascadable multi-region is estimated and can be enhanced by increasing the peak power of pulse source and decreasing the width of pulse source. The third main result is that this pulse-correlation-based fiber optic sensing system also can reach up to 30 Km long-distance remote measurement in laboratory and 66 km in theory by using optical partial reflectors.

# Table of Contents

Abstract ..... I
Table of Contents ..... i
Chapter 1 Introduction ..... 1
1.1 Background: Environment Monitoring and Distributed Sensor ..... 1
1.2 Fiber Optic Sensor History ..... 4
1.3 Objective and Scope of This Work ..... 8
Chapter 2 Optical Pulse Correlation Sensing System ..... 13
2.1 Introduction ..... 13
2.2 Principle of Differential Optical Correlator Based on QPM SHG ..... 15
2.2.1 Theory of QPM SHG ..... 15
2.2.2 Theory of Temperature and Strain Measurement ..... 17
2.2.3 Principle of Differential Optical Pulse Correlator ..... 19
2.3 Setup of Optical Pulse Correlation Sensing System ..... 24
2.4 Result and Discussion of Temperature and Strain Experiment ..... 26
2.4.1 Temperature Experiment and Result ..... 26
2.4.2 Strain Experiment and Result ..... 27
2.5 Field Experiments and Results ..... 28
2.6 Summary ..... 31
Chapter 3 High-sensitivity and Wide-dynamic-range Fiber Optic Sensing System Based on Pulse Correlation and TDM ..... 34
3.1 Introduction ..... 34
3.2. Principle ..... 36
3.2.1 Optical Switch ..... 36
3.2.2 Principle of Combination with Short and Long Monitoring Fiber ..... 39
3.3 Experimental Methods ..... 43
3.4 Results and Discussion ..... 46
3.5 Conclusions ..... 47
Chapter 4 Selectable-Regions Distributed Fiber Optic Sensing System Based on Pulse Correlation and Region Separation ..... 50

4.1 Introduction ..... 50
4.2 Principle ..... 51
4.2.1Region Separation Technique Based on WSRs ..... 51
4.2.2 Regions Separation Technique Based on IPRs ..... 53
4.3 Experimental Results ..... 55
4.3.1 Using Wavelength Scanning with WSRs ..... 55
4.3.2 Using Time-Position Scanning with IPRs ..... 58
4.4 Discussion ..... 61
4.4.1 Time Resolution and Stability ..... 61
4.4.2 Estimation of the Number of Cascadable Regions ..... 63
4.4.3 Comparison ..... 67
5.Summary ..... 69
Chapter 5 Reliable Long-Distance Remote Fiber Optic Sensing System Based on Pulse Correlation and Partial Reflector ..... 72
5.1 Introduction ..... 72
5.2 Principle of Remote Pulse-Correlation-Based Reflectometry ..... 74
5.2.1 Single-Region Remote Pulse-Correlation-Based Sensing System ..... 74
5.2.2 Multi-Regions Remote Pulse-Correlation-Based Sensing System ..... 75
5.3 Experimental Setups and Results ..... 77
5.3.1 Single-Region Remote Pulse-Correlation-Based Sensing System ..... 77
5.3.2 Multi-Regions Remote Pulse-Correlation-Based Sensing System ..... 82
5.4 Discussion of Maximum Distance for Remote Sensing ..... 86
5.4.1 Loss Effect ..... 87
5.4.2 Dispersion Effect ..... 90
5.4.3 Nonlinear Effect ..... 91
5.5 Summery ..... 94
Chapter 6 Conclusions ..... 96
Acknowledgement ..... 99
Publications List ..... 100

# Chapter 1 Introduction

This section analyzes the monitoring needs in real industry engineering: ocean sensing and civil structures. After giving an overview of fiber optic sensor (FOS) that can benefit from a deformation measuring system, the characteristics of the existing monitoring methods of FOS will be analyzed. Finally the possibility of developing a new generation of sensors based on optical pulse correlation as replacement of existing measurement methods or as enabling technology to open new possibilities will be discussion.

## 1.1 Background: Environment Monitoring and Distributed Sensor

Currently, the most important environment of earth is global climate change which mainly refers to global warming. For global warming monitoring, it is very important for monitoring the global ocean temperature changing. Usually, the high sensitivity electrical instrument Conductivity-Temperature-Depth (CTD) [1] is popularly used for ocean temperature monitoring as shown in Figure 1-1. It can reach 0.001 ℃ high sensitivity of temperature measurement from -5 to 35 ℃. However, it cannot isolate the Electromagnetic Interference (EMI). Therefore, high sensitivity and dynamic measurable range of fiber optic sensors are required.

Another important environment monitoring is geological environmental monitoring such as distortion or collapse of hillside as shown in Figure 1-2. Usually, multiplexing point sensors marked by point ticks in Figure 1-2 are used for monitoring the distortion or collapse of the hillside. However, their main drawback is the missing of the degradation measurement between sensors marked by cross ticks in Figure 1-2. Therefore, distributed sensors are required as the bold line with deferent colours marked in Figure 1-2. The different colours mean the different sensing regions. In other word, region selectable distributed sensing technology is requirement. For easily observation of the geological environment information in office, long distance remote sensing is also required.

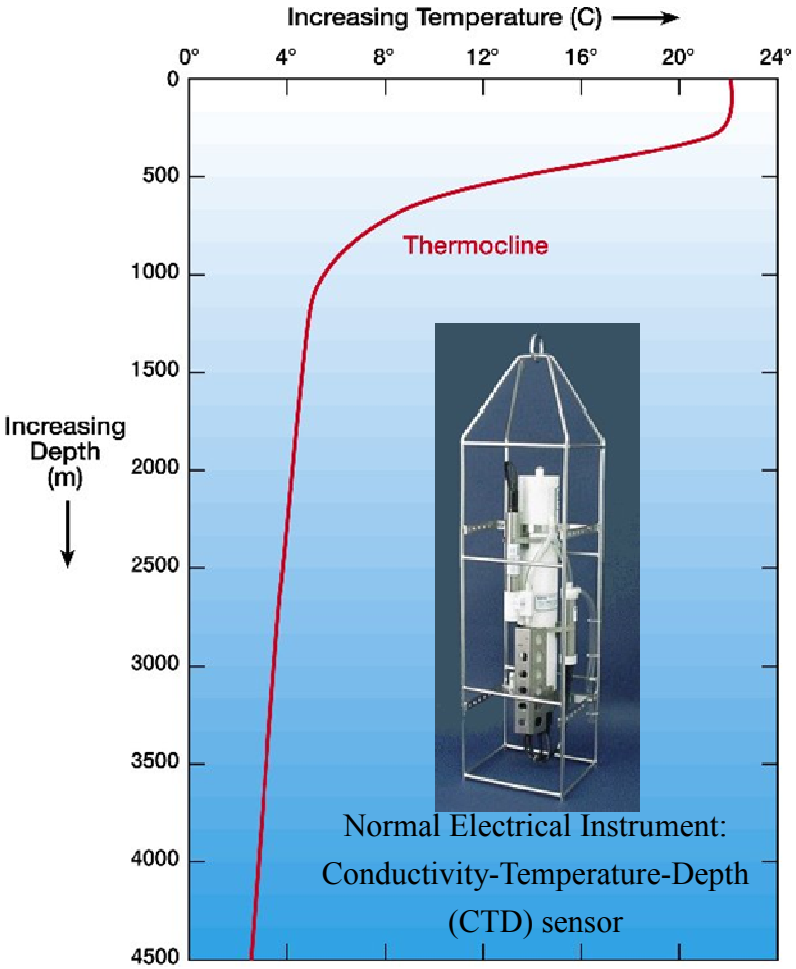


**Figure 1-1**: Ocean Temperature Monitoring

**Figure 1-2**: Geological Environmental Monitoring

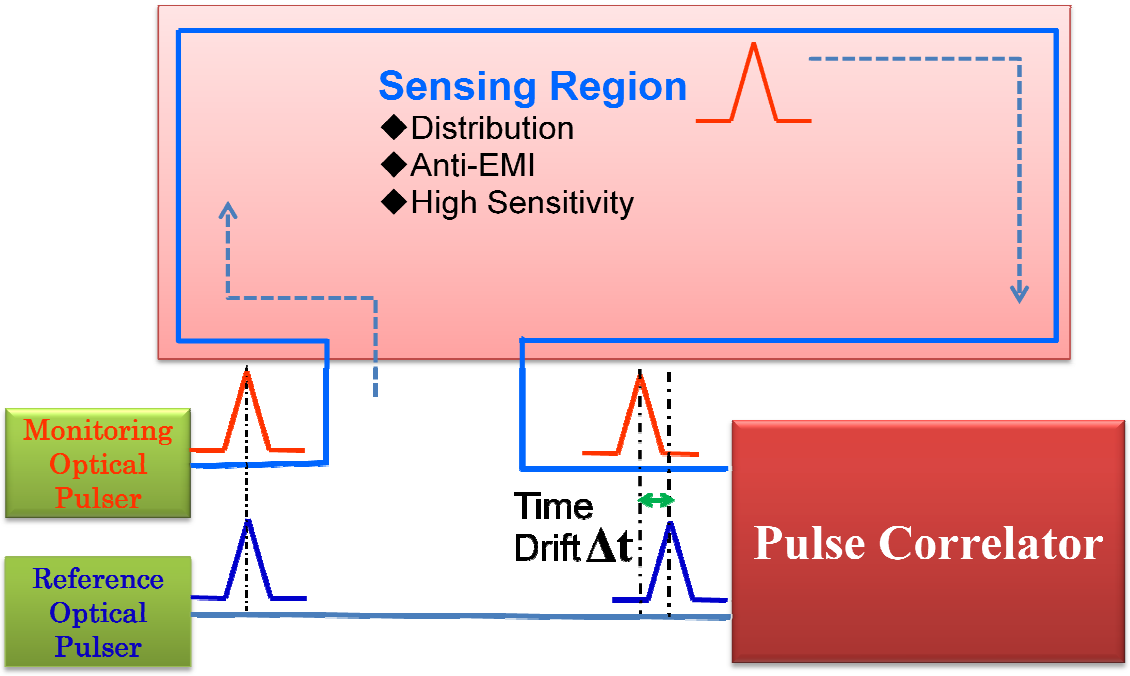


**Figure 1-3:** Scheme of Optical Pulse Correlation Fiber Optic Sensor

For high sensitivity, distributed and anti-EMI environment monitoring, a novel optical pulse correlation fiber optic sensor [2-5] has been developed for several years as shown in Figure 1-3. This sensing system use two same pulse train, monitoring and reference pulse trains. The monitoring pulse train is input to the sensing region fiber, and the reference pulse passes through the reference fiber. In the two pulse train source, their times are same. After different propagation paths, there is a time drift between the two pulses. Reference line keeps constant condition; monitoring line is put in the sensing region for environment monitoring. If the strain or temperature environment changes, the monitoring line length will be extended or stretched. At that time, the time drift of two pulse train will also change. The pulse correlator can monitor the time drift exactly with low frequency electronic circuit which cost so low. Therefore, this optical pulse correlation fiber optic sensing system can easily measure the environment change with high sensitivity and distribution. The research of this thesis will contributed in high-sensitivity, wide- dynamic-range and selectable-region sensing for environment monitoring such as ocean temperature measurement and geologic environment sensing.

## 1.2 Fiber Optic Sensor History

Any environment effect that can be conceived of can be converted to an optical signal to be interpreted [6]. During the past decade, physicists have been developing new sensory capabilities to measure the internal parameters of structures as part of so-called smart civil structures. For civil structures, the primary sensing issues are measuring the reaction of the structure to external loads and determining the internal state-of-health of the structure. For these purposes, small fibre optic sensors (FOSs) are embedded and spatially distributed in the structure. FOSs have been developed to detect variations in crack formation, strain, temperature and corrosion. A significant advantage of FOS is the ability to multiplex a number of continuous or discrete sensors on one fibre to form a distributed sensor system [7].

As shown in Table 1-1, with the invention of the laser in 1960's, a great interest in optical systems for data communications began. From 1966 to 1969, several scientists concluded that impurities in the fiber material caused the signal loss in optical fibers. The first patents on the subject precede the original suggestions from Kao and Hockham [8, 9]. In 1967, the "fotonic" sensor [10] was conceived to measure positions and spacings in the machine tool industry and its attraction combined a noncontact measurement with immunity to electromagnetic interference, factors which still continue to feature in the benefits list of fiber sensor technology. These fibers could have a significant role in telecommunications. By removing these impurities, construction of low-loss optical fibers was possible. In 1970, Corning Glass Works made a multimode fiber with losses under 20 dB/km for fiber optic communication. In parallel with these developments, fiber optic sensor technology has been a significant user of technology related with the optoelectronic and fiber optic communication industry. Some early work by Snitzer made the very important observation that optical fibers could usefully convey phase information which may be related to physical modulation of the fiber parameters in 1971[11]. In 1975, when fiber communications was beginning to look competitive, saw also the first definitive papers on optical fiber phase modulated sensors notably hydrophones and the gyroscope (Sagnac interferometer) and the beginnings of an appreciation that these sensors had something

different to offer [12, 13].

The backscattering method was invented by M. Barnoskim and M. Jensen in 1976 [14]. The backscattering was the Rayleigh backscattering developed to OTDR. Then, the first in-fiber Bragg grating was demonstrated by Ken Hill in 1978 [15]. Initially, the gratings were fabricated using a visible laser propagating along the fiber core. In 1989, Gerald Meltz and colleagues demonstrated the much more flexible transverse holographic technique where the laser illumination came from the side of the fiber. This technique uses the interference pattern of ultraviolet laser light to create the periodic structure of the Bragg grating [16]. Then, the FBG is widely used for sensing.

Dakin et al proposed in 1985 for the first time to use a non-elastic scattering for distributed sensing [17]. The spontaneous scattering process is generated by thermally-activated acoustic waves and their phonon population follows a Bose-Einstein distribution. This makes the scattering cross-section temperature-dependent and the spontaneous Raman scattering suitable for temperature distributed sensing.

The possibility to use the other inelastic scattering – Brillouin scattering – for sensing purposes was proposed in 1989 [18, 19]. The mechanism used in this type of sensor is not based on an intensity measurement, but on the frequency positioning of the Brillouin scattered wave. It makes the measurement very immune to any loss effects. The photonic-crystal fiber (PCF) was coined by Philip Russell in 1991 [20], and then the PCF as a microstructure fiber optic has been widely utilized in fiber optic communication and sensing. For the research of this thesis, optical pulse correlation fiber optic sensor was first published by Prof. Koji Nonaka [3].

**Table 1-1:** the history of fiber sensing

| Time | Fiber Optic Sensor Technology |
|---|---|
| 1960 | Optical Communication begin |
| 1966-1969 | First Fiber Optic patents |
| 1967 | First "fotonic" sensor |
| 1970 | Fiber Optic Communications |
| 1971 | Fiber Optic Sensors |
| 1976 | Rayleigh Backscattering fiber optic sensor (OTDR) |
| 1977 | Gyroscope ( Sagnac Interferometer) |
| 1978 | In-fibre Bragg Grating (FBG) producing |
| 1983 | **Raman Distributed Fiber Optic Sensor** |
| 1989 | **FBGs Fiber Optic Sensor** |
| | **Brillouin Distributed Fiber Optic Sensor** |
| 1991 | photonic-crystal Fiber (PCF) |
| 2005 | Optical pulse correlation fiber optic sensor begin |

Fiber optic sensors have been widely used to monitor a wide range of environmental parameters such as position, vibration, strain, temperature, humidity, viscosity, chemicals, pressure, current, electric field and several other environmental factors.

Fiber optic sensors are excellent candidates for monitoring environmental changes and they offer many advantages over conventional electronic sensors as listed below:

• Easy integration into a wide variety of structures, including composite materials, with little interference due to their small size and cylindrical geometry.

• Inability to conduct electric current.

• Immune to electromagnetic interference and radio frequency interference.

• Lightweight.

• Robust, more resistant to harsh environments.

• High sensitivity.

• Multiplexing capability to form sensing networks.

• Remote sensing capability.

• Multifunctional sensing capabilities such as strain, pressure, corrosion, temperature

and acoustic signals.

There are many types of fiber optic sensors as shown in Table 1-2 [21, 22]. According to the optical physics modulation parameter, normal fiber optic sensors are classified to intensity, phase, wavelength and Frequency. For the sensing mechanism of intensity modulation, the micro bending sensor (MBS) and OTDR sensor have an advantage of simple structure and disadvantages of low sensitivity and insertion loss dependence. For the sensing mechanism of phase modulation, interferometer sensors have an advantage of high sensitivity and disadvantages of coherence length dependence and unable to wide-range. For the sensing mechanism of wavelength modulation, FBG sensors have advantages of real time, multipoint and intensity independence, and have disadvantages of need of broadband light source and special fiber. For the sensing mechanism of frequency modulation, Brillouin OTDR have advantages of distributed and long-distance remote monitoring and have disadvantages of high cost and none-real time.

Optical pulse correlation fiber optic sensing system monitors the pulse correlation to measurement the environment. It has the advantages of simple, high sensitivity, real time, distributed and long distance remote monitoring ability which include most advantages of normal fiber optic sensors of foregoing statement. It also needs phase-locked optical pulse source. However, model locked laser diode (ML-LD) and model locked fiber laser (ML-FL) can provide high quality phase-locked optical pulse source. Therefore, Optical pulse correlation fiber optic sensing system has so much advantages and conquered disadvantages, and will contribute to fiber optic sensing area.

**Table 1-2:** Different Fiber Optic Sensors

| Characteristic | OTDR | Interferometer | FBG | BOTDR | Pulse Correlator |
|---|---|---|---|---|---|
| **Measurand** | Intensity | Phase | Wavelength | Frequency | Correlation |
| **Low cost** | △ | ◎ | ○ | × | ○ |
| **Wide range** | ◎ | × | × | ◎ | ◎ |
| **Real-time** | × | ◎ | ○ | △ | ◎ |
| **High sensitivity** | × | ◎ | ○ | × | △→○ |
| **Distribution** | ◎ | △ | △ | ◎ | △→○ |
| **Long distance** | ◎ | × | △ | ◎ | △→○ |
| **Intensity independence** | × | △ | ◎ | ○ | △ |
| **Coherence independence** | ◎ | × | ◎ | ○ | ○ |

× : Impossible △ : Sometimes Possible ○: Possible ◎ : Completely Possible

## 1.3 Objective and Scope of This Work

The simple, real time optical pulse correlation fiber sensor had been investigated for several years by previous researchers. A subpicosecond pulse timing monitoring and stabilization system based on optical pulse cross-correlation and SHG differential signal detection was proposed, and the time resolution is better than 0.1 picosecond [2]. Therefore, the pulse correlation fiber optic sensing system was investigated. This sensing system used optical pulse correlation measurement mechanism and differential detection technique between reference double-pulse and monitoring signal pulse to detect the environment condition such as temperature, stress and pressure. It also has

very high time resolution of less than 0.04ps [3]. A polarization fluctuation suppressed optical correlation sensing system was proposed by utilizing the birefringence compensation approach in a retraced fiber path using Faraday Rotator Mirror elements. Therefore, a higher resolution and stable operation were realized within the designed pulse monitoring range. The time resolution had reached to 0.02ps [4].

The object of this research is to develop the previous optical pulse correlation sensor to a novel high sensitivity, wide dynamic range and selectable sensing region distributed sensing system based on pulse correlation. Therefore, for achieved those objects, there are several important studies as follow as:

(1) How to achieve simultaneously high sensitivity and wide measurable range? For sensing technology, it is well know that the high sensitivity and wide measurable range were trade off relationship. How to resolve the conflict between temperature sensitivity and measurable temperature range is required.
(2) How to achieve multiplexing sensing regions? Optical pulse correlation sensor can inquire the total strain or temperature value of the whole sensing fiber, and cannot identify in which sensing region the strain or temperature is located. Therefore, a compact and simple cascadable multi-regions distributed sensing system based on pulse correlation is required. Moreover, sensing region separation techniques are required to investigate.
(3) How to achieve long-distance remote sensing? Fiber optic sensor can be used in extreme environments, and monitor of fiber optic sensor should be isolated the extreme environments. In the other word, the human interface of fiber optic sensing system should be far away the sensing region. Therefore, long-distance remote pulse correlation sensing system is required to investigate.

The organization of this dissertation is shown in Figure 1-4. The introduction of this dissertation is presented in Chapter 1. The concepts of optical pulse correlation sensing system are presented in Chapter 2. For industrial practical applications of ocean temperature monitoring, by combining long and short sensing fibers, a high-sensitive and dynamic-range fiber optic sensing system based on the pulse correlation measurement is investigated and presented in Chapter 3. For practical application such

as civil structure monitoring, by employing wavelength multiplexing or time multiplexing techniques, a regional selectable distributed fiber optic sensing system based on the pulse correlation measurement is presented in Chapter 4. For long distance remote sensing application, a long-distance remote fiber optic sensing system based on pulse correlation measurement is investigated and presented in Chapter 5. The summaries of the main results in this work are presented in Chapter 6.

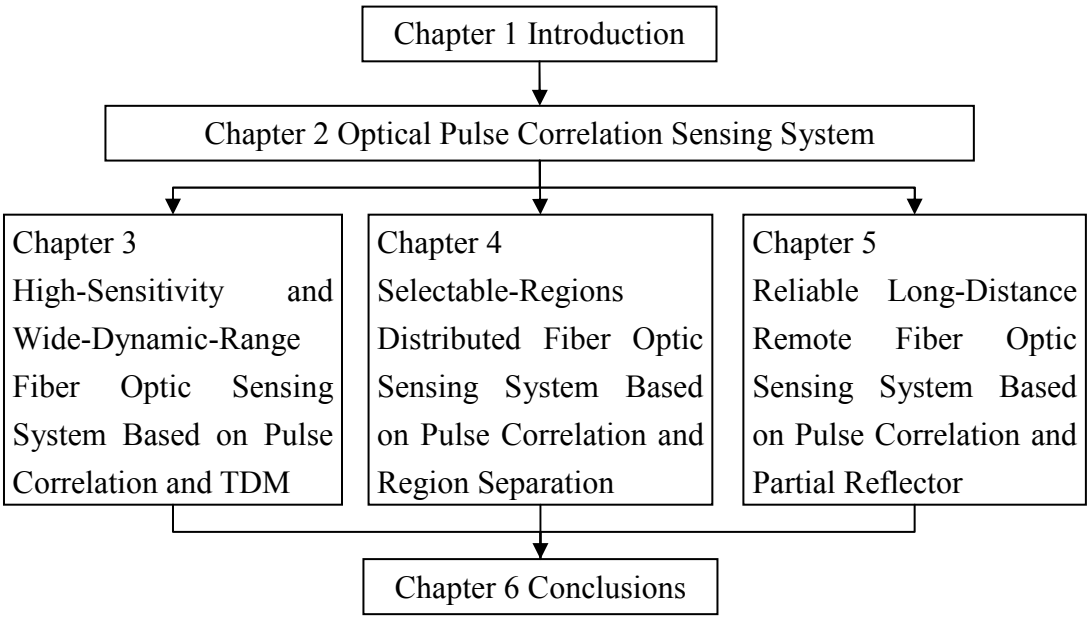


**Figure 1-4:** Organization Chart of the Dissertation

# Reference


[1] http://www.windows2universe.org/earth/Water/CTD.html.

[2] K. Uchiyama, K. Nonaka, and H. Takara: "Subpicosecond timing control using optical double-pulse correlation measurement", IEEE Photonics Technol. Lett., vol. 16, p. 626, 2004.

[3] K. Nonaka, M. Sako, T. Suzuki: "Optical pulse timing drift sensing for fiber delay monitoring using pulse correlation and differential detection", 17th International Conference on Optical Fiber Sensors, Proceeding of SPIE, vol. 5855, p. 76, Bruges, 2005.

[4] H. B. Song, T. Suzuki, M. Sako, and K. Nonaka: "High time resolution fiber optic sensing system based on correlation and differential technique", Meas. Sci. Technol. vol. 17, p. 631, 2006.

[5] H. B. Song, T. Suzuki, T. Fujimura, K. Nonaka, T. Shioda, and T. Kurokawa: "Polarization fluctuation suppression and sensitivity enhancement of an optical correlation sensing system", Meas. Sci. Technol., vol. 18, p. 3230, 2007.

[6] Eric Udd: "Fiber Optic Sensors", John Wiley & Sons, Inc., p. 3, 1991.

[7] Brian Culshaw: "Optical Fiber Sensor Technologies: Opportunities and Perhaps Pitfalls", Journal of Lightwave Technology, vol. 22, 2004.

[8] C. K. Kao and G. A. Hockham: "Dielectric fiber surface waveguides for optical frequencies", Proc. Inst. Elect. Eng., vol. 113, p. 1151, 1966.

[9] http://en.wikipedia.org/wiki/Optical_fiber.

[10] C. Menadier, C. Kissenger, and H. Adkins: "The fotonic sensor," Instrum. Control Syst., vol. 40, p. 114, 1967.

[11] E. Snitzer: "Apparatus for controlling the propagation characteristics of coherent light within an optical fiber," U. S. Patent 3 625 589, Dec. 7, 1971.

[12] J. A. Bucaro, H. D. Dardy, and E. F. Carome: "Fiber optic hydrophone," J. Acoust. Soc. Amer., vol. 52, p. 1302, 1977.

[13] B. Culshaw, D. E. N. Davies, and S. A. Kingsley, "Acoustic sensitivity of optical fiber waveguides," Electron. Lett., vol. 13, p. 760, 1977.

[14] J. K. Barnoski, S. M. Jensen: “Fiber waveguides: A novel technique for investigation attenuation characteristics”, Appl. Opt., vol. 15, p. 2112, 1976.

[15] Hill, K.O.; Fujii, Y.; Johnson, D. C. Kawasaki: “Photosensitivity in optical fiber waveguides: application to reflection fiber fabrication”, Appl. Phys. Lett., vol. 32, p. 647, 1978.

[16] G. Meltz, et al.: “Formation of Bragg gratings in optical fibers by a transverse holographic method”, Opt. Lett., vol. 14, p. 823, 1989.

[17] Dakin, J.P., Pratt, D.J., Bibby, G.W. and Ross: “Distributed Optical Fibre Raman temperature sensor using a semiconductor light source and detector”, Electron. Lett., vol. 21, p. 569, 1985.

[18] D.Culverhouse, F.Ferahi, C.N.Pannell, D.A.Jackson: “Exploitation of stimulated Brillouin scattering as a sensing mechanism for distributed temperature sensors and as a mean of realizing a tunable microwave generator”, Optical Fibre Sensors conference OFS'89, Springer Proceedings in Physics 44, p. 552, Springer-Verlag, Berlin, 1989.

[19] T.Horigushi, M.Tateda: “Optical- fiber-attenuation investigation using stimulated Brillouin scattering between a pulse and a continuous wave”, Optics Letters, vol. 14, p. 408, 1989.

[20] http://en.wikipedia.org/wiki/Photonic-crystal_fiber.

[21] Minako Sako, “Optical Pulse Correlation Measuring Technique for Fiber-Optic Temperature and Strain Sensor”, Mater Thesis. Kochi University of Technology, 2005.

[22] Hongbin Song, “Development of High-Sensitivity Optical Fiber Sensor Based on Optical Pulse Correlation”, PhD. Thesis. Kochi University of Technology, 2008.

# Chapter 2 Optical Pulse Correlation Sensing System

## 2.1 Introduction

Temperature sensors are widely utilized during industrial application. There are many main kinds of temperature sensors such as liquid (alcohol/mercury) thermometer, bi-metal mechanic thermometer, electrical resistance thermometer, silicon band-gap temperature sensor, infrared thermometer and fiber optic temperature sensor [1]. The range of usefulness of the liquid thermometer is set from the freezing point to the boiling point of the liquid used, which makes it just useful for measuring day and night-time temperatures and to measure body temperature, although not for anything much hotter than these [2]. Bi-metal mechanic thermometer used two strips of different metals which expand at different rates as they are heated to covert a temperature change into mechanical displacement. It can be measured high temperature (about 200 ℃) but no electronic signal output just scale display, so it could not widely used in industry temperature monitoring and usually used in kitchens for oil and oven temperature measurement. Electrical resistance thermometers are temperature sensors that exploit the predictable change in electrical resistance of some materials which are almost invariably made of platinum with changing temperature and widely used in many industrial applications below 600 ℃, but they cannot isolate electromagnetic interference. The silicon band-gap temperature sensor is an extremely common form of temperature sensor (thermometer) used in electronic equipment and its main advantage is that it can be included in a silicon integrated circuit at very low cost. But it also cannot isolate the electromagnetic interference. Infrared thermometers measure temperature using blackbody radiation (generally infrared) emitted from objects, so they can no contact to measure temperature but very low measurement precision. Fiber optic temperature sensors generally measure temperature by using the thermal expansion of fiber optic, and they have no electrical signals and only use optical signals, so they can isolate the electromagnetic interference and have wide measurement range and high resolution due to extremely high temperature of melting point of fiber optic material. Moreover fiber optic temperature sensors can be utilized in very dangerous situation

such as oil tank, nature gas pipe, coal mine, high voltage power transformer and so on. Therefore, a simple, real-time fiber optic sensor is required. Double-pulse correlation measurement is alternative method [3]. In this research, a novel simple, high resolution, wide region fiber optic temperature sensor is proposed.

As description in Chapter 1, optical pulse correlation sensing system has a simple, low cost, high time resolution and real time characteristics. This chapter focuses on basic optical pulse correlation sensing system with double channels differential technology. A fiber optic temperature sensing system based on optical pulse correlation measurement and SHG differential detection technique has been proposed and demonstrated during recently several years [3-9]. A subpicosecond pulse timing monitoring and stabilization system based on optical pulse cross-correlation and SHG differential signal detection was proposed, and the time resolution is better than 0.1 picosecond [3]. A simple fiber optic sensing system was investigated. This sensing system used optical pulse correlation measurement mechanism and differential detection technique between reference double-pulse and signal pulse to detect the environment condition such as temperature, stress and pressure. It also has very high time resolution of less than 0.04ps [3-6]. A polarization fluctuation suppressed optical correlation sensing system was proposed by utilizing the birefringence compensation approach in a retraced fiber path using Faraday Rotator Mirror elements. Therefore, a higher resolution and stable operation were realized within the designed pulse monitoring range. The time resolution had reached to 0.02ps [7, 8]. In order to obtain wide measurement range, an optical pulse correlation unit dynamic range redesigned time bias from 7ps to 20ps using longer birefringent crystal for double reference pulsed generation in this research. And in order to more enhance the time resolution of this temperature sensing system, an electrical faint signal amplifier module is used in this research, and the time resolution can reach to 0.005ps [9].

In order to establish the reliability of this fiber optic temperature sensing system, a long-term wide region outside temperature monitoring experiment with a new designed 20ps time-bias optical pulse correlation unit for wide measurement rang was carried out. The temperature measured by means of a correlation sensor had the same variation as and higher sensitivity and quick measurement response than the digital thermometer.

The resolution of the correlation sensor is approximately ±0.01 ℃. This fiber optic temperature sensor can measure even in very tough environment and low and high temperature range. Not only point temperature but also a field area average temperature can monitor by this system.

In this chapter, the basic concept of optical pulse correlation sensing system will be investigated. In section 2, the principle of differential optical correlator based on QPM SHG will be shown; in section 3, the experimental setups of optical pulse correlation sensing system will be carried out; in section 4, temperature and strain experiment results will be discussed; in section 5, a summery for this chapter will be given.

## 2.2 Principle of Differential Optical Correlator Based on QPM SHG

### 2.2.1 Theory of QPM SHG

As an important parameter of optical signal, the propagation time of optical signal reflects the condition of the optical path. So the sensing can be realized by monitoring the time information of optical signals will contributes to a novel optical fiber sensing system. The mature of short-pulse generation technique enables the sensor based on the time modulation of optical pulse to have high sensitivity. The time information of the optical pulse is included in the optical pulse correlation, which makes the novel sensing feasible [8].

One of the most well-known aspects of nonlinear optics is second-harmonic generation (SHG), which means that light is generated at a frequency double that of the input (fundamental) wave. This is an intrinsic property of a non-centrosymemetric nonlinear medium.

In order to achieve SHG efficiently, the photon momentum has to be conserved, which is called phase-matching condition. A common method to fulfill this condition is using birefringence and dispersion.

A more efficient way of achieving SHG was already known since the early years of nonlinear optics namely quasi-phase-matching (QPM) [8, 10-13]. A QPM crystal

consists of domains whose nonlinear coefficients alternate in the sign. The domains usually have a size of few microns and were originally equally sized depending on the center frequency of the incident fundamental wave. The advantages of this method in comparison to the first method are: high conversion efficiency, free choice of the nonlinear tensor element, a broad conversion bandwidth and no Poynting-vector walk-off.

However, until the early 1990s such a structure could not be fabricated with the required uniformity. By applying a high voltage to the crystal it became possible to pole the crystal [10] and manufacture a QPM crystal in this way. A common material is lithium niobate ($LiNbO_3$).

Quasi-phase matching utilizes a material with spatially modulated nonlinear properties instead of a homogeneous nonlinear crystal material to realize the phase matching [10]. The spatial modulation nonlinear properties are realized by the periodically poling. The growth of second harmonic power is shown in Figure 2-1 Comparing the conversion efficiency in the case of phase matching, quasi-phase matching and non-phase matching, it can be seen that, the efficiency of quasi-phase matching is lower than that the phase matching condition but much higher than the non-phase matching condition. However, by utilizing the material with high effective nonlinearity, the conversion efficiency can be enhanced as high as that in the case of phase matching [10].

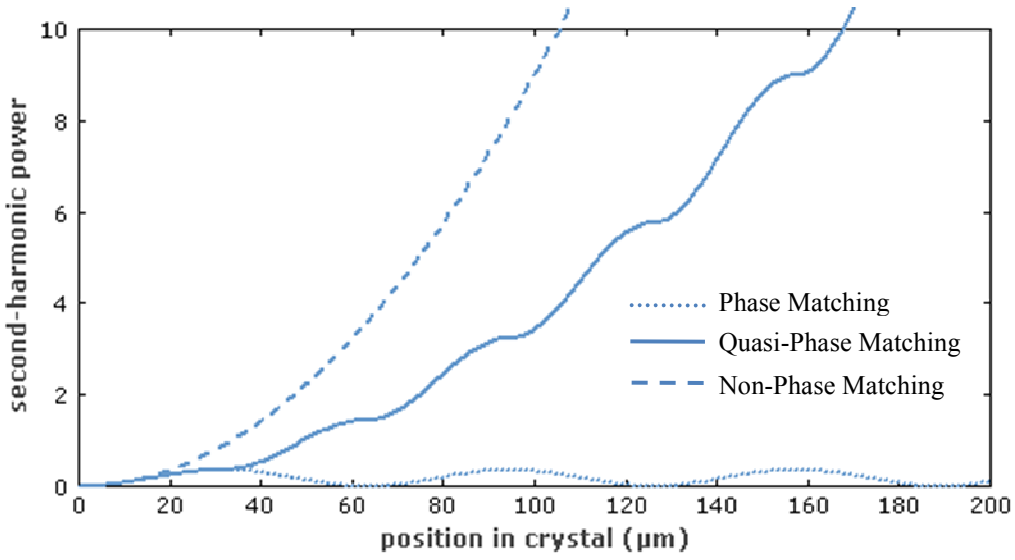


**Figure 2-1:** the SH power with and without phase matching and quasi-phase matching

### 2.2.2 Theory of Temperature and Strain Measurement

As the optical path *S* is the function of stress (σ) and temperature (*T*) exerted on the sensing fiber, therefore the propagation time along the monitoring path under the exertion of strain and temperature is

$$\mathrm{t} = \frac{\mathrm{S}(\sigma,\mathrm{T})}{\mathrm{c}} = \mathrm{t}(\sigma,\mathrm{T}) \tag{2-1}$$

The increment t can be expressed as

$$\mathrm{dt} = \frac{\partial \mathrm{t}}{\partial \sigma}\mathrm{d}\sigma + \frac{\partial \mathrm{t}}{\partial \mathrm{T}}\mathrm{dT} \tag{2-2}$$

The propagation time $t$ along the monitoring path can be expressed as

$$\mathrm{t} = \frac{\mathrm{n}\cdot\mathrm{L}}{\mathrm{c}} \tag{2-3}$$

Where the n and L are the refractive index of the optical fiber core and the length of sensing propagation path in monitoring fiber. The c is the vacuum speed of light. And the partial differential of t can also be expressed as

$$\begin{cases} \frac{\partial \mathrm{t}}{\partial \sigma}\mathrm{d}\sigma = \frac{\mathrm{n}}{\mathrm{c}}\cdot\frac{\partial \mathrm{L}}{\partial \sigma}\,\mathrm{d}\sigma + \frac{\mathrm{L}}{\mathrm{c}}\cdot\frac{\partial \mathrm{n}}{\partial \sigma}\,\mathrm{d}\sigma \\ \frac{\partial \mathrm{t}}{\partial \mathrm{T}}\mathrm{dT} = \frac{\mathrm{n}}{\mathrm{c}}\cdot\frac{\partial \mathrm{L}}{\partial \mathrm{T}}\,\mathrm{dT} + \frac{\mathrm{L}}{\mathrm{c}}\cdot\frac{\partial \mathrm{n}}{\partial \mathrm{T}}\,\mathrm{dT} \end{cases} \tag{2-4}$$

Where $\mathrm{d}\sigma$ and $\mathrm{dT}$ are the local change of stress and temperature, respectively. The $\frac{\partial \mathrm{t}}{\partial \sigma}$ and $\frac{\partial \mathrm{t}}{\partial \mathrm{T}}$ are the partial differential of *t* with respect to σ and *T*, respectively. If the strain ε , the Young's modulus $\mathrm{E_f}$ and expansion coefficient $\alpha_\mathrm{T}$ are defined as

$$\varepsilon = \frac{\Delta \mathrm{L}}{\mathrm{L}},\ \mathrm{E_f} = \frac{\sigma}{\varepsilon}, \alpha_\mathrm{T} = \frac{\varepsilon}{\Delta \mathrm{T}} \tag{2-5}$$

Then we have

$$\begin{cases} \frac{\partial \mathrm{L}}{\partial \sigma} = \frac{\mathrm{L}\cdot\partial\varepsilon}{\partial \sigma} = \frac{\mathrm{L}}{\mathrm{E_f}} \\ \frac{\partial \mathrm{L}}{\partial \mathrm{T}} = \frac{\mathrm{L}\cdot\partial\varepsilon}{\partial \mathrm{T}} = \mathrm{L}\cdot\alpha_\mathrm{T} \end{cases} \tag{2-6}$$

Substituting Eq. (2-6) to (2-4), we have

$$\begin{cases} \frac{\partial t}{\partial \sigma} d\sigma = \frac{n \cdot L}{c \cdot E_f} ( 1 + \frac{1}{n} \cdot \frac{\partial n}{\partial \varepsilon}) d\sigma \\ \frac{\partial t}{\partial T} dT = \frac{n \cdot L}{c} (\alpha_T + \frac{1}{n} \cdot \frac{\partial n}{\partial T}) dT \end{cases} \tag{2-7}$$

Where $C_\varepsilon$ and $C_T$ are the refractive index strain and temperature coefficients respectively, which are defined as

$$\begin{cases} C_\varepsilon = \frac{1}{n} \cdot \frac{\partial n}{\partial \varepsilon} \\ C_T = \frac{1}{n} \cdot \frac{\partial n}{\partial T} \end{cases} \tag{2-8}$$

Substituting Eq. (2-9) and (2-8) to (2-4), we have

$$dt = \frac{n \cdot L}{c \cdot E_f} ( 1 + C_\varepsilon) d\sigma + \frac{n \cdot L}{c} (\alpha_T + C_T ) dT \tag{2-9}$$

$\Delta t$, $\Delta \sigma$ and $\Delta T$ are the changing of time drift, stress and temperature. Because of Eq. (2-9) we can have

$$\Delta t = \frac{n \cdot L}{c \cdot E_f} ( 1 + C_\varepsilon) \Delta \sigma + \frac{n \cdot L}{c} (\alpha_T + C_T ) \Delta T \tag{2-10}$$

Thus, the time drift changing of during the monitoring path can be used to measure the strain and temperature changing by Eq. (2-10).

If the monitoring fiber is in the free space, the strain can be neglected and $d\sigma = 0$. Assuming that the initial length of sensing propagation path in monitoring fiber is $L_0$ at temperature $T_0$. As the temperature changing from $T_0$ to T, the length of sensing propagation path in monitoring fiber will be changed from $L_0$ to L. Therefore, the optical path of the sensor gauge will be varied due to thermal expansion ($\alpha_T$) and the change of refractive index of the fiber core ($C_T$). The time drift $\Delta t$ related with the ambient temperature T can be represented as follows in terms of Eq. (2-10):

$$\begin{aligned} \Delta t &= \frac{n \cdot L}{c} (\alpha_T + C_T ) (T - T_0) \\ &= \frac{n \cdot [L_0 + (L - L_0)]}{c} (\alpha_T + C_T ) (T - T_0) \\ &\approx \frac{n \cdot L_0}{c} (\alpha_T + C_T ) (T - T_0) \end{aligned} \tag{2-11}$$

Then the ambient temperature can be measured as

$$T = \frac{\Delta t}{\frac{n \cdot L_0}{c}(\alpha_T + C_T)} + T_0 \tag{2-12}$$

Because of the FRM in the end of monitoring fiber, the optical pulse is double-passed in the monitoring fiber. If the $l$ is the length of monitoring fiber, $l_0$ is the initial length of monitoring fiber during $T_0$ temperature. Therefore the length of monitoring path is double of the length of the monitoring fiber as follows

$$L = 2l\,, L_0 = 2l_0 \tag{2-13}$$

Then we can have

$$T = \frac{\Delta t}{\frac{n \cdot 2l_0}{c}(\alpha_T + C_T)} + T_0 = \frac{\Delta t}{S \cdot l_0} + T_0 \tag{2-14}$$

Where $S$ is a sensitivity coefficient, which are defined is

$$S = \frac{2n}{c}(\alpha_T + C_T) \tag{2-15}$$

For the standard commercial communication single mode fiber at wavelength $\lambda = 1550$ nm the parameters are n=1.4675, $\alpha_T = 5.5 \times 10^{-7}/℃$ , $C_T = 0.811 \times 10^{-5}/℃$ are taken from Ref. [14]. Using these data, for the unit optical fiber length, the sensitivity coefficient S of this kind fiber temperature sensor can be calculated as $0.085 ps/(m \cdot ℃)$ in theory.

### 2.2.3 Principle of Differential Optical Pulse Correlator

A schematic of the temperature measurement system with a monitoring fiber is shown in Figure 2-2. An optical pulse is split into a reference pulse and a monitoring pulse by a coupler. The monitoring pulse is reflected by a mirror and doubled through the monitoring fiber and a circulator, and then input to an optical correlation unit with the reference pulse in different ports. There is a time drift t between the reference and monitoring pulses because of their different propagation paths. When the temperature or strain of the monitoring fiber is changed, the propagation path of the monitoring pulse is changed owing to the length expansion and contraction of the monitoring fiber.

Therefore, the change in time drift Δt is proportional to the temperature change in the monitoring fiber.

Then the time drift between reference and monitoring pulse can be detected by QPM SHG crystals. The output signal of SHG is called correlation signal. The relationship between the time drift of monitoring pulse and correlation signal is shown in Figure 2-3. It is found that the correlation signal reached maximum value when reference pulse and monitoring pulse completely overlapped. Also the correlation signal reached minimum value when the two pulses did not overlap any. A good linear relationship area between the time drift and correlation signal is found about 5 ps range as shown in the ellipse of Figure 2-3.

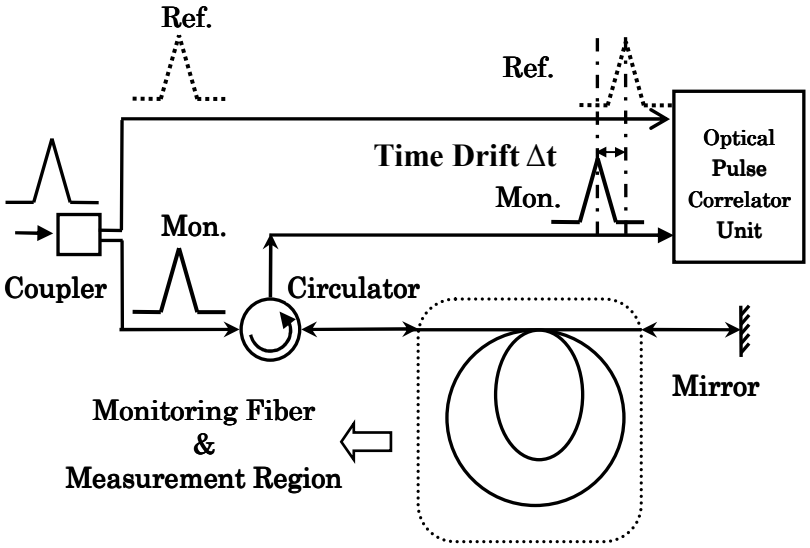


**Figure 2-2:** Schematic of temperature measurement with monitoring fiber based on optical pulse time drift.

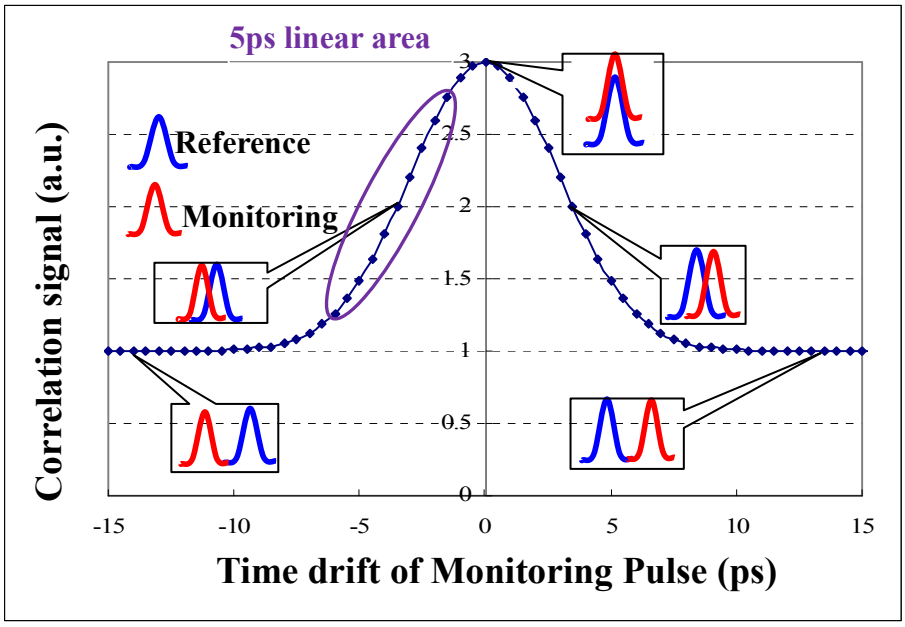


**Figure 2-3:** Correlation signal Vs. Time drift of monitoring pulse

The correlation signal can be detected by optical to electronic converter. Finally a voltage will be obtained, which is related to the correlation of two optical pulses caused by the timing delay. Therefore the monitoring of the temperature around the optical fiber will be realized.

To realized a temperature sensing with high sensitivity and wide range, the optical pulse correlation in orthogonal polarization planes with two channels are carried out by using an optical pulse correlation unit shown in Figure 2-4 (a). For the purpose of obtaining much larger measurement range rather than high-sensitivity, an optical pulse correlation unit with 20ps time-bias was used instead of pervious 7ps time-bias for high-resolution. Besides the difference of the time delay bias from the previous correlation unit, two pieces of polarizer are added in orthogonal polarization planes, respectively, which is helpful to enhance the stability. The optical pulse correlation unit is composed of a birefringence crystal, a half mirror (HM) and a polarization beam splitter (PBS). When the reference beam passes through the birefringence crystal, it is split into two beams, Refα and Refβ, which polarize in orthogonal polarization planes *p* and *s*. Simultaneously, a time delay about 20ps is produced between Refα and Refβ,

which makes it possible to realize the optical pulse correlation measurement in two channels and the differential detection is available. Therefore the high sensitive sensing can be realized. By using a polarization controller, the polarization state of the monitoring beam can be adjusted to 45°. Then equal components Sig ξ and Sigζ will be obtained in polarization plane *p* and *s*, respectively. At the half mirror, Refα and Refβ will combine with Sig ξ and Sigζ in plane *p* and *s*, respectively. After that, the polarization beam splitter will divide the two correlation signals into Ch1 and Ch2. The whole correlation process of two pulses is realized in a compact component with a size of 9.4 cm×4.0 cm ×1.0 cm. The top view of the optical pulse correlation unit and the SHG correlation detection & O/E unit are shown in Figure 2-4 (b).

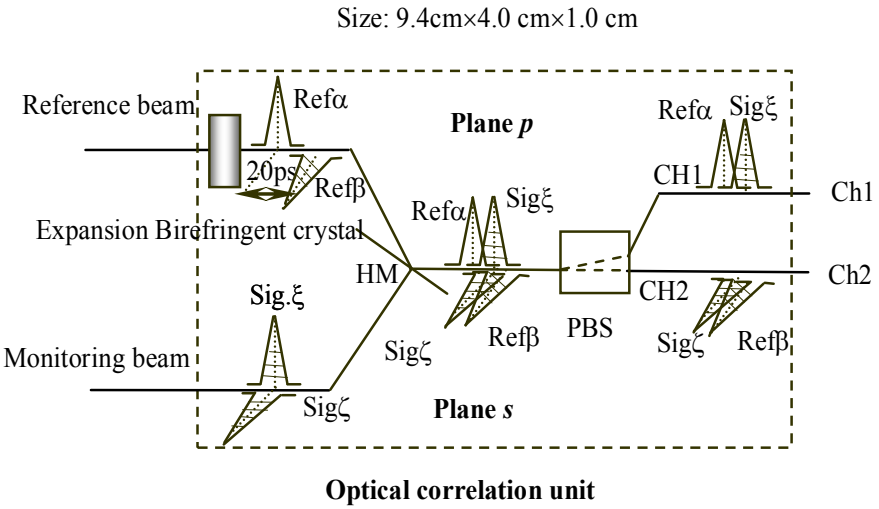


(a) Diagram of optical pulse correlation unit (HM: Half Mirror; PBS: Polarization beam splitter)

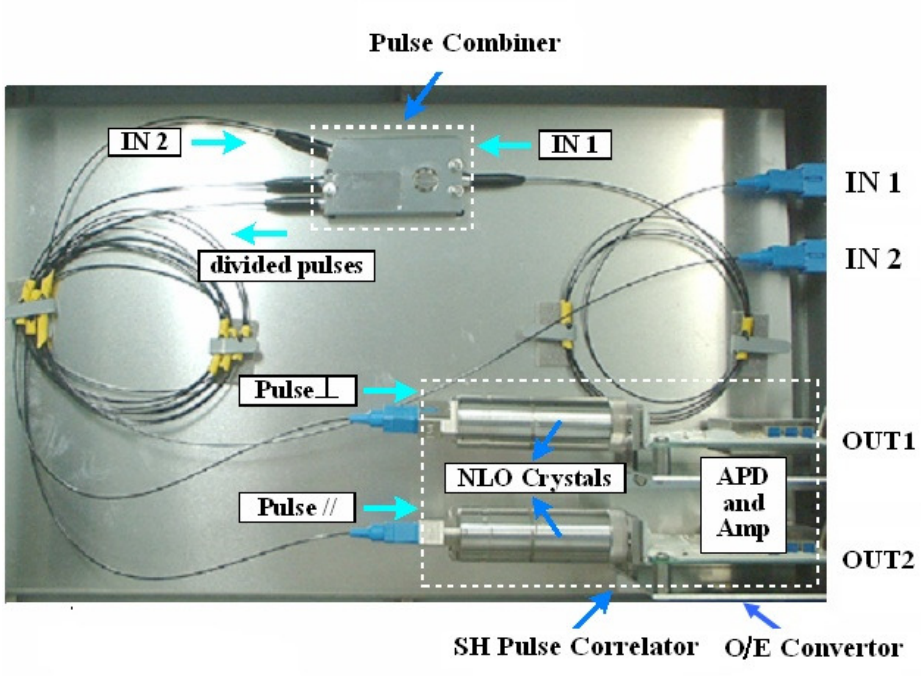


(b) Top view of optical pulse correlation unit and SHG Correlation detection & O/E unit

**Figure 2-4:** Optical pulse correlation unit

When the time delay in the monitoring beam is increased due to the temperature changed around the monitoring fiber, Sig ξ and Sigζ will drift backwardly. Then the correlation signal of Ch1 will increase, while Ch2 decreases. Thus the timing relationship between the reference beam and the monitoring beam can be obtained. And the temperature around the monitoring fiber can be monitored. The relationship between the correlation signal versus the timing drift and the optical timing relationship is shown in Figure 2-5.

The optical pulse source has a period of 50 ps. Because the optical pulses are doubled through the monitoring fiber, the relationship between the correlation signals and the time drift of the monitoring fiber becomes a 25 ps period. The differential correlation signal of Ch1-Ch2 contains a 10 ps good linear and a 15 ps approximately linear area b from real measurement, as shown in Figure 2-5. The 10 ps linear area is used in the short monitoring fiber for a wide measureable range but low sensitivity, and the entire 25 ps period areas a and b are used in the long monitoring fiber for a high sensitivity but narrow measureable range. And the 10 ps linear area is twice of single channel SHG. In other word, double channel differential pulse correlation unit increased the linear range to twice and also can isolate the fluctuation of pulse power.

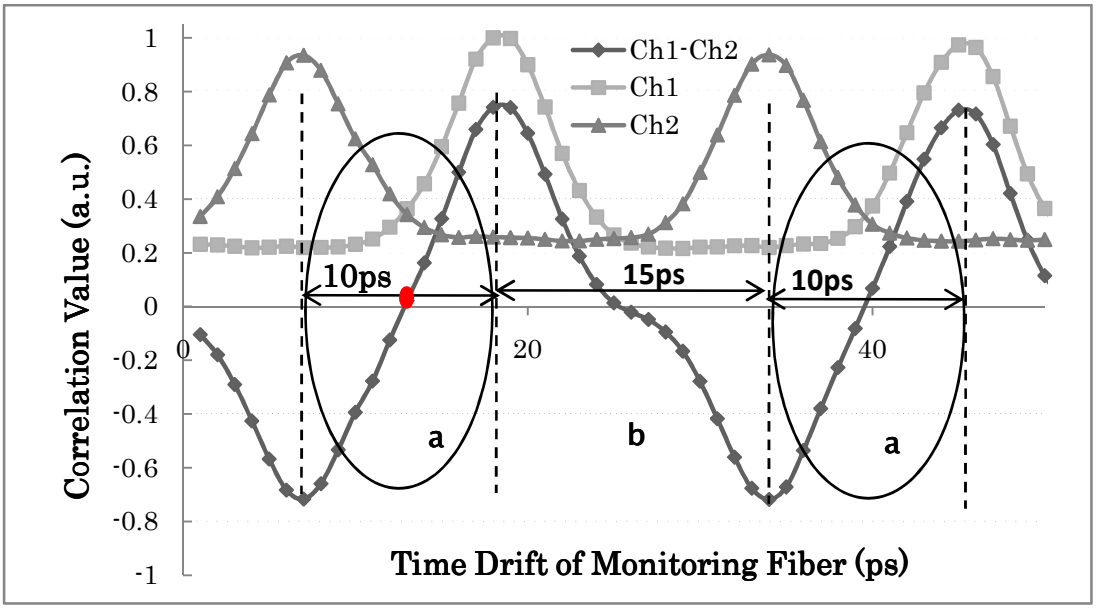


**Figure 2-5:** Monitoring pulse time drift Vs correlation signal.

## 2.3 Setup of Optical Pulse Correlation Sensing System

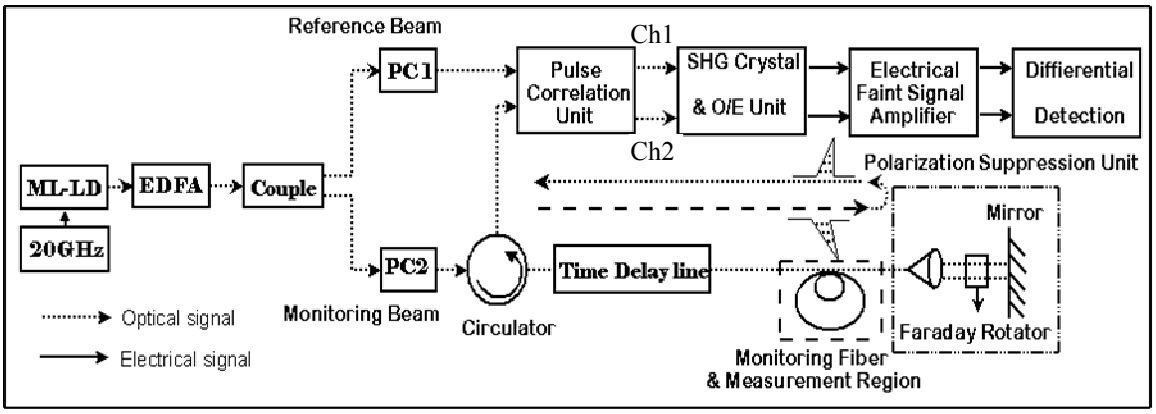


**Figure 2-6:** Configuration of the optical correlation temperature sensing system with polarization suppression

ML-LD: Mode-Locked Laser Diode; EDFA: Erbium-doped Fiber Amplifier;

PC1&2: Polarization Controller 1&2; SHG: Second Harmonic Generator

A higher time resolution optical correlation sensing system has been developed by using an electrical faint signal amplifier in the polarization fluctuation suppressed optical correlation sensing system [9]. The configuration of the sensing system was

shown in Figure 2-6. In this sensing system, a mode-locked laser diode (ML-LD) was used as the light source, which is modulated by optical pulse with a repetitious rate approximately 20 GHz. After being amplified by an EDFA, the optical pulse was split into a reference pulse and a monitoring pulse by a coupler. The Reference pulse is input to the pulse correlation unit through a polarization controller PC1. The monitoring pulse is input to a circulator through other polarization controller PC2. (The PC1 and PC2 are used to adjust the polarization angle offset by 45°, and the circulator is used to isolate the incoming and outgoing optical pulse.) Then the monitoring pulse accesses to a faraday rotate mirror (FRM) through a time delay line and the monitoring fiber. The monitoring pulse is refracted by the FRM which can make the polarization fluctuation of the correlation signal to be isolated effectively, and then accesses to the pulse correlation unit by the circulator again.

The pulse correlation unit is used for double orthogonal paired pulse generation, combination and separation [9]. Figure 2-4 (b) shows the diagram of the pulse correlation unit. Then the correlation signals of Ch1 and Ch2 can be obtained by the second harmonic generation (SHG) crystal and be converted to electrical signals by the optical-to-electrical (O/E) unit. After that, they are amplified by the electrical faint signal amplifier which be made up of low noise instrument amplifier INA128 and low-pass filter circuit and are detected by the differential detection unit. The signal-to-noise ratio (SNR) of the correlation signals is increased from 6 dB to 24 dB. Therefore the time resolution of this sensing system is increased from 0.02ps to 0.005ps.

Therefore, the optical pulse time drift in monitoring fiber is vulnerable to variation of the environment such as temperature, strain and stress. And this time drift can be obtained by using the SHG correlation technique as the foregoing statement and Figure 2-6 shown. By controlling the step motor of the time delay line to simulate the time drift in monitoring fiber, the output signals of correlation value vs. time drift are shown as Figure 2-5. Ch1 and Ch2 are the correlation signals of the double paired pulse CH1 and CH2 respectively. The optical pulse source is period of 50ps, and the reference double pulse is 20ps time-bias during the pulse correlation unit. The optical pulse is double

through the time delay line and monitoring fiber and. Therefore, the signal of Ch1-Ch2 with 25ps period, which is the differential of Ch1 and Ch2, contains a 10ps good linear area ∅ and 15ps approximately linear area ψ as shown as Figure 2-5.

## 2.4 Result and Discussion of Temperature and Strain Experiment

### 2.4.1 Temperature Experiment and Result

The schematic diagram of the temperature sensor experimental setup is shown in Figure 2-6. Before practical field measurements , a reliable calibration is required. The scheme of calibration system is shown in Figure 2-7. It contains three parts, an incubator to control the temperature around monitoring fiber, a commercial available thermometer (SK-L200 TII) to roughly calibrate the sensing value and the optical pulse correlation sensor. The incubator can change the temperature in the range from -10 °C $^{to}$ 50 °C. Then the temperature around the monitoring fiber can be changed continuously and the time delay of the monitoring pulse will be generated and detected by the correlation signal. By using a commercial available digital thermometer with a USB interface, the temperature change generated by the incubator can be displayed and recorded in a PC. Unfortunately, the resolution of the digital thermometer is 0.1°C and the accuracy is ± 0.1°C within the measurement range of -9.9 °C ~205 °C.

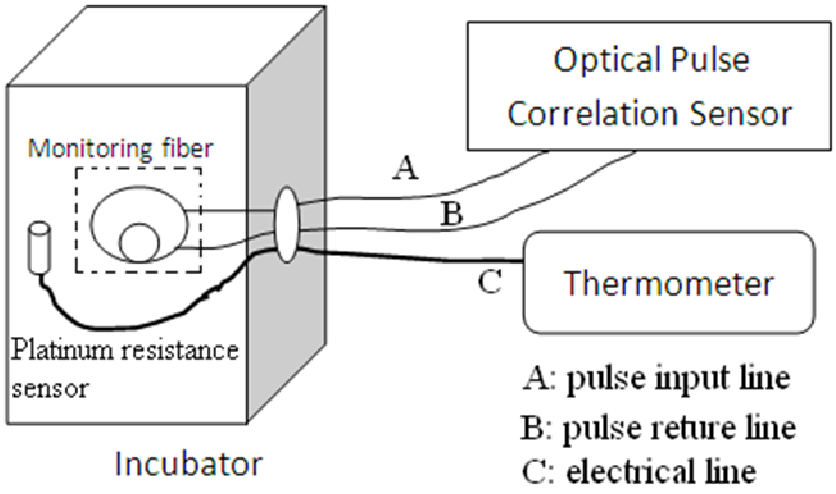


**Figure 2-7**: Schematic diagram of calibretion system

The sensing of correlation signal with the temperature was shown in Figure 2-8. An excellent linearity was observed, when the water bath temperature was increased from 19 °C to 50 °C within about 1 hour. By fitting the experimental data with least square method, a curve correlation coefficient of 99.24 % was obtained. A resolution about 0.04 m·°C was obtained, which showed different temperature resolution could be realized with different fiber length to satisfy the corresponding applications. Some fluctuations appeared when the temperature was higher. The main reasons were discussed in the next part.

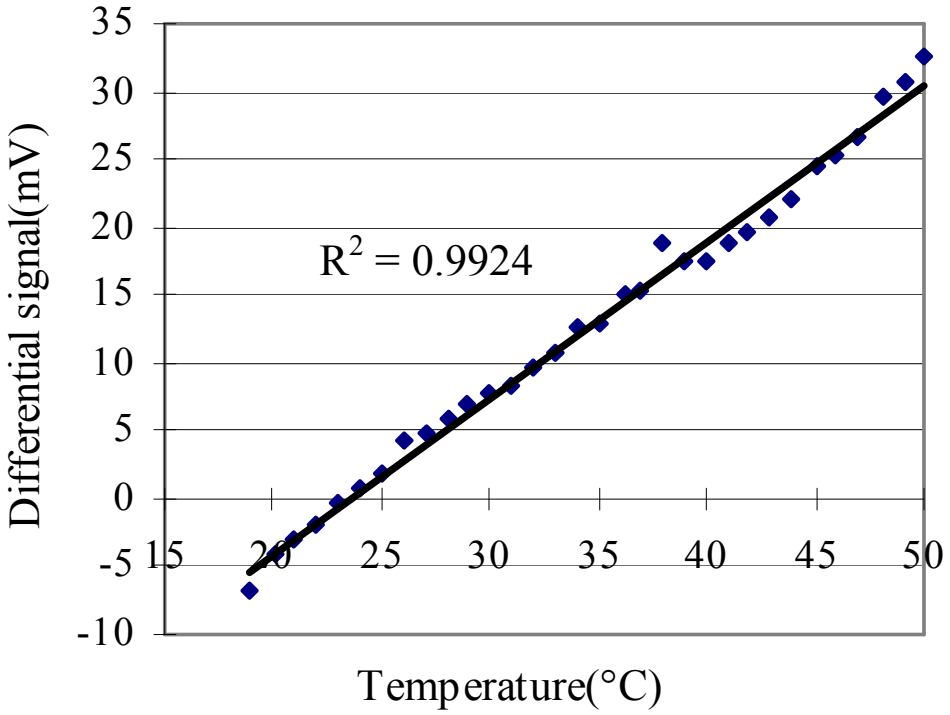


**Figure 2-8:** Temperature calibration result

### 2.4.2 Strain Experiment and Result

In addition, an experiment for strain measurement with a single mode fiber of length 56 cm was carried out by the similar approach. Due to the strain, the fiber optic was extended, which yielded a timing delay for the optical pulse through it. The relationship between the differential signal and the manipulator position was shown to be extremely

linear with a correlation coefficient rate of 99.78% as is indicated in Figure 2-9. According to further experimental study, a resolution of 0.2 με was obtained.

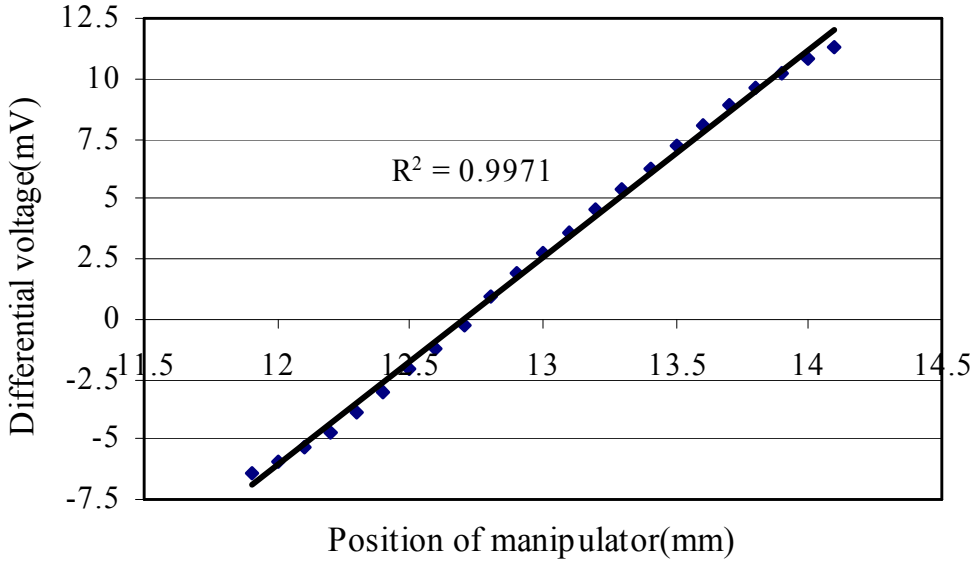


**Figure 2-9:** Strain experiment result

## 2.5 Field Experiments and Results

In order to use practical field sensing, utility, stability and reliability of sensing system is very important. The polarization insensitive, bit-rate flexible and electronics response speed, and electronic noise insensitive were already realized [3]. Before a sensor is used to the practical field measurement , a reliable calibration is required. We use an incubator to control the temperature around monitoring fiber and a commercial available thermometer (SK-L200 TII) to roughly calibrate the sensing value and the optical pulse correlation sensor. The incubator can change the temperature in the range from -10℃ to 50 ℃. Then the temperature around the monitoring fiber can be changed continuously and the time delay of the monitoring pulse will be generated and detected by the correlation signal. By using a commercial available digital thermometer with a USB interface, the temperature change generated by the incubator can be displayed and recorded in a PC. Unfortunately, the resolution of the digital thermometer is 0.1℃ and the accuracy is ±0.1℃ within the measurement range of -9.9 ℃ ~205℃.

As show in Figure 2-5, the linearity is around the decision point α. If the initial position of the time delay line is located at the decision point as shown in red point of Figure 2-5, not only the difference of the temperature can be measured, but also the change the direction (increase or decrease) is available, which is determined by the sign of the difference between two correlation signals. Before the calibration, in order to reduce the hysteresis of the optical fiber cable sleeve, the natural heat-up and cool-down process was carried out by leaving the monitoring fiber outside of the room for 4 days and nights. Then a single-mode fiber with a length of 3.37 m was calibrated by changing the temperature of the incubator step by step. The accuracy around ±0.17 ℃ was obtained.

To investigate the performance of the optical pulse correlation sensor in the practical measurement, a field experiment was carried out. The air temperature outside of the laboratory was measured as shown in Figure 2-10 (a). To confirm the performance of the correlation sensor, a reference digital thermometer (SK-L200) with a resolution of 0.1℃ was placed near the monitoring fiber. The temperature outside of the lab was monitored from 0 o'clock to 8:30 am. During the experiment, besides the real-time data recording from the thermometer and correlation sensor, the temperature change measured by the digital thermometer also was recorded with 20 minutes interval. To balance the reference arm length and monitoring arm, a length compensation fiber was inserted after PC1.

The result from the optical pulse correlation sensor is shown in Figure 2-10 (b), from which it can be seen that the temperature measured from correlation sensor has the same variation with the thermometer. It is obvious that the result from correlation sensor changes much larger than that of the thermometer, so that some fluctuations were observed. However, these fluctuations are not noise, they reflects the temporary temperature fluctuation around the optical fiber by much faster response and much higher resolution. The larger changes of the temperature from correlation sensing system implied the higher sensitivity and response speed than the digital thermometer. The air temperature outside of the lab was successfully monitored by the optical pulse correlation sensor with a high sensitivity, which confirmed the monitor ability of the correlation sensor to the environment around the optical fiber transmission line.

Because the length of the monitoring fiber is 3.37m, this fiber optic temperature sensor can measure the average temperature of a field area with a length of 3.37m. And then if the monitoring fiber is rolled with a small diameter not less than 6 cm, it can measure a very small area temperature as similar as point measurement. Therefore this fiber optic temperature sensor can measure not only point temperature but also a field area average temperature.

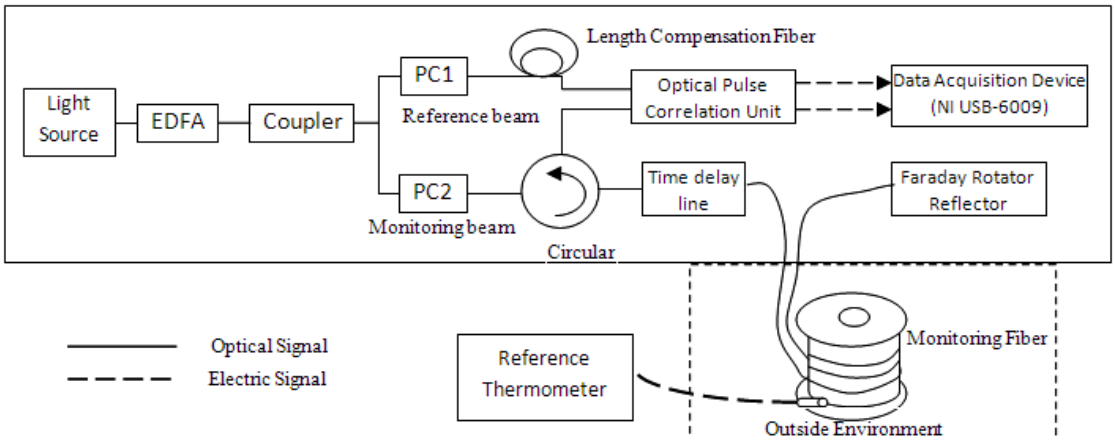


(a) Configuration of temperature measurement

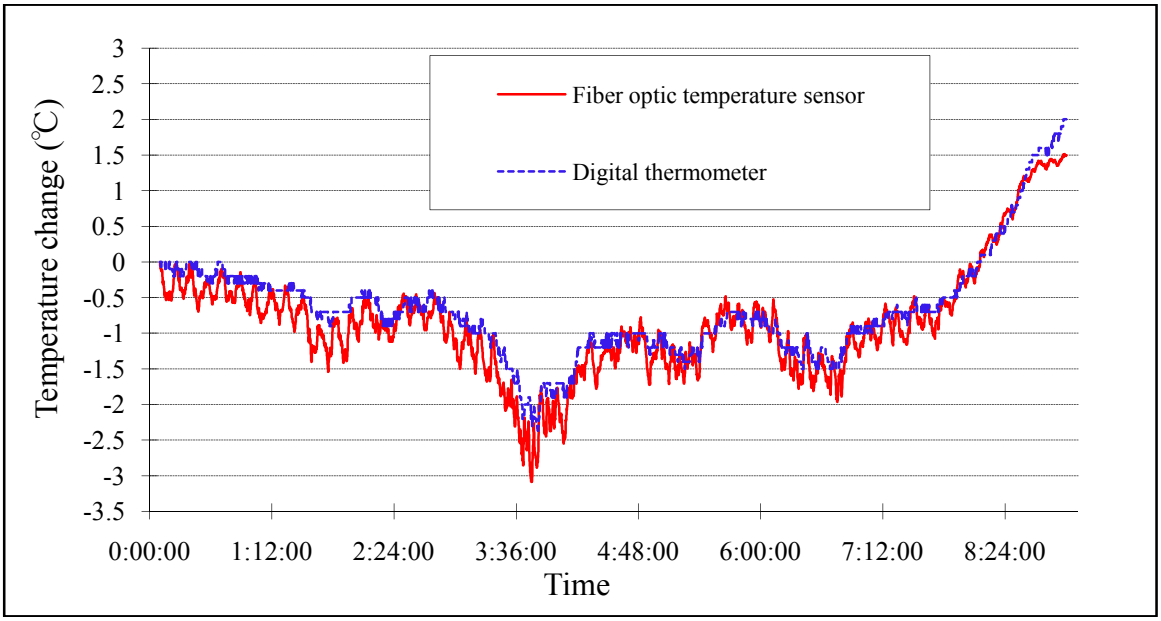


(b) Comparison of the temperature changes measured from the thermometer and correlation sensor

**Figure 2-10:** Field Temperature measurement experiment

## 2.6 Summary

Using quasi-phase matching (QPM) SHG method to measure the correlation between reference and monitoring pulse train, the optical pulse correlation fiber optic sensor has been developed. The experiment result of temperature and strain are investigated. The good linear, real time and low cost high performances are demonstrated. The field testing of the optical pulse correlation temperature sensing system demonstrated that the temperature measured by the correlation sensor had the same variation as and higher sensitivity than the reference digital thermometer. The accuracy of the correlation sensor was approximately ±0.17℃. This fiber optic wide range temperature sensor can be used in oil tank, power transformer and high resolution temperature controller for its anti-electromagnetic interference characteristic. However, for practical applications, the high-sensitivity, wide-dynamic-range and selectable-regions distributed measurement requirements are carried out.

## Reference


[1] Jaime Wisniak: “The Thermometer—From the Feeling to the Instrument”. The Chemical Educator, Vol. 5 No. 2 (2000).

[2] R. P. Benedict, “Fundamentals Temperature, Pressure, and Flow Measurements”, ISBN 0-471-89383-8, p. 4 (1987).

[3] K. Uchiyama, K. Nonaka, and H. Takara: “Subpicosecond timing control using optical double-pulse correlation measurement”, IEEE Photonics Technol. Lett., vol. 16, p. 626, 2004.

[4] K. Nonaka, M. Sako, T. Suzuki: “Optical pulse timing drift sensing for fiber delay monitoring using pulse correlation and differential detection”, 17th International Conference on Optical Fiber Sensors, Proceeding of SPIE, vol. 5855, p. 76, Bruges, 2005.

[5] Minako Sako, “Optical Pulse Correlation Measuring Technique for Fiber-Optic Temperature and Strain Sensor”, Mater Thesis. Kochi University of Technology, 2005.

[6] H. B. Song, T. Suzuki, M. Sako, and K. Nonaka: “High time resolution fiber optic sensing system based on correlation and differential technique”, Meas. Sci. Technol. vol. 17, p. 631, 2006.

[7] H. B. Song, T. Suzuki, T. Fujimura, K. Nonaka, T. Shioda, and T. Kurokawa: “Polarization fluctuation suppression and sensitivity enhancement of an optical correlation sensing system”, Meas. Sci. Technol., vol. 18, p. 3230, 2007.

[8] Hongbin Song, “Development of High-Sensitivity Optical Fiber Sensor Based on Optical Pulse Correlation”, PhD. Thesis. Kochi University of Technology, 2008.

[9] X. J. Xu, K. Nonaka and H. B. Song; “Fiber optic wide region temperature sensing system”, Photonics and Optoelectronics Meetings: Fiber Optic Communication and Sensors, Wuhan of China, Proc. SPIE, vol. 7278, p. 72781F, 2008.

[10] http://www.rp-photonics.com/phase_matching.html

[11] G. Imeshev: “Tailoring of Ultrafast Frequency Conversion with Quasi-Phase-Matching Gratings,” PhD. Dissertation, Stanford University, 2000.

[12] H. Ishizuku, T. Suhara, M. Fujimura and H. Nishihara: “Wavelength-conversion type picosecond optical switching using a waveguide QPM-SHG/DFG device”, Optical and Quantum Electronics, vol. 33, p. 953, 2001.

[13] J. Yang, X. P. Hu, P. Xu, X. J. Lv, C. Zhao, H. J. Zhou and S. N. Zhu: “Chirped-quasi-periodic structure for quasi-phase-matching”, Optics Express, vol. 18, p. 127630, 2010.

[14] L. B. Yuan, J. Yang: “Multiplexed Mach-Zehnder and Fizeau tandem white light interferometric fiber optic strain/temperature sensing system”, Sensors and Actuators A, vol. 105, p. 40,2003.

# Chapter 3 High-sensitivity and Wide-dynamic-range Fiber Optic Sensing System Based on Pulse Correlation and TDM

## 3.1 Introduction

Fiber optic temperature sensors generally measure temperature by using the thermal expansion of fiber optic, and they only use optical signals for sensing, hence they can isolate the electromagnetic interference and have wide measurable range and high resolution due to extremely high temperature of melting point of fiber optic material. FBG temperature sensor is simple, however FBG signal monitor is complex needed high resolution optical spectrum analyzer [1]. Some interferometers are simple but are more limited in measurement resolution, dynamic range or multiplexing; others provide better resolution but are more complicated, expensive or unstable [2]. Therefore, a simple, real-time fiber optic sensor is required. Double-pulse correlation measurement is alternative method [3-5]. A subpicosecond pulse timing monitoring and stabilization system based on optical pulse cross-correlation and SHG differential signal detection was proposed, and the time resolution is better than 0.1 picosecond [3]. A simple fiber optic sensing system was investigated. This sensing system used optical pulse correlation measurement mechanism and differential detection technique between reference double-pulse and monitoring signal pulse to detect the environment condition such as temperature, stress and pressure. It also has very high time resolution of less than 0.04ps [4]. A polarization fluctuation suppressed optical correlation sensing system was proposed by utilizing the birefringence compensation approach in a retraced fiber path using Faraday Rotator Mirror elements. Therefore, a higher resolution and stable operation were realized within the designed pulse monitoring range. The time resolution had reached to 0.02ps [5].

Moreover, this research increases the time resolution of the system to 0.005ps by enhancing the signal to noise rate with using an electrical faint signal amplifier. A long monitoring fiber has high measurement resolution but small measureable dynamic range. Short monitoring fiber has long measureable dynamic range but low measurement resolution. The wide range is contradicted by high resolution. Therefore, in order to resolve the contradiction of temperature resolution and measurable range, this paper shows a new idea to realize the simultaneous high resolution and large dynamic range using periodical characteristic between differential signal and time drift. The temperature sensing high-resolution and large measurement range method which is combined the short and long monitoring fiber simultaneously by using optical switch and time-division multiplexing (TDM) technique is proposed. Therefore, wide dynamic range measurement and high resolution are simultaneity able to monitor.

There are many industrial applications for high-sensitivity temperature sensors. These fall into two main classes, electrical temperature sensors and optical temperature sensors. The electrical temperature sensor class includes platinum thin-film resistance temperature detection (RTD) sensors, metal oxide semiconductor temperature sensors, and quartz resonator temperature sensors. Electrical temperature sensors have high sensitivity, stability, and reliability advantages but are limited by electromagnetic interference [1-4]. The optical temperature sensor class includes the fiber Bragg grating (FBG) sensors, fiber-optic Fabry-Perot interferometers, fiber-optic white light interferometers, plastic optical fiber temperature sensors using thermo sensitive clouding materials, fiber-optic temperature sensors using a grating on an angled fiber tip, fiber-optic fluorescence temperature sensors, black-body source sensors, and fiber-optic thin-film temperature sensors [5-12]. The majority of these optical fiber sensors have low temperature sensitivity. One FBG temperature sensor, which is described in ref. 5, has high sensitivity and can reach 0.005 °C resolution but its measurable range is limited. There are a few other types of temperature sensors, such as acoustic reflector temperature sensors, that also have low temperature sensitivity [13].

To address this problem, a high-sensitivity, simple, real-time fiber-optic temperature sensing system has been developed. This sensing system is based on an optical pulse correlation measurement mechanism and differential detection technique and uses a

single-mode fiber as the monitoring fiber to measure temperature [14-16]. However, the high sensitivity is sacrificed for a wide measurable range and vice versa [14].

To resolve the conflict between temperature sensitivity and measurable range, in this study, we design and demonstrate a novel optical pulse correlation sensing system which is combined with short and long monitoring fibers by a time-division multiplexing (TDM) technique. This new approach differs from previously demonstrated measurement schemes in that only one monitoring fiber was used [14-17]. In this new approach, the two different length monitoring fibers are combined in one system. This greatly increases the temperature sensitivity and maintains an acceptable measurable range.

## 3.2. Principle

### 3.2.1 Optical Switch

In telecommunication, an optical switch is switch that enables signals in optical fibers or integrated optical circuits (IOCs) to be selectively switched from one circuit to another. An optical switch may operate by mechanical means, such as physically shifting an optical fiber to drive one or more alternative fibers, or by electro-optic effects, magneto-optic effects, or other methods. Slow optical switches, such as those using moving fibers, may be used for alternate routing of an optical transmission path, such as routing around a fault. Fast optical switches, such as those using electro-optic or magneto-optic effects, may be used to perform logic operations; also included in this category are the semiconductor optical amplifiers, which are optoelectronic devices that can be used as optical switches and be integrated with discrete or integrated microelectronic circuits.

There are many kinds of optical switch as follow as [18]:

- MEMS approaches involving arrays of micromirrors that can deflect an optical signal to the appropriate receiver;
- Piezoelelectric Beam Steering involving piezoelctric ceramics providing enhanced optical switching characteristics

- Inkjet methods involving the intersection of two waveguides so that light is deflected from one to the other when an inkjet-like bubble is created ;
- Liquid crystals that rotate polarized light either 0 degrees or 90 degrees depending on the applied electric field to support switching;
- Thermal methods that vary the index of refraction in one leg of an interferometer to switch the signal on or off;
- Nonlinear methods that vary the diffraction pattern in a medium by taking advantage of the material nonlinear properties to deflect light to the desired receiver;
- Acousto-optic methods that change the refractive index as a result of strain induced by an acoustic field to deflect light;
- Amplifiers and attenuators in output fibers that adjust the signal to the digital "0" power range (when the fiber is not switched to) or to the normal power range when it is.

Considering for the low price and high performance, a MEMS optical switch FSW1×2-SM from China Electronics Technology Group Corporation (CETC) was utilized in this research as Figure 3-1 shown.

Its features are showed as follows:

- Wide Wavelength Range
- Low Insertion Loss
- Low Back Reflection
- High Reliability、High dependability
- No glue in the Route
- Latching and Non-latching control

Applications includes as follow as:

- Configurable& OADM
- Metropolitan Area Networks
- System Monitoring
- Component Testing
- For R&D in Laboratory

The performance specification of the optical switch is shown in Table 3-1.

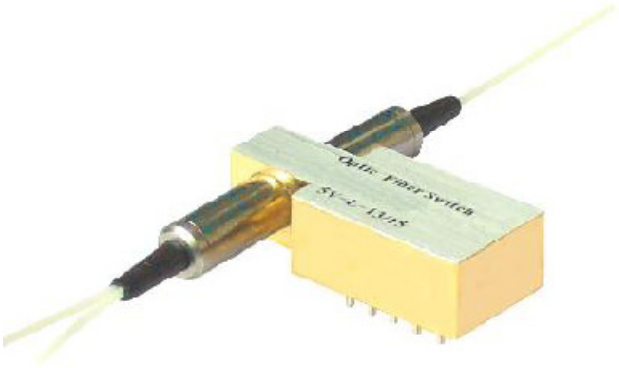

**Figure 3-1: MEMS optical switch** FSW1×2-SM

**Table 3-1:** the Performance specification of optical switch FSW1×2-SM

| | | | | | | |
|---|---|---|---|---|---|---|
| Type | 1×1、1×2、2×2、2×2B | | | | | |
| Wavelength Range nm | 1310 or 1550(SM) | | 1310 & 1550(SM) | | 850 or 1310(MM) | |
| Insertion Loss dB | Typ:0.3 | Max:0.5 | Typ:0.5 | Max:0.8 | Typ:0.5 | Max:0.8 |
| PDL dB | ≤0.05 | | | | | |
| Return Loss dB | SM≥55、MM≥30 | | | | | |
| Wavelength RelativeLoss dB | ≤0.25 | | | | | |
| Cross-Talk dB | ≤-60 | | | | | |
| Repeatability dB | ≤±0.02 | | | | | |
| Operating Voltage v | 3.0 or 5.0 | | | | | |
| Durability(Life) times | ≥107 | | | | | |
| Switching Time ms | Bar→Cross≤3 Cross→Bar≤8 | | | | | |
| Transmission Power mw | ≤500 | | | | | |
| Operating Temperature ℃ | -5～+50 | | | | | |
| Storage Temperature ℃ | -20～+85 | | | | | |
| Dimension mm | (L)29.0×(W)12.5×(H)8.0 | | | | | |

### 3.2.2 Principle of Combination with Short and Long Monitoring Fiber

If the strain change in the monitoring fiber can be neglected, the optical path of the sensor gauge will be varied owing to thermal expansion ($\alpha_T$) and the change in refractive index of the fiber core ($C_T$). Therefore, the change in time drift $\Delta t$ related with the ambient temperature T can be represented as

$$\Delta t = t - t_0 = \frac{n \cdot 2L_0}{c}(\alpha_T + C_T)(T - T_0), \tag{3-1}$$

where $L_0$ is the initial length of the sensing propagation path in the monitoring fiber at the initial ambient temperature $T_0$, and $t_0$ is the initial time drift.

Then, the ambient temperature can be measured as

$$T = \frac{\Delta t}{\frac{n \cdot 2L_0}{c}(\alpha_T + C_T)} + T_0 = \frac{t - t_0}{S \cdot L_0} + T_0, \tag{3-2}$$

where *S* is a sensitivity coefficient, which is defined as

$$S = \frac{2n}{c}(\alpha_T + C_T). \tag{3-3}$$

For the standard commercial communication single-mode fiber at wavelength $\lambda = 1550$ nm, the parameters are n=1.4675, $\alpha_T = 5.5 \times 10^{-7}/℃$ , $C_T = 0.811 \times 10^{-5}/℃$, as taken from ref. 13. Using these data for the unit optical fiber length, the sensitivity coefficient S of this fiber temperature sensor can be theoretically calculated as $0.085 ps/(m℃)$.

Because the resolution and range of the time drift $\Delta t$ of monitoring path are fixed to 0.01ps and 20ps respectively. Therefore the range of temperature measurement is inversely proportional to the $l_0$ which is the length of monitoring fiber. And the resolution of temperature measurement is directly proportional. Therefore we can know that the temperature resolution and measurable range were contradictory and related to the length of monitoring fiber in this system from theory.

The temperature measurement result by using 3m monitoring fiber is shown as Figure 3-2 (a). The resolution is about $0.03℃/mV$, measurable range is 20℃. And the other one by using 100m monitoring is shown as Figure 3-2 (b). The resolution and

measurable range are about 0.001 ℃/mV and 0.7 ℃, respectively. Therefore we can know that the temperature resolution and measurable range were contradictory and related to the length of monitoring fiber in this system from the real measurement result as shown in Table 3-2.

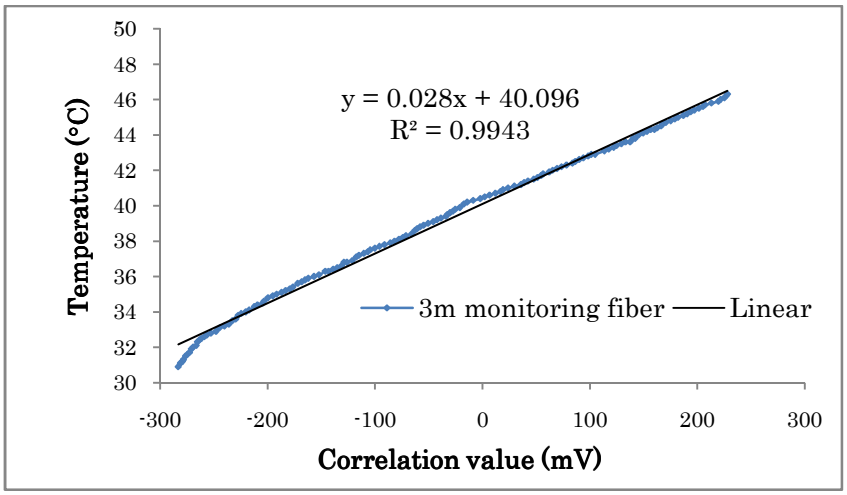


(a)

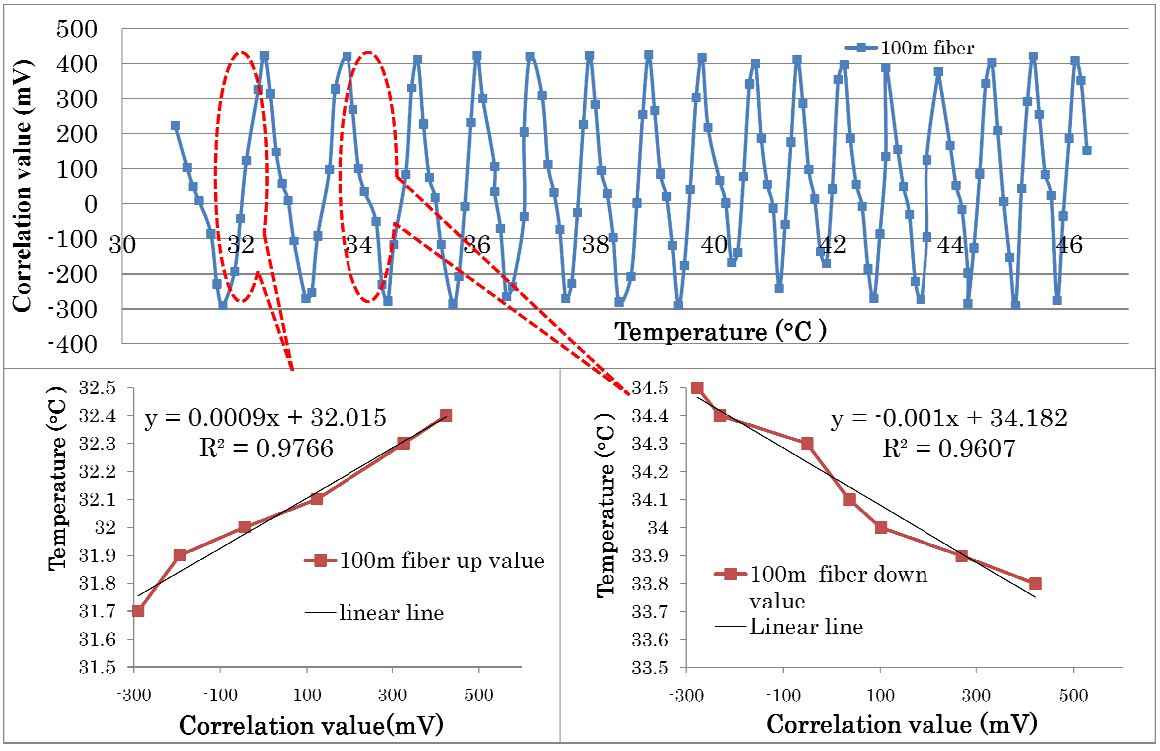


(b)

**Figure 3-2:** Temperature resolution calibration for 3m short and 100m long fibers. (a)3m short fiber (b)100m long fiber

**Table 3-2:** Comparing the performance of temperature experiment with different length of monitoring fibers.

| The length of monitoring fiber | Measure Range | Temperature Resolution |
|---|---|---|
| 3 m short fiber | 20℃ | 0.03℃/mV |
| 100m long fiber | 0.7℃ | 0.01 ℃/mV |

In order to enhance higher resolution of fiber optic temperature sensing system and increase the wide measure range simultaneously, a new principle of the temperature sensing system is proposed here. The principle of this fiber optic temperature sensor system is similar with the spiral micrometer as shown in Figure 3-3. It contains two sensing parts, a short monitoring fiber A with large measure range $nT_0$ and low resolution $T_0$, the other long monitoring fiber B with small measure range $T_0$, high resolution $\frac{T_0}{m}$ and periodic characteristic. The n and m are constant integer. The measure resolution of monitoring fiber A equals to the measure range of the monitoring fiber B. And the measure signal of the monitoring fiber B is periodical characteristic. Therefore, combing the monitoring fiber A and B can achieve large measure range and high resolution simultaneously. Because the signal of long monitoring fiber B is periodic, monitor A and B can be combined and achieve large measure range $nT_0$ and high resolution $\frac{T_0}{m}$.

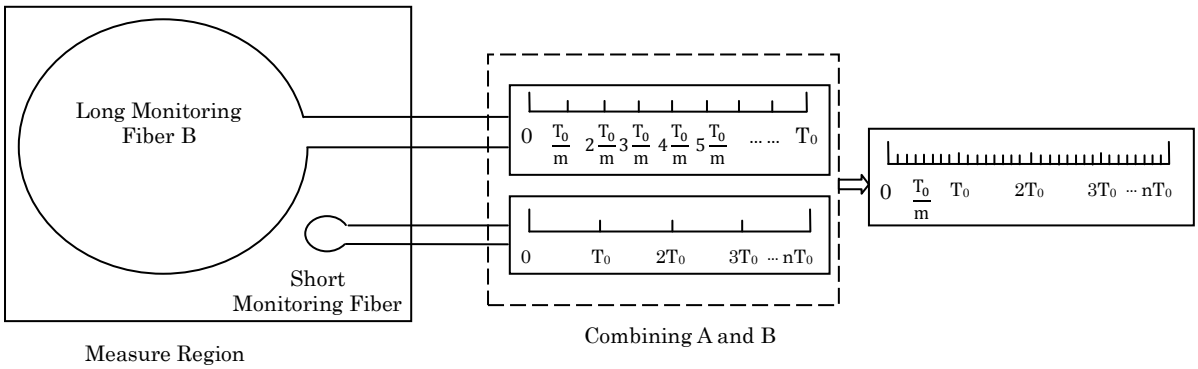


**Figure 3-3:** Schematic diagram of the combining measure (n and m are constant integer)

We already know that a wide range is contradicted by high sensitivity [15]. By combining short and long monitoring fibers, we can achieve a high sensitivity and wide measureable range in one sensing system. Therefore, a method that combines the correlation signals of short and long monitoring fibers and converts them to a temperature value is required. Because the correlation signal and temperature have an exceptional linear relationship, using the linear trend line is a simple and applicable method. Figure 3-4 is a schematic drawing that illustrates the principle of the conversion of the combined correlation signal to a temperature value. The short monitoring fiber has a low sensitivity $T_0/V_0$ and wide measurable range $nT_0$ (n is an integer). The long monitoring fiber has a high sensitivity $aT_0/[nV_0(a+b)]$ and narrow measurable range $aT_0/(a+b)$ in the increase areas, and high sensitivity $bT_0/[nV_0(a+b)]$ and narrow measurable range $bT_0/(a+b)$ in the decrease areas (n is an integer, and a and b are the widths of the increase and decrease areas of the short fiber, respectively). Therefore, the combined system has a wide measurable range $nT_0$ and high sensitivity $aT_0/[nV_0(a+b)]$ and $bT_0/[nV_0(a+b)]$ in theory for temperature measurement.

When combining long and short fibers in a sensing system, $V_L$ and $V_S$ are the real-time correlation values of long and short fibers, respectively. $\mathrm{mod}(V_S, V_0)$ is the remainder after $V_S$ is divided by $V_0$ .

When $\mathrm{mod}(V_S, V_0) \le a/(a+b)\, V_0$ , the real-time temperature T is expressed as

$$T = \left[\frac{V_S}{V_0} - \mathrm{mod}(V_S, V_0)\right] T_0 + \frac{V_L}{nV_0} \cdot \frac{aT_0}{(a+b)} \quad . \tag{3-4}$$

When $\mathrm{mod}(V_S, V_0) > a/(a+b)\, V_0$ , the real time temperature T is expressed as

$$T = \left[\frac{V_S}{V_0} - \mathrm{mod}(V_S, V_0) + 1\right] T_0 - \frac{V_L}{nV_0} \cdot \frac{bT_0}{(a+b)} \quad . \tag{3-5}$$

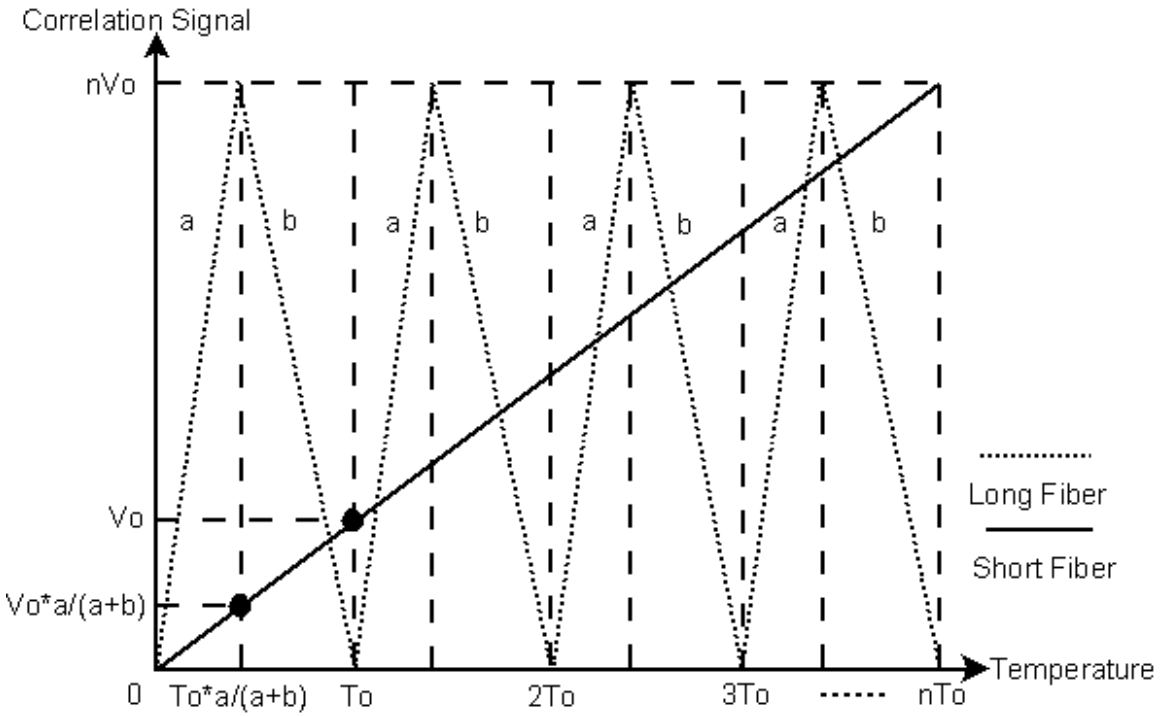


**Figure 3-4:** Schematic diagram of combining long and short fibers (n is a constant integer, and a and b are the widths of the long fiber increase and decrease areas, respectively).

## 3.3 Experimental Methods

The experimental setup is shown in Figure 3-5. The ML-LD optical pulse source has a power of 441.6 μW and a full width at half maximum (FWHM) of 8.9 ps with Gaussian shape. The optical pulse power is amplified to 15 mW by erbium-doped fiber amplifier (EDFA). The reference pulse power is 4.743 mW and the monitoring pulse power is 10.265 mW. A 1×2 optical switch, which has a switch speed of less than 10 ms, is inserted before the two monitoring fibers. The TDM technique using an optical switch to combine the short and long monitoring fibers is thereby made available. The optical switch is controlled by the detection driver NI USB6009, which can detect the correlation signal from the O/E unit with 1.0 mV resolution. The NI USB6009 output signal is connected to a computer, which is interfaced using Labview software.

In this sensing system, we coil the 3-m and 100-m-long fibers in one metal constructer to form a sensor head, which is 8 × 8 × 4 $cm^3$. This combined sensor is not simply a point measurement sensor and measures the average temperature of an 8 ×8 ×4 $cm^3$ space. This compact sensor can accurately and conveniently measure the average temperature of a volume or space.

To demonstrate the applicability of the combined sensing system in high-sensitivity temperature measurements, a temperature experiment is carried out by inserting the 3- and 100-m-long-fiber sensor head and a platinum resistance thermometer (PRT) as the reference temperature sensor into an incubator, and measuring the correlation value of the fiber-optic sensing system and the temperature of PRT.

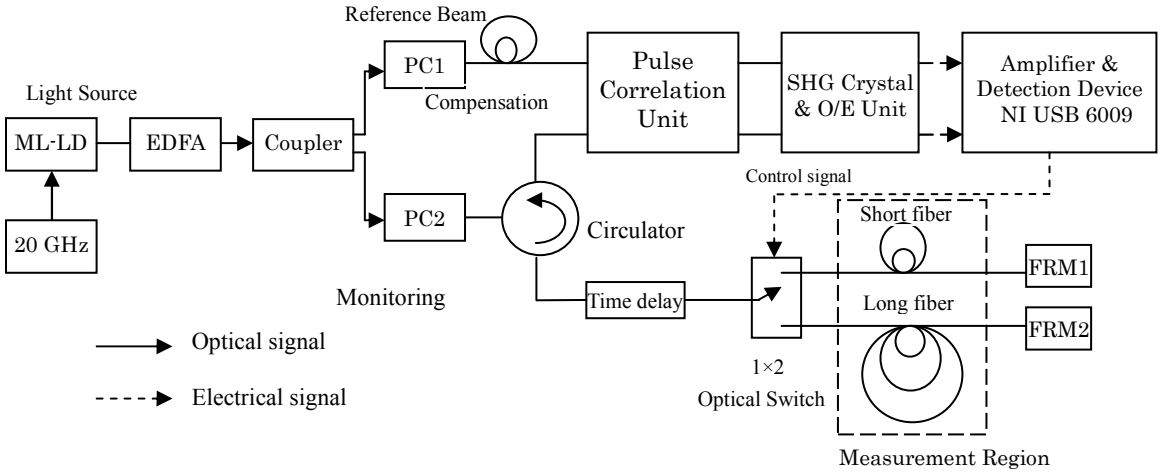


**Figure 3-5:** Schematic diagram of high-sensitivity and wide-range fiber-optic temperature sensing system. ML-LD: mode-locked laser diode; EDFA: erbium-doped fiber amplifier; PC1 and PC2: polarization controllers 1 and 2, respectively; SHG: second harmonic generator.

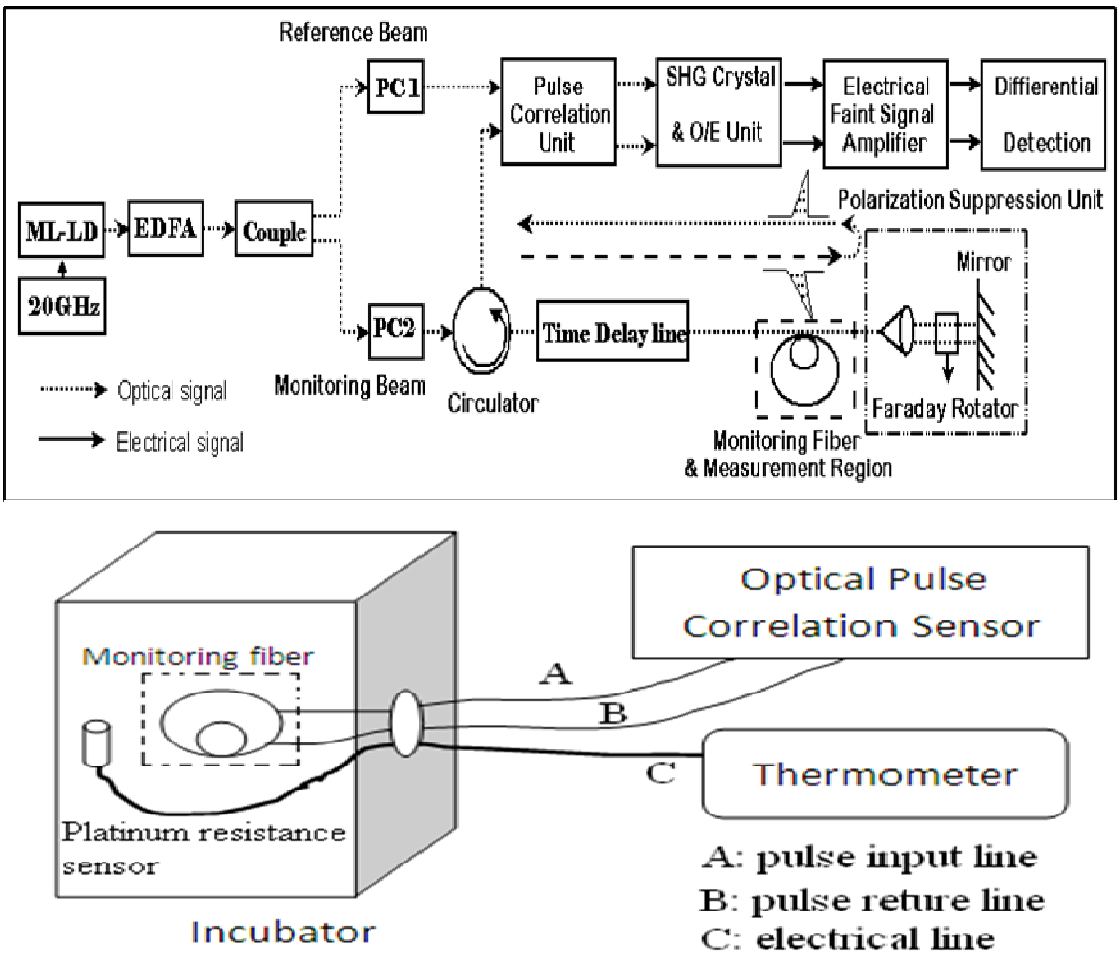


**Figure 3-6:** Temperature sensitivity calibration for 3- and 100-m-long fibers.

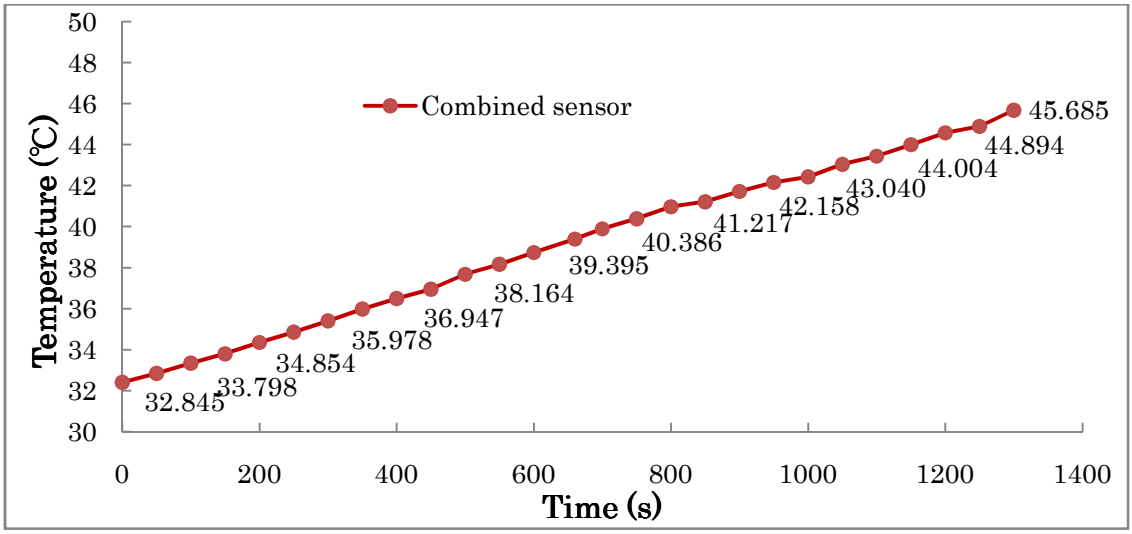


**Figure 3-7:** Real temperature measurement result.

## 3.4 Results and Discussion

The temperature measurement result of combining 3- and 100-m-long fibers in a sensor head over the range from 31 to 47 °C is plotted in Figure 3-6. The result of the 3-m long monitoring fiber is linear, and the result of the 100-m long monitoring fiber is a triangular wave, which contains an increasing and decreasing linear line. The calibration coefficient of the 3-m-long fiber can be calculated as 0.17 ps/(m°C), and it is also about 34 μm/(m°C). The temperature sensitivity of the short fiber sensor is about 0.03 °C/mV. The calibration coefficient of the 100-m-long fiber can be calculated as 0.143 ps/(m°C), and it is also about 28.6 μm/(m°C). The entire temperature sensitivity of the 100-m-long fiber is 0.001°C/mV. Moreover, the temperature measurable ranges of the 3- and 100-m –long monitoring fibers are 20 °C and 0.7 °C, respectively, as shown in Table 3-3.

From this we can determine that the temperature sensitivity and measurable range were contradictory and related to the length of the monitoring fiber. However, the combined sensing system can resolve the contradiction by combining the long and short monitoring fibers in one sensing system. The results of using the linear trend-line method, as described in eqs. (3-4) and (3-5), are to convert the correlation signals of the combined sensor to real temperature values are shown in Figure 3-7.

In this experiment the temperature measured using the PRT has 0.1°C resolution. By calculation from the experimental data, the RMS errors of the temperature data are 0.33 °C for short fiber measurement, 0.056 °C for long fiber increase area measurement, and 0.057 °C for long fiber decrease area measurement. Therefore, by using the 0.1 °C temperature resolution of the PRT to measure the temperature of the sensor head, the temperature resolution of this combined fiber sensor is just 0.1 °C in this experiment, even though it has high sensitivity.

If the fibers are bundled very tightly, the thermo-fiber-stretching information and thermo-mechanical-stress information will be simultaneously measured. We are preparing to distinguish these two features. However, in this experiment, it was difficult to separate them. In this experiment, two bare fibers of different length are inserted into

the same region by lose bundling in the small drum to reduce the tensile strain. Therefore, the two bare fibers should be quasi-free from their own strain impacts from the stretching mechanical stress.

It should be mentioned that the dynamic measurement ranges are dependent on the optical time delay line component, as shown in Fig. 5. Even if the measurable range of the short fiber is fixed, the optical time delay line component can dynamically change the measurable range by changing the initial temperature such as from 10-30 to 30-50 °C.

**Table 3-3:** Comparison of performance of fiber-optic temperature sensors with different lengths of monitoring fibers.

| | Temperature measurable range (°C) | Temperature sensitivity (°C /mV) |
|---|---|---|
| 3-m-long fiber | 20 | 0.03 |
| 100-m-long fiber | 0.7 | 0.001 |
| Combination of 3- and 100-m-long fibers | 20 | 0.001 |

## 3.5 Conclusions

A fiber-optic temperature sensing system based on correlation and the TDM technique combined with 3- and 100-m-long monitoring fibers for achieving high sensitivity and a dynamic measurable range has been proposed and demonstrated. By using the optical switch to combine the short and long fibers, high sensitivity is available in this sensing system. By using the optical time delay line component to change the measurable range, a wide dynamic measurable range is also available. By using the linear trend-line method to combine the correlation values of the short and long monitoring fibers, a high-sensitivity temperature measurement of 0.001 °C/mV with an approximately 20 °C measurable range is successfully carried out. This system can be used in oil tanks, power transformers, ocean water temperature measurements, and high-resolution temperature controller applications owing to its high sensitivity and anti-electromagnetic interference characteristics.

## Reference


**[1]** J. Kim, J. Kim, Y. Shin, and Y. Yoon: “A study on the fabrication of an RTD (resistance temperature detector) by using Pt thin film”, Korean J. Chem. Eng., vol. 18, p. 61, 2001.

[2] C. M. Jha, G. Bahl, R. Melamud, S. A. Chandorkar, M. A. Hopcroft, B. Kim, M. Agarwal, J. Salvia, H. Mehta, and T. W. Kenny: “High resolution microresonator-based digital temperature sensor”, Appl. Phys. Lett., vol. 91, p. 4101, 2007.

[3] J. He, Z. Y. Zhao, J. Lin, and J. M. Dai: “A new low-cost high-performance quartz tuning-fork temperature sensor”, Sens. Rev., vol. 23, p. 134, 2003.

[4] L. Spassov, E. Yossiffov, V. Georgiev, and L. Vergov: “A rotated Y-cut quartz resonator with a linear temperature-frequency characteristic”, Sens. Actuators A, vol. 58, p. 185, 1997.

[5] S. L. Tsao, J. S. Wu, and B. C. Yeh: “High-resolution neural temperature sensor using fiber Bragg grating”, IEEE J. Quantum Electron., vol. 35, p. 1590, 1999.

[6] E. Ishikawa and K. Mizutani: “Temperature Measurement Using a Dual Frequency Acoustic Delay Line Oscillator”, Jpn. J. Appl. Phys., vol. 42, p. 5372, 2003.

[7] L. B. Yuan and J. Yang: “Multiplexed Mach-Zehnder and Fizeau tandem white light interferometric fiber optic strain/temperature sensing system”, Sens. Actuators A, vol. 105, p. 40, 2003.

[8] T. Fukui, M. Kodera, K. Kumagai, T. Shimada, T. Masuda, R. Tanaka, and A. Yamashita: “High precision temperature measurement system using SmartLink at SPring-8”, Proc. Int. Conf. Accelerator and Large Experimental Physics, p. 90, 1999.

[9] B. S. Lee, D. H. Cho, G. R. Tack, S. C. Chung, J. H. Yi, J. H. Jun, S. H. Son, and S. Y. Cho: “Feasibility study of development of plastic optical fiber temperature

sensor using thermosensitive clouding material", Jpn. J. Appl. Phys., vol. 45, p. 4234, 2006.

[10] S. W. Kim: "High-temperature fiber optic sensor using a grating on an angled fiber tip", Jpn. J. Appl. Phys., vol.41, p. 1431, 2002.

[11] Y. J. Rao: "In-fibre Bragg grating sensors", Meas. Sci. Technol. vol. 8, p. 355, 1997.

[12] M. C. Wang, Z. Y. Hsien, Y. T. Tseng, F. G. Tseng, H. S. Huang, J. E. Wang, and H. F. Taylor: "Dual fiber-optic Fabry-Perot interferometer temperature sensor with low-cost light-emitting diode light source", Jpn. J. Appl. Phys., vol. 47, p. 3236, 2008.

[13] K. Kudo and K. Mizutani: "Temperature measurement using acoustic reflectors", Jpn. J. Appl. Phys., vol. 43, p. 3095, 2004.

[14] K. Uchiyama, K. Nonaka, and H. Takara: "Subpicosecond timing control using optical double-pulse correlation measurement", IEEE Photonics Technol. Lett., vol. 16, p. 626, 2004.

[15] H. B. Song, T. Suzuki, M. Sako, and K. Nonaka: "High time resolution fiber optic sensing system based on correlation and differential technique", Meas. Sci. Technol. vol. 17, p. 631, 2006.

[16] H. B. Song, T. Suzuki, T. Fujimura, K. Nonaka, T. Shioda, and T. Kurokawa: "Polarization fluctuation suppression and sensitivity enhancement of an optical correlation sensing system", Meas. Sci. Technol., vol. 18, p. 3230, 2007.

[17] X. J. Xu and K. Nonaka: "High-sensitivity fiber-optic temperature sensing system based on optical pulse correlation and time-division multiplexer technique", Jpn. J. Appl. Phys., vol. 48, p. 102403, 2009.

[18] http://www.fiberer.com/P/1x1_1x2_2x2_2x2B_optical_Switch.html

# Chapter 4 Selectable-Regions Distributed Fiber Optic Sensing System Based on Pulse Correlation and Region Separation

## 4.1 Introduction

To monitor the damage and environmental condition on civil structures is becoming an important research field for civil engineers. It is very important to know the structural health and the degradation of these structures during their lifetime. Nowadays, there are many types of electrical sensors (like strain gauges or thermo-couplers) and also optical sensors. In the optical field, many sensing techniques have been developed. These techniques can be sorted into two types depending on the way to measure the physical magnitude: the point and the distributed sensing techniques. The point sensing technique consists in the point measurement of a physical magnitude in a large number of locations with a large number of sensors, while distributed sensing technique consists in the measurement along a fiber link that can be as long as several meters. The most popular point sensing techniques are the Fibre Bragg Gratings (FBGs) based techniques [1]. Their main drawback is the missing of the degradation measurement between sensors. Also, most of the point sensors used to have a limited maximum range to detect strain. On the other hand, the most common distributed sensing techniques are based on Stimulated Brillouin Scattering (SBS), Stimulated Raman Scattering (SRS), Optical Time/Frequency Domain Reflectometer and interferometers [2]. However, they require more complex information handling, have slower response time and usually need higher input optical power requirement. Thus, measurement regions are strongly limited by the length due to the signal to noise ratio of backscattering intensity. Optical pulse correlation sensing system can inquire the total strain value of the monitoring fiber, but cannot identify in which region the strain is located [3-6].

Therefore, we propose and demonstrate a compact and simple cascadable multi-region distributed sensing system for wide region sensing [7-10]. It is based on optical pulse correlation measurement with region separation techniques. The system uses

inline-multiple monitoring fibers connected by wavelength partial reflectors or intensity partial reflectors for cascadable multi-region measurement. Then, using wavelength scanning with wavelength selective reflectors (WSRs) by employing FBG or using time-position scanning with intensity partial reflectors (IPRs) by employing reflective index gap in fiber connectors, the system can successfully detect very short length changes in multiple regional monitoring fibers for temperature or strain measurement. In this paper, firstly we will show the principle of pulse correlation sensing system and region separation and the identification techniques. Then, we will show the experimental setups for two different region measurements with no crosstalk using two region separation techniques. Later, we will discuss the comparison of the two methods of wavelength and intensity separation and their applications. Finally, we will give some conclusions about the presented techniques.

## 4.2 Principle

### 4.2.1Region Separation Technique Based on WSRs

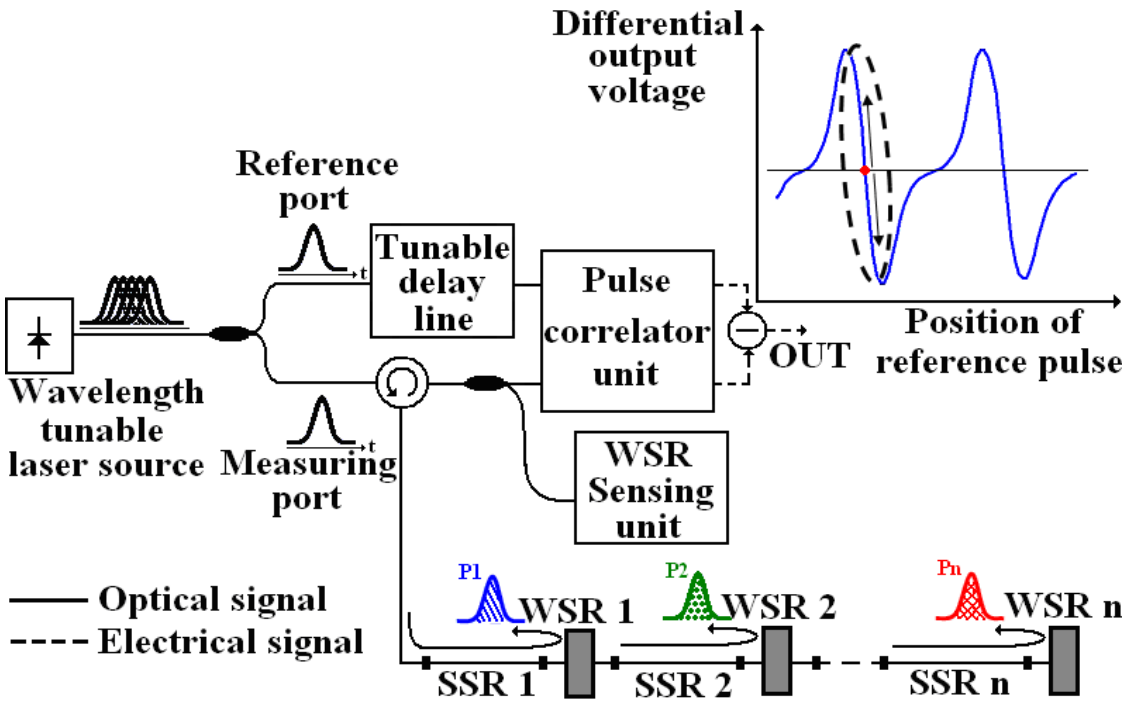


**Figure 4-1:** Scheme of point temperature and distributed strain measurement, WSR: wavelength selective reflector, SSR: Strain Sensing Region.

The interrogation system scheme for point temperature sensors and multi-region distributed strain measurements based on the pulse correlation technique [7] is shown in Figure 4-1. The light source is a wavelength tunable laser that generates a pulse train. The pulse repetition rate is determined by the modulation frequency. The pulse train is coupled into two different ports named "*reference port*" and "*measuring port*". In the measuring port, the pulses pass through an optical circulator and then enter in a cascade of Strain Sensing Regions (SSRs) separated by the Wavelength Selective Reflectors (WSRs). The SSRs are fixed along the structure to monitor the strain changes induced in the structure. The WSRs are released free from the structure. The WSRs change their resonance with variations in temperature acting as a point temperature sensor. The scanning of the wavelength of the pulse source allows the temperature point sensors to be interrogated, also to monitor the different SSRs. In essence, the pulse in the WSR1, the pulse round-trip reaches until the region SSR1 and it only contains information about the strain changes in this region, whereas the reflected pulse in the WSR 2 crosses both SSR1 and SSR2 regions. Using the reflected signals from WSR1 and WSR2, the information of the strain changes in SSR 2 can be retrieved. This scheme can be easily upgraded to the SSRn region.

The reflected pulses return to reach one input port of the pulse correlator unit. The other input of the correlator unit is fed with the pulses coming from the reference port. The reference pulses and the measuring pulses arrive at different time position due to the different lengths of the optical paths. A tunable delay line is placed in the reference arm to allow a partial overlap of both train pulses. The tunability range of the tunable delay line has to be at least half of the inverse of the frequency repetition rate. If the strain in a sensing region is changed, the optical path in the measuring branch produces a time drift between reference and measuring pulse trains and there is a change in the overlapped energy between both train pulses. This change can be monitored by the optical pulse correlation unit. Differential detection technique is used after the pulse correlation unit.

The relationship of the typical differential output voltage is shown in an inset graph in Figure 4-1. It has the same speed of the pulse train from the laser source. The most important area of the differential output voltage curve, which is used for sensing, is

highlighted inside a dashed oval (inset graph in Figure 4-1). The dot indicates the central position (also known as "decision point") in order to perform the highest excursion and to detect fiber compression and elongation. It is very important to mention that the output relationship is linear in this region and it is very useful for sensing applications. Each SSR is adjusted to have its initial value at the central position. This is done by adjusting the tunable delay line for each region response. The initial values of the tunable delay lines are recorded and used as references. Then, any strain applied is transformed in a change of the output voltage value.

### 4.2.2 Regions Separation Technique Based on IPRs

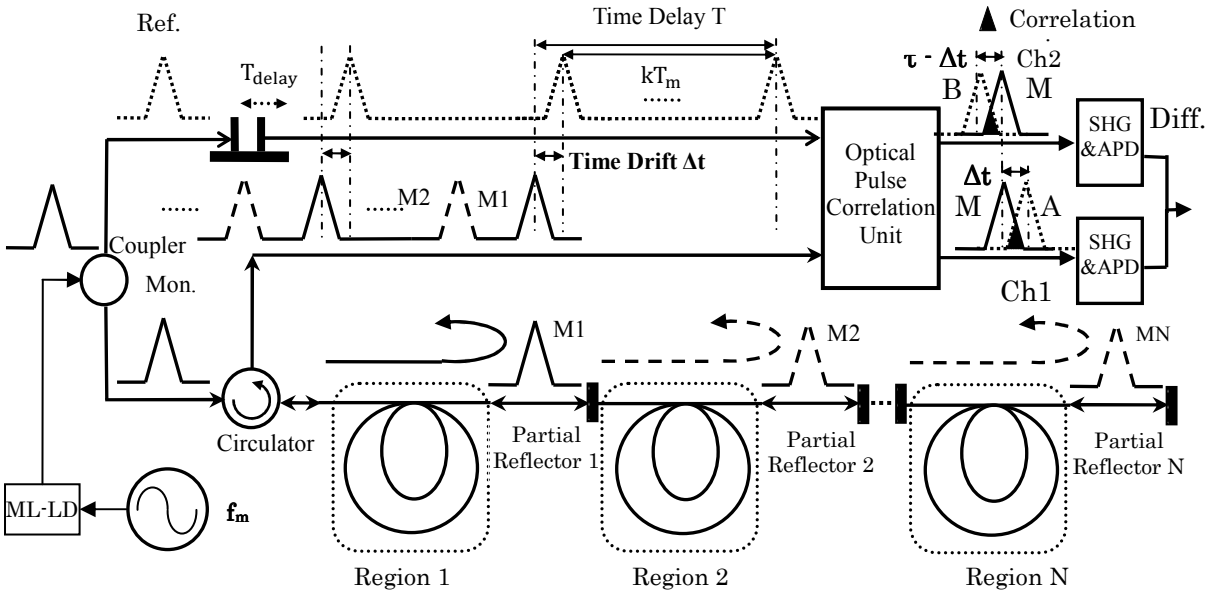


**Figure 4-2:** Schematic of selectable region distributed sensor based on reflected optical pulse correlation measurement,
ML-LD: Mode Locked – Laser Diode, IPR: Intensity Partial Reflector.

The schematic of a cascadable regional distributed sensor based on optical pulse correlation measurement and intensity partial reflectors (IPRs) [8] is shown in Figure 4-2. IPRs are made with thin-file of metal, and are coated with the metal gold on the end of optical fiber by magnetron sputter method. A mode locked laser diode (ML-LD) modulated by a synchronized source with frequency $\mathbf{f_m}$ produces a short optical pulse-train. The optical pulse-train is split into a reference (Ref.) pulse and a monitoring

(Mon.) pulse by a coupler. The monitoring pulse accesses monitoring fibers in regions 1 and 2 (which are used to measure the strain change) through a circulator. Then, the monitoring pulse is reflected back by intensity partial reflectors 1 and 2 (IPR1 and IPR2), respectively, which become two region monitoring pulses M1 and M2. (There are multiple reflections (back and forth) between the two reflectors, which are attenuated quickly because of the low reflectivity of the first reflector and the absorption of optical pulse power in the long sensing fiber) The reflected back pulses M1 and M2 access to the monitoring fibers again and then they reach the input port of an optical pulse correlation unit whereas the reference pulse is connected at a different port.

Thus, M1 passes only through region 1 while M2 passes through both regions 1 and 2. Using the optical pulse correlation unit to detect the time drifts between the reflected pulses M1, M2, and the reference pulse, the information on the strain changes in regions 1 and 2 can be obtained. This scheme can be easily upgraded to the region N.

Therefore, the time drifts between the monitoring pulses reflected by partial reflector 1, 2, ···, N (PR 1, PR 2, ···, PR N) and their adjacent reference pulses are given by

$$\Delta t_i = \frac{n}{c}\Delta L_i + T_{delay} - k_i T_m \tag{4-1}$$

where subscript i = 1, 2,···, N, which indicate PR1, PR2, ···, PRN; $T_m$ is the period of modulated signal equal to $1/f_m$, $\Delta L_i (i = 1, 2, \cdots, N)$ are the differential propagation lengths between the reflected monitoring pulses and the reference pulses; $k_i (i = 1, 2, \cdots, N)$ are the constant integers standing for $\Delta t_i$ less than $T_m$, and $T_{delay}$ is the time position of the optical delay line device. Equation (4-1) indicates that $\Delta L_i$ is proportional to the $T_{delay}$ and $T_m$ when other parameters remain constant. Therefore, we can use a scanning of time position method to monitor temperature and strain changes of different sensing regions. As Figure 4-2 shows, when moving the time position of the time delay line device in the reference propagation path, the time position of the reference pulse will change, the time drift between the reference and monitoring pulses will change, and so the correlations of each channel as well. While the differential correlation value is located at the peak point, the monitoring pulse completely overlaps with the reference

pulse. In other words, the peak points of differential correlation indicate the monitoring pulse positions of each region, as shown in Figure 4-3. Therefore, by scanning the time position of the reference pulse we can detect the change in the monitoring fiber length in each region.

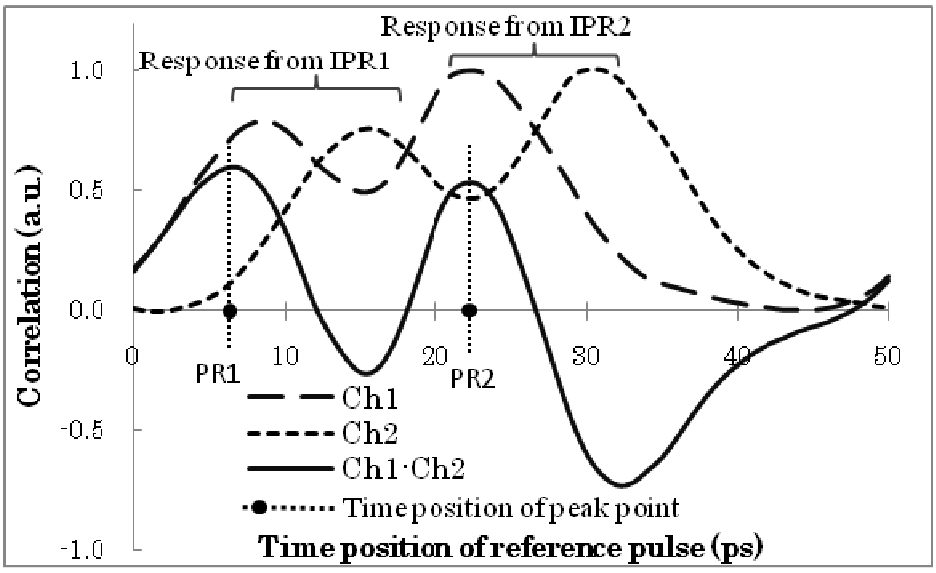


**Figure 4-3:** Correlation vs. Time position of reference pulse

## 4.3 Experimental Results

### 4.3.1 Using Wavelength Scanning with WSRs

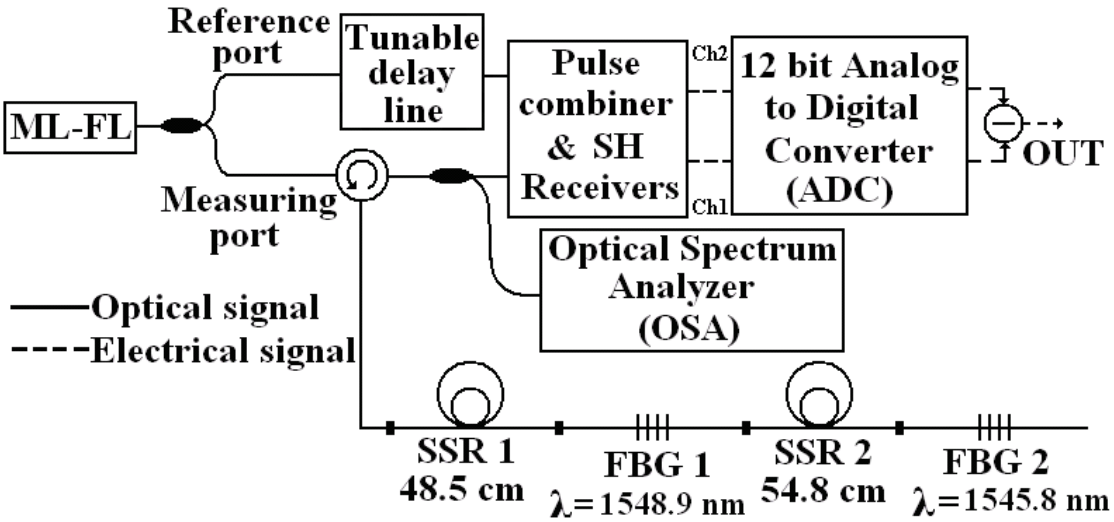


**Figure 4-4:** Experimental setup of pulse correlation and differential technique with wavelength sensing region separation. ML-FL: Mode Locked – Fiber Laser, SH: Second Harmonic, SSR: Strain Sensing Region.

The experimental setup is shown in Figure 4-4. A Mode-Locked Fiber Laser (ML-FL) has been used as a laser source. The laser source is wavelength tunable and its pulse width can be adjusted between 10 ps and 20 ps. In this experimental setup, a pulse width of 12.9 ps has been used, 3.4 dBm of output power and a frequency of 9.956104 GHz, that implies a 100.4 picoseconds pulse repetition rate. To divide the train pulses into reference and measuring ports, a 90/10 ratio optical coupler has been employed.

In the reference port, a delay line has been placed that can be manually adjusted. On the other port, an optical circulator is used to route the pulses to the sensing region and to the correlation unit. Two Fiber Bragg Gratings (FBGs) have been used as a demonstration of WSRs. FBGs central wavelengths are 1548.86 nm for FBG 1 and 1545.81 nm for FBG 2, with 0.26 nm of Full Width at Half Maximum (FWHM) and 80 % of reflectivity in both FBGs. The SSRs have been implemented with two standard single mode optical fibers of 48.5 cm and 54.8 cm length, respectively. The pulse correlation unit and the dual SH Receivers (SHR) have been connected to a 12-bit Analogy to Digital Converter (ADC) to obtain the voltage values of the two single channels. Finally, the output differential signal of these channels is stored in a personal computer. The temperature variations have been sensed by the FBGs using an Optical Spectrum Analyzer (OSA).

The interrogation system has been characterized by checking its linearity, stability and resolution. In the first experiment, the laser source has been tuned at 1545.8 nm. Then, some strain has been applied to SSR2 in 0.1 mm steps (182.5 micro strains for a fiber of 54.8 centimetres length) and the differential output voltage values have been obtained. To calculate the strain applied, the first step is to adjust the decision point when SSR2 is relaxed (central point in the solid curve of inset graph in Figure 4-1). Then, any change in the applied strain (elongation or compression) is converted automatically in a change of the output differential voltage. The results are shown in Figure 4-5. It can be seen that the sensor has a linear response. The vertical error-bars at each strain measurement point show the maximum range of deviations after dozens of cycles. The stability in the measurements is quite high, fluctuations of less than 0.2% have been observed even in the worst case.

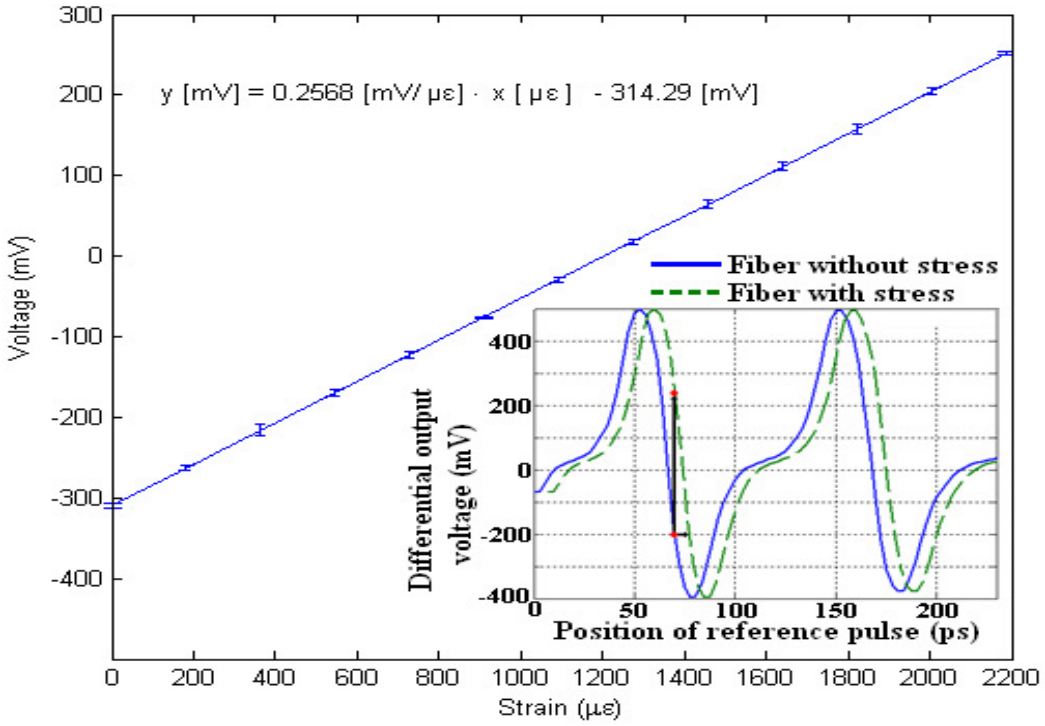


**Figure 4-5:** Differential output voltage when stress is applied to SSR2 with laser source tuned at 1545.8 nm. Subplot shows differential curves of relaxed fiber and 1.2 mm stressed fiber so that a time shift is observed.

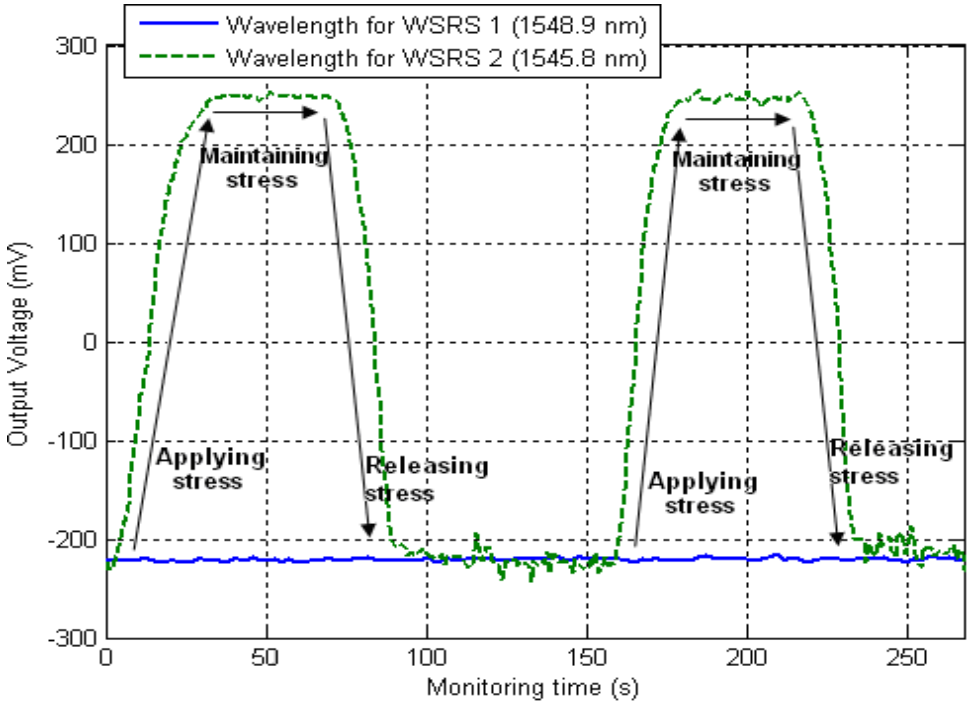


**Figure 4-6:** Output differential voltage with stress applied to the SSR2 using different central wavelengths from the laser source

To demonstrate the absence of crosstalk between the two strain sensing regions, the laser source has been tuned to 1545.8 nm to select WSR 2. Then, a stress has been applied in the SSR2. The dashed line of Figure 4-6 shows the changes in the output voltage. Later, the laser has been tuned to 1548.9 nm to select WSRS 1 and a similar stress has been applied to the same sensing region (SSR2). No change in the differential output voltage has been detected (solid line) showing the absence of crosstalk._At the same time, the temperatures of FBG 1 & 2 with free strain can be sensed by measuring the central wavelength shifting with an OSA. Then the strains of SSR 1&2 can be corrected by using the measured temperature value of FBGs.

### 4.3.2 Using Time-Position Scanning with IPRs

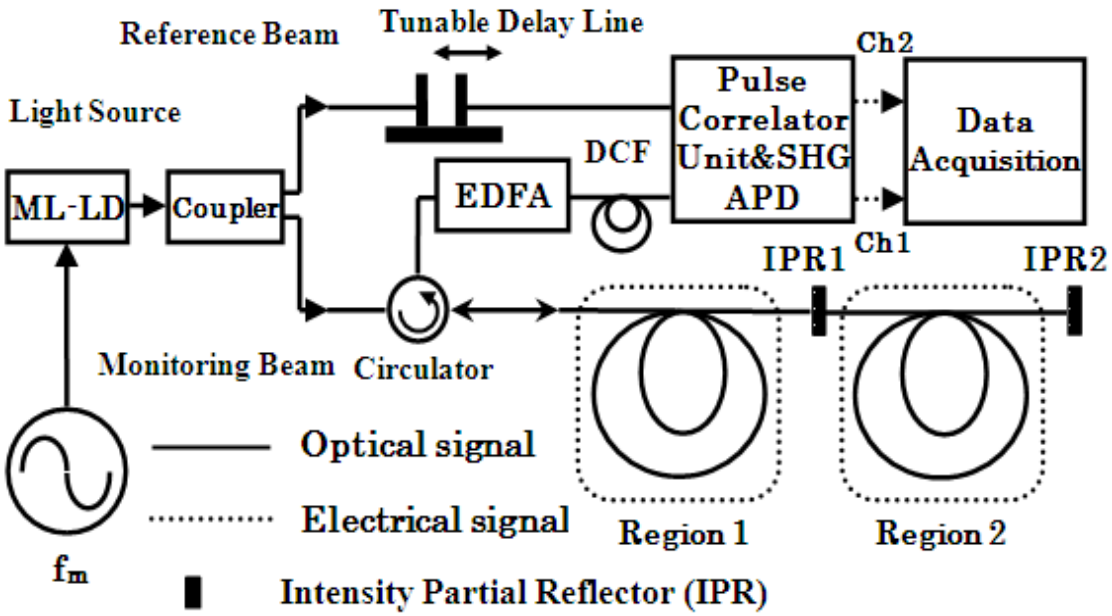


**Figure 4-7:** Experimental setup of quasi-distributed optical pulse correlation sensing system. ML-LD: Mode Locked – Laser Diode, DCF: Dispersion Compensated Fiber

The experimental setup is shown in Figure 4-7. The mode locked laser diode (ML-LD) optical pulse source with 1555 nm centre wavelength is modulated with a frequency of 20 GHz. The generated pulse width and repetition period are 8.7 ps and 50 ps, respectively. (The pulse width can be extended to 10 ps in the monitoring fiber.) In this study, two partial reflectors are used to connect multi-region monitoring fibers. Two 600 mm single mode fibers are connected, acting as sensing regions. Then the

correlation is detected by a data acquisition device whose output signal is uploaded to computer interfaced using Labview software. For well connected fiber ends, the air gap is smaller than the wavelength of the pulse source, in which case the typical reflectivity of each IPR is nearly equal to 1%.

In order to demonstrate the applicability of the system in real multi-region distributed deformation measurement, strain calibration experiments were first carried out by deforming a 600 mm long fiber segment of region 1 in 0.2 mm steps (333.3 με for a fiber of 600 mm length) and measuring the time shift in the peak point of differential correlation by scanning the time position of the optical delay line device in the reference propagation path. The linear relationship between the peak shift of correlation and strain over the range from 0 to 4300 με is plotted in Figure 4-8. It can be seen that the sensor has a linear response. The stability in the measurement is quite high; the fluctuation in the measurement is less than 1%. The calibration coefficient can be calculated as 238 με/ps. The time resolution of the system is less than 0.02 ps, and therefore the strain resolution of the system is less than 5 με.

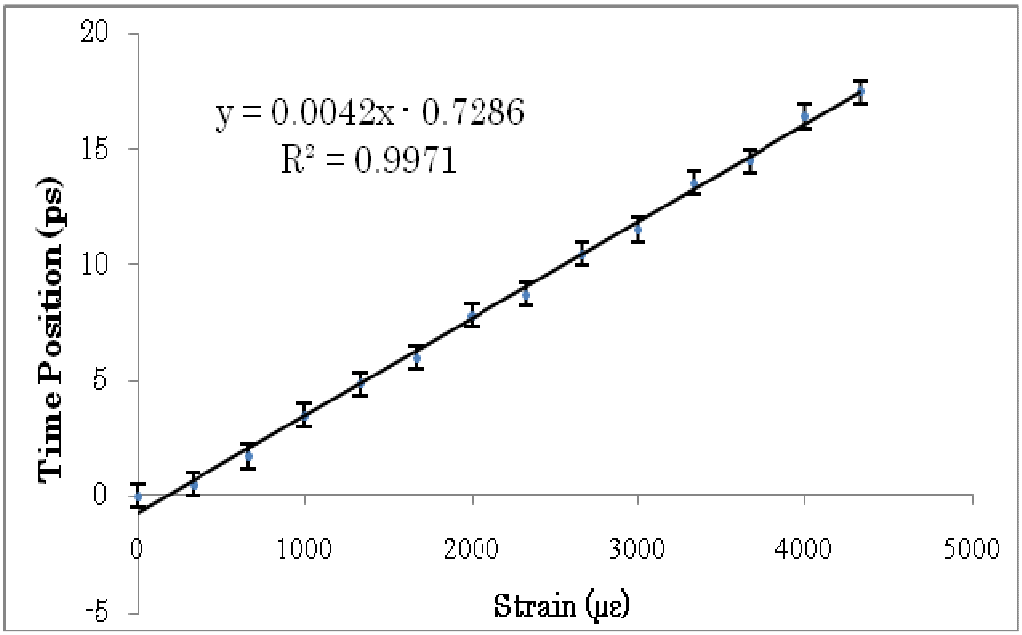


**Figure 4-8:** Strain calibration result for a fiber with a 600 mm gauge

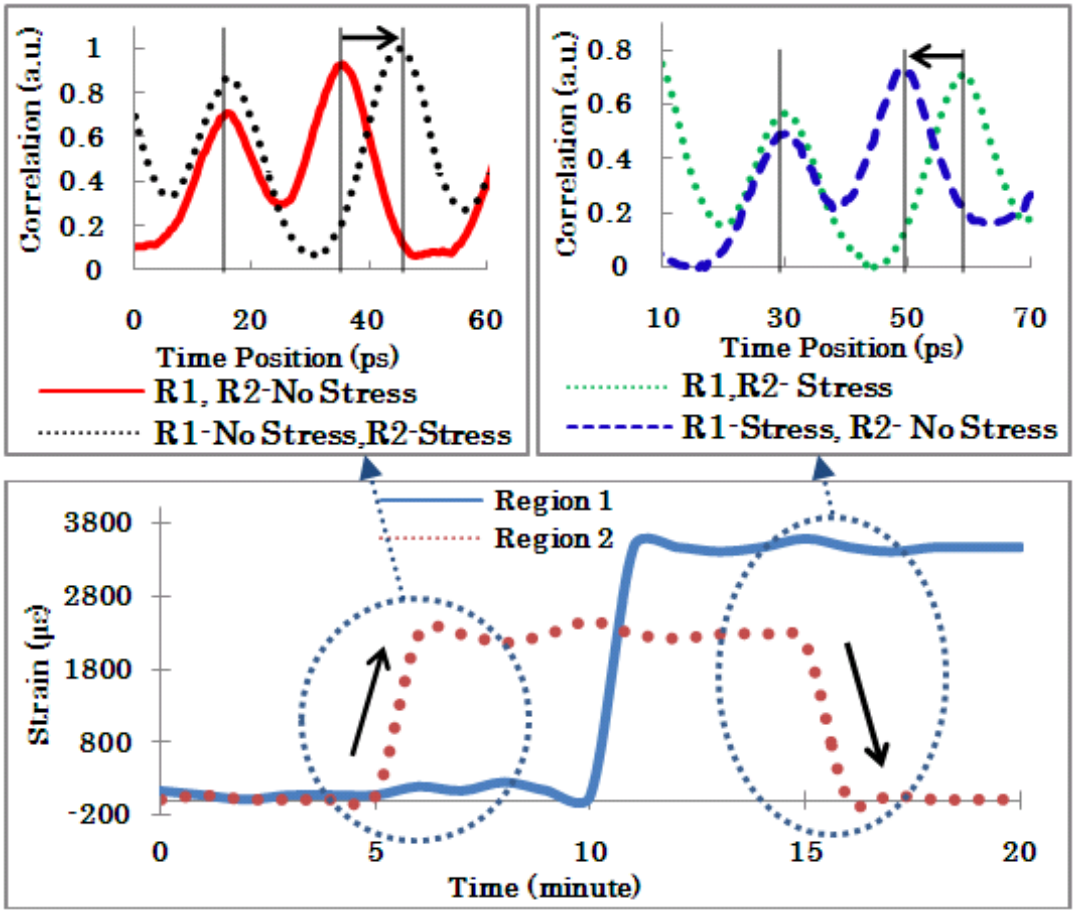


**Figure 4-9:** Results of the strain distribution measurement of Region 1(R1) and Region 2 (R2)

Then, multi-region strain experiments were carried out in sensing region 1 (R1) and region 2 (R2). For investigating the two regions' strain measuring, there were four cases for the stress of sensing regions, which included case 1: R1 and R2 without stress; case 2: R1 without stress and R2 with stress; case 3: R1 with stress and R2 with stress; and case 4: R1 with stress and R2 without stress. The sensing fibers of R1 and R2 were applied, maintained or released stress according to cases 1, 2, 3, and 4, orderly. Every case remained 5 minutes. The experiment results are shown in below part of Figure 4-9. The four different cases can be identified correctly. For the detail of experiment data, a comparison between case 1 and case 2 is shown in the upper left of Figure 4-9. R1 has no stress and R2 was applied stress from case 1 to case 2. Therefore, the peak point of the response from R1 remained in a constant time position, while the peak point of response from R1+ R2 shifted forward. The other comparison between case 3 and case

4 is also shown in upper right of Figure 4-9. R1 remained stressed and R2 was released from stress. The peak point of response from R1+R2 shifted backward and R1 showed no shifting. It can be seen that the multi-region sensor can measure the variations in the strain distribution without crosstalk.

## 4.4 Discussion

### 4.4.1 Time Resolution and Stability

The actual time resolution is not limited by SHG crystal length (pulse walk-off) because the combined double pulses have the same wavelength [3]. It is limited by the peak power and the dispersion of the monitoring pulse. The correlation time resolution of SHG is less than 0.02 ps [3-5]. Other more, in the time multiplexing with IPRs, the time resolution is also limited by the time resolution of optical delay line device. The optical delay line consists in beam collimators, a moving stage and a high accuracy step-motor controlled by computer from OZ Company, and is an ODL300 with 0.005 ps min step and 0 to 350 ps range. In other words, the time resolution of the optical delay line device is very high and reaches to 0.005ps. Therefore, the time resolution of both systems can reach to 0.02 ps.

The time drift stability is estimated from time jitter of the pulse source. In the two proposed systems, mode-locked pulse sources were used with a very low time jitter (less than 1 ps). The time stability also concern to the polarization of the pulses. In the wavelength multiplexing system with WSRs (FBGs), the time stability depended completely on the polarization fluctuation of the pulse, so that a polarization controller was used in this system [5]. In the time multiplexing system with IPRs, the time stability is isolated from the fluctuation of pulse polarization. Because this system only detects the time shifting of the peak point of the optical pulse, an standard single mode fiber was used, which has a much smaller polarization mode dispersion (PMD) and much lower differential group delay (DGD) [9]. Moreover, the differential correlation method was used in both the two sensing systems. This method can isolate the pulse power fluctuation completely and the pulse time jitter fluctuation partially. Furthermore, the timing stability concerns the stability of transmission path. The two systems

proposed are based on the pulse correlation measurement. The stability of the systems mainly depended on the differential transmission path between the reference pulse and the monitoring pulse. When the transmission fibers (except the fiber in the sensing region) are maintained in a temperature and strain stable environment, the sensing system can maintain stability for a very long time. For these reasons, the timing stability of both systems is less than 1 ps.

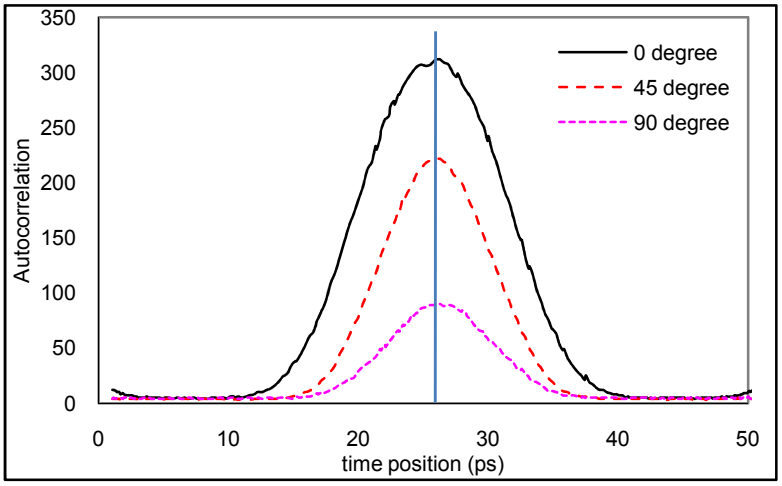


(a) Single mode fibre

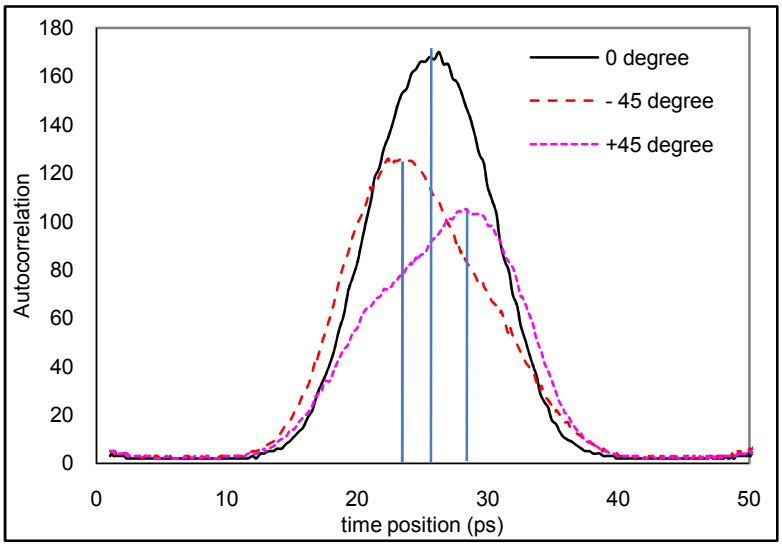


(b) Panda fibre

**Figure 4-10:** Comparison of polarization fluctuation of the system using single mode fibre and panda fibre

As far as the detail of polarization fluctuation, in the previous correlation sensing system, a Faraday rotator mirror (FRM) was used to suppress the polarization

fluctuation dependences of the correlation signals in the monitoring fibre [4]. However, the FRM is expensive and cannot be used to connect the cascadable multi-region fibers in current strain sensing systems. In order to investigate the polarization influence using single mode fibre and panda fibre, a fibre polarization controller was inserted in front of the monitoring fibre and after the circulator in the setup shown in Figure 4-7. When using the single fibre, the polarization controller was tuned and polarization perturbation was added to the correlation signals. There was no time shifting of the peak point of the correlation signals shown in Figure 4-10 (a). This means that, using the single mode fibre, it is possible to isolate the polarization influence in this system because it only detects the time shifting of the peak point of the optical pulse, and standard single mode fibre has a much smaller polarization mode dispersion (PMD) and much lower differential group delay (DGD) [11].

When we used the panda fiber (polarization maintenance fibre) as the monitoring fibre, the corresponding experimental results are shown in Figure 5-10 (b). We found that the peak point of the correlation signals moved because the polarization direction of pulse was not parallel to the fast or slow axis of the panda fibre and autocorrelation of the pulse occurred in the panda fibre [7]. If the polarization direction of pulse is adjusted to be parallel to the fast or slow axis of the panda fibre, this system can also isolate the polarization influence. However, panda fibre is more expensive than single mode fibre.

### 4.4.2 Estimation of the Number of Cascadable Regions

For the wavelength multiplexing system with WSRs (FBGs), the maximum number of cascadable sensing regions mainly depends on the number of wavelengths in the pulse source. The key point is to use a multi wavelength mode-locked pulse source. In this experiment, a tunable wavelength mode-locked fiber laser source was used. If the pulse power can be amplified enough, the maximum number of sensing regions can be very high.

For the time multiplexing system with IPRs, the number of cascadable regions is limited by the combination of the repetition frequency of the pulse source, the width of the pulse source and the detection sensitivity limit of the back reflected optical signal. Then, the maximum number of cascadable regions can be calculated by separating the

several different cases as follows:

*Case 1*. The number of cascadable regions depends on the repetition period of the optical pulse and inversion of pulse width as shown in figure 4-11. When we use a 100 MHz repetition (10 ns period, 2 ps pulse width) typical mode locked fibre laser (ML-FL) pulse source instead of our 20 GHz repetition ML-LD (50 ps period, 10 ps pulse width) pulse source, the number of cascadable regions can be calculated to $\frac{T_m}{d} = 5000$ (where $T_m$ is the repetition period, 10ns, and *d* is the pulse width, 2 ps) as shown in the table 1. In that case, the max number of cascadable regions is potentially 5000 when we use 100MHz ML-FL. However, the large delay time position control is required using combinations of fiber delay line and tunable optical delay component.

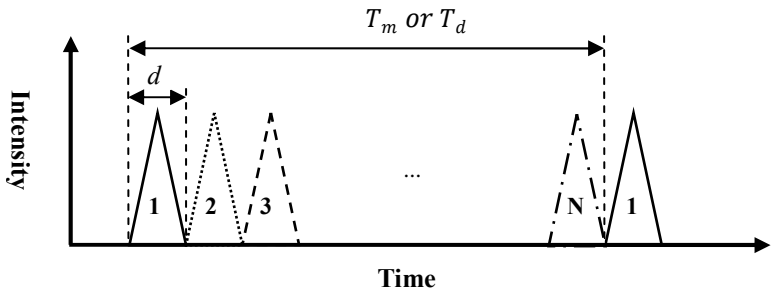


**Figure 4-11:** Schematic of the maximum number of cascadable regions using optical pulse source

*Case 2.* The number of cascadable regions also depends on the time position controllable range of the optical delay line device. If the range of the optical delay line device and the width of the optical pulse are $T_d$ and *d,* respectively, the number of cascadable regions can also be calculated to $\frac{T_d}{d}$ similarly to case 1. For example, typical tunable delay value, $T_d$ =350ps and *d*=2ps, hence, the number *N*=350/2≈170 as Table 1 shown.

*Case 3.* The number of cascadable regions also depends on whether the reflected power $I_R(i)$ is more than $I_{min}$, the detection limit of the reflected back optical signal, as Equation (3) shows.

$$I_R(i) \geq I_{min},\ i=1, 2, \ldots, N. \tag{4-2}$$

In this experiment with 10 ps pulse width, our reflected back light detection system has a detection sensitivity limit power of 0.01 mW and S/N larger than 20 dB. It means that the $I_{min}$ is 0.01mW in this study. As Figure 4-12 shows, at each regional fiber's end surface, the optical pulse partly reflects and partly transmits due to the air gap in the connector. For well connected fibre ends, the air gap is smaller than the wavelength of the pulse source, in which case the typical reflectivity $R$ is nearly equal to 1%. The transmission coefficient $T$ can be calculated as $T$ = 0.89, and the typical fiber optic connection insertion losses (except reflective losses) coefficient $\beta$ can be calculated as $\beta$ = 0.9 [12]. The insertion losses coefficients of the circulator are $\alpha_1 \approx 0.84$ from port A to port B and $\alpha_2 \approx 0.85$ from port B to port C. Therefore, the received optical pulse reflected from the partial reflector i, $I_R(i)$, can be given by

$$I_R(i) = I_0 \alpha_1 \alpha_2 R T^{2(i-1)} \beta^{2(i-1)},\ i=1, 2, \ldots, N \tag{4-3}$$

where $I_0$ is the input power to the circulator. Then, the normalized optical signal power vs. the fiber optic sensor number $i$ is plotted in Figure 5-13.

When we use the 20GHz ML-LD pulse source, the input power is 10.7 mW in this study. According to Equations (4-3) and (4-4) and taking account of the above data, the number of cascadable regions can be calculated as $N$ = 6. When we use the ML-FL, the input power can reach to 1W because of the extremely sharp shape of output pulse. In that case, the sensing region numbers can be upgraded to 600 as Table 1 shown.

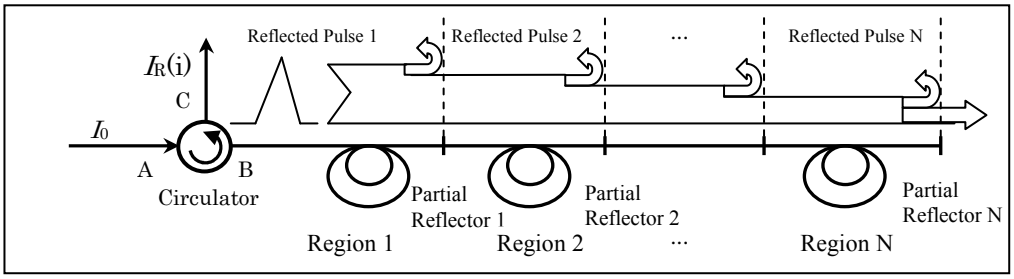


**Figure 4-12:** Schematic of power fluxes of transmissive and reflective optical pulse in the cascadable fibre sensors

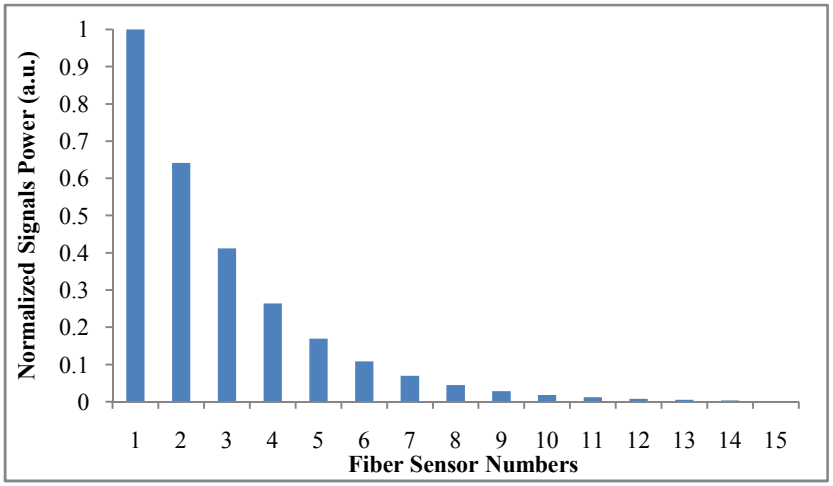


**Figure 4-13:** Normalized optical signal power vs. Fibre-optic sensor number

**Table 4-1:** The number of cascadable regions limited by different cases (with 1% reflectivity)

| | | | |
|---|---|---|---|
| **Conditions** | Light sources | 20GHz ML-LD | 100MHz ML-FL |
| | Pulse width $d$ | 10ps | 2ps |
| | Period of Pulse $T_m$ | 50ps | 10ns |
| | Range of optical delay line $T_d$ | 350ps | 350ps |
| | Input Power $I_0$ | 10.7mW | 1w |
| | Detection limit $I_{min}$ | 10μW | 10μW |
| **Number of cascadable Sensing Regions** | **Number of Case 1** | **5** | **5000** |
| | **Number of Case 2** | **35** | **170** |
| | **Number of Case 3** | **6** | **600** |
| | **Minimum Number** | **5** | **170** |
| | **Dynamic measurable time range of each region** | **10ps** | **2ps** |

It is very important to mention that the number of cascadable regions is estimated to 5 depending on the minimum value of the number of sensing regions in the above three cases as shown in table 4-1 when we used the 20GHz ML-LD. And the number of

sensing regions can be upgraded to 170 when we used 100MHz ML-FL. The dynamic measurable time range of each region is equal to the width of pulse source.

"To obtain a greater maximum number of cascadable regions, one approach is to increase the detection limit of this sensing system. Additional improvement is usage of different designed reflectivity to control the power of each reflected signal equal to the detection limit ($I_R(i) = I_{min}$, i = 1, 2, ... , N). Moreover, to decrease the pulse width by using a pulse compression technique and to increase the pulse peak power, the number of sensing regions can be easily be upgraded. To correctly operate the sensing system, the dynamic delay range of the optical delay line device should be longer than the pulse repetition period. And to allow the system requirement of each user, repetitions rate flexible pulse source is desirable key components.

### 4.4.3 Comparison

Using the region separation and identification techniques, these sensing systems can successfully achieve the multiple region distributed strain sensing. Compared with other fiber-optic sensors, such as FBG sensors, the region separation pulse correlation sensing systems have a number of distinguishing advantages. (1) They can give hybrid intelligent sensing combination of the distributed and point sensors for WSRs. (2) They can use a cascadable standard single mode fiber as the sensing gauge for WSRs. (3) They can supply real time measurement, high resolution and high speed measurement. (4) The position resolution is not so high, but wide region monitoring does not require very high spatial resolution, thus they can apply in a very wide region infrastructure monitoring. One of the most important applications of these sensors that have been demonstrated is the so called fiber optic smart structure health monitoring, where multiplexed optical fiber sensors are embedded into the structure to monitor its strain distribution.

In order to see the characteristics of region separated pulse correlation sensors, a comparison between the two region separation technologies would be as follows: The WSRs have the advantages of high resolution and high speed measurement, making it ideal for short distance and high speed measurement in fiber optic for smart structures, such as an intelligent building. Meanwhile, the IPRs have the advantages of low cost,

large sensing regions and low speed measurement speed, making it ideal for long distance, medium precision measurement situations, such as large build, long oil/gas pipeline, and power supply cable/line. However, temperature compensation of the strain error caused by thermal fluctuation is essential for practical applications.

In order to see the significance of region separated pulse correlation sensors, a comparison between the two region separation technologies is given in table 1. It can be seen that the WSRs has the advantages of high resolution and high speed measurement, making it ideal for short distance, high speed measurement fibre-optic smart structures, such as smart building. Moreover, the IPRs has the advantages of low cost, large sensing regions and low speed measurement speed, making it ideal for long distance, medium precision measurement situations, such as large build, long oil/gas pipeline, and power supply cable/line. However, temperature compensation of the strain error caused by thermal fluctuation is essential for practical applications.

Table 4-2 the comparison between of two regions separation techniques of WSRs and IPRs

| | WSRs | IPRs |
|---|---|---|
| Quasi-real-time | yes | yes |
| Linearity | yes | yes |
| Dynamic range to strain resolution | high | high |
| Sensor gauge length | long | long |
| Mechanical Control | no | yes |
| Measurement speed | high | medium |
| Polarization independence | no | yes |
| Multiplexed numbers | high[a] | high[b] |
| Potential cost | high | medium |
| Tele-monitoring | yes | yes |
| Mass production | yes | yes |

[a] dependence on the number of wavelength of optical pulse source [5].

[b] dependence on the width and repetition of optical pulse source [4].

## 5.Summary

We successfully proposed and demonstrated the optical pulse correlation sensing system for multiple region distributed fiber strain measurement with two kinds of region separation techniques, WSRs and IPRs. Using these regions separation techniques, the sensor measures the correlations between the reference pulse and the monitoring pulse from cascadable selected sensing regions. The system uses inline-multiple monitoring fibers connected by FBG or air gap for cascadable multi-region measurement. Then, using wavelength scanning with WSRs (FBG) or time position scanning with IPRs (air gap), the system can successfully detect the length change of multiple regional monitoring fibers for strain measurement. With WSRs, the system can be used for short distance, high precision and high speed for distributed strain measurement. With IPRs, the system can be used for long distance, large sensing regions and low speed for distributed strain measurement. This novel sensing system with WSRs and IPRs can select the regions and know the distributed strain information in any different sensing regions.

We have developed a regional selectable fibre-optic sensing system based on monitoring the length fluctuation of optic fibers by optical pulse correlation measurement. The multiple regional sensing fibers are cascadable and are connected by partial reflectors. The measurable regions are easily upgraded by a scanning of time position method. The results of strain experiments confirmed their linear response. These multiplex regions sensing techniques were experimentally operated within a resolution of less than 5 με and over 4300 με for sensing a region of 600 mm in length. A high number of sensing regions of in-line fibers can be exploited by the wide period, narrow width, and high intensity of the pulse source and the high sensitivity of the optical signal detecting system.

## Reference


[1] Yun-Jiang Rao: “In-fibre Bragg Grating Sensors”, Meas. Sci. Technol., Vol.17, pp. 355-375 (1997).

[2] L. Thevenaz: “Review and progress on distributed fiber sensing”, OFS-18 Conf. (Cancún, Mexico) paper Thc1 (2006).

[3] K. Uchiyama, K. Nonaka, and H. Takara: “Subpicosecond timing control using optical double-pulse correlation measurement”, IEEE Photon. Technol. Lett., Vol.16, No.2 pp. 626 -628 (2004).

[4] H. B. Song, T. Suzuki, M. Sako, and K. Nonaka: “High time resolution fiber optic sensing system based on correlation and differential technique”, Meas. Sci. Technol., Vol.17, pp. 631-634 (2006).

[5] H. B. Song, T. Suzuki, T. Fujimura, K. Nonaka, T. Shioda, and T. Kurokawa: “Polarization fluctuation suppression and sensitivity enhancement of an optical correlation sensing system”, Meas. Sci. Technol., Vol.18, pp. 3230-3234 (2007).

[6] X. J. Xu and K. Nonaka: “High-sensitivity fiber-optic temperature sensing system based on optical pulse correlation and time-division multiplexer technique”, Jpn. J. Appl. Phys., Vol. 48, pp. 102403-8 (2009).

[7] A. Bueno, K. Nonaka, and S. Sales: “Hybrid interrogation system for distributed fiber strain sensors and point temperature sensors based on pulse correlation and FBGs”, IEEE Photon. Technol. Lett., Vol. 21, No 22, pp. 1671-1673 (2009).

[8] X. J. Xu and K. Nonaka: “Regional selectable distributed sensor based on reflected optical pulse correlation measurement”, 20th International Conference on Optical Fibre Sensors, Edited by Jones, Julian D. C., Proceedings of the SPIE, Vol. 7503, pp. 75036J-75036J-4 (2009).

[9] X. J. Xu and K. Nonaka: “A regional selectable distributed fiber-optic sensing system based on pulse correlation and partial reflectors”, Meas. Sci. Technol., vol. 21, p. 094018, 2010.

[10] X. J. Xu, A. Bueno, K. Nonaka and S. Sales: “Fiber Strain Measurement for Wide Region Quasidistributed Sensing by Optical Correlation Sensor with Region Separation”, Journal of Sensors, vol. 2010, ID 839803, 2010.

[11] T. Luo, C. Yu, L. S. Yan, S. Kumar, Z. Pan and A. E. Willner: “Simple autocorrelation technique based on degree-of-polarization measurement”, IEEE Photonics Technol. Lett., vol. 18, p. 1606, 2006.

**[12]** L. B. Yuan, J. Yang: “Multiplexed Mach-Zehnder and Fizeau tandem white light interferometric fiber optic strain/temperature sensing system”, Sensors and Actuators A, Vol. 105, pp. 40-46 (2003).

# Chapter 5 Reliable Long-Distance Remote Fiber Optic Sensing System Based on Pulse Correlation and Partial Reflector

## 5.1 Introduction

A remote sensor system is a continuous, long-distance and all-weather sensing system which provides monitoring of activity in selected areas. The system consists of monitoring equipment, leading line, and sensors [1] as figure 5-1 shown. Sensors are placed adjacent to the desired sensing areas. System components are emplaced at selected points on the sensing area to provide an integrated sensor network.

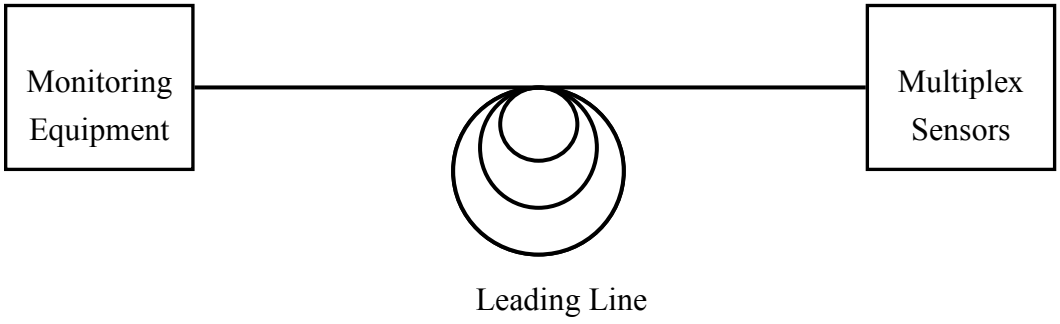


**Figure 5-1:** Remote sensor systems schematic

For long-distance remote fiber optic sensing system, optical time domain reflectometry (OTDR) is a well-know method for the diagnostics and measurement of fiber optic systems. Many techniques have been reported for enlarging the dynamic range of OTDRs and improving their spatial resolution, such as Brillouin OTDR (OTDR) [2], Coherence OTDR (COTDR) [3], Polarization OTDR (POTDR) [4], and Tunable OTDR (TOTDR) [5] and so on. These OTDR systems have well-distributed continuity measurements, but also slow measurement scanning cycles and low time resolution due to the optical pulse width which lies in several ns. It is insufficient.

As previous chapter's discussion, we already knew that the simple, low cost and real-time optical pulse correlation sensors have high-sensitivity, wide-dynamic-range and multiplex sensing regions characteristics. Long distance remote sensing is requirement.

Therefore, I have proposed a novel pulse-correlation-based reflectometry that detects the reflection point by measuring the optical pulse correlation using the overlap of reference and reflected pulses. The pulse overlap produces second harmonic signal in proportion to the intensity correlation of two pulses without using complicated high-speed electrical components. This pulse-correlation-based reflectometry can detect the reflectometry pulse with high time resolution better than 0.02 ps and can achieve real-time 30 km long-distance remote sensing but only one sensing region. In addition, comparing to the classical OTDR, all the system components are simple and low-cost. Replacing the short pulse with fixed light phase from a 20 GHz mode locked laser diode (ML-LD) to a low-time-jitter flexible repetition pulse source gain switching laser diode (GS-LD); we have shown the feasibility of pulse correlation OTDR measurement with very high time resolution 0.02 ps. A multi-region fiber sensing system with 10 km remote distance with high resolution is achieved. It means 4 με strains or 0.1 °C environmental changes per 1 meter sensing fiber can detect with more than 17 of separated regions within 10 km tele-monitoring. Using the pulse feedback and moving average technology, the noise factors of this system are suppressed. In this chapter, in order to achieve long distance remote sensing based on pulse correlation measurement, in section 2, I will show the principle of long distance remote pulse-correlation-based reflectometry; in section 3, I will show the two experiment setups and results of single region and multi-regions sensing system; in section 4, I will discuss the maximum distance for remote sensing in theory; in section 5, I will give a summery for this chapter.

## 5.2 Principle of Remote Pulse-Correlation-Based Reflectometry

### 5.2.1 Single-Region Remote Pulse-Correlation-Based Sensing System

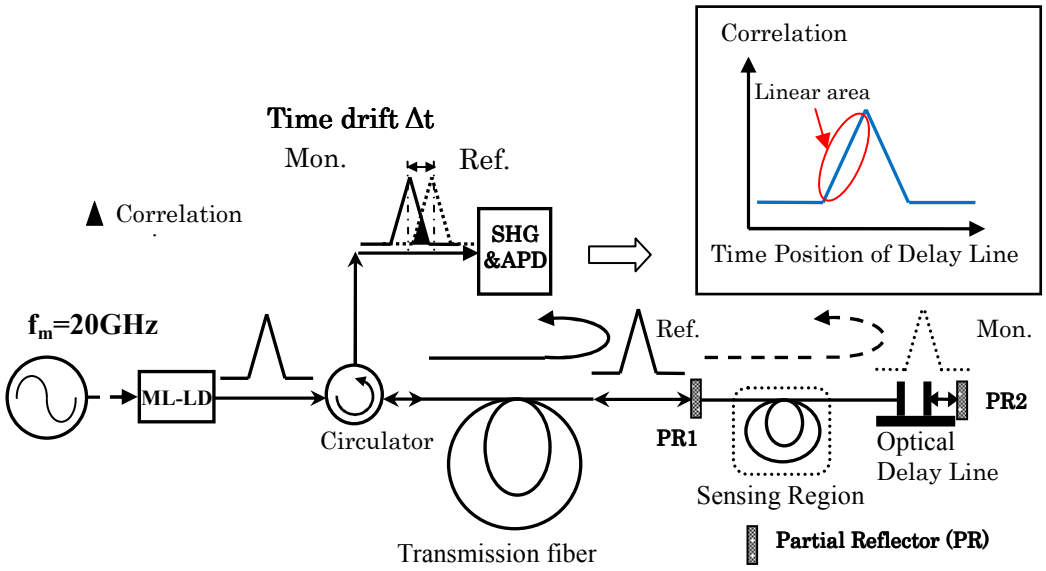


**Figure 5-2:** Scheme of remote pulse-correlation-based sensing system

The remote pulse-correlation-based sensing system is shown in Figure 5-2. A mode locked laser diode (ML-LD) modulated by a synchronized source with frequency $f_m$=20GHz produces a low-time-jitter phase-locked short optical pulse-train. The optical pulse-train is input into the transmission fiber through an optical circulator. Then, the pulse is split into a reference (Ref.) pulse and a monitoring (Mon.) pulse by partial reflector 1 (PR1) which is made by coating metal thin-film at the end of fiber. The reference pulse is reflected back to the transmission fiber again by the PR1. The monitoring pulse accesses sensing fibers and an optical delay line in sensing region, through the PR1. Then, the monitoring pulse is reflected back by partial reflectors 2 (PR2), which becomes a reflected monitoring pulse (Mon.). The reflected pulses access to the monitoring fibers again and then input to a SHG & APD unit. Thus, Ref. passes only through transmission fiber pulse while Mon. passes through both transmission fiber and sensing region. Using the SHG & APD unit to detect the correlation value between the reflected monitoring pulse Mon., and the reference pulse Ref., the

information on the strain or temperature changes in sensing region can be received. This is the principle of single-region remote pulse-correlation-based sensing system.

When controlling the optical delay line in front of PR2 to simulate the sensing fiber length changing, the correlation value between reference and monitoring pulse will be changed as shown in upper right of Figure 5-2. The output curve from optical pulse correlation unit is blue color in the Figure 5-2, and is similar with the shape of pulse source from ML-LD. For easily measurement, the linear area in the red ellipse is used to measure the sensing fiber length changed by strain or temperature change.

### 5.2.2 Multi-Regions Remote Pulse-Correlation-Based Sensing System

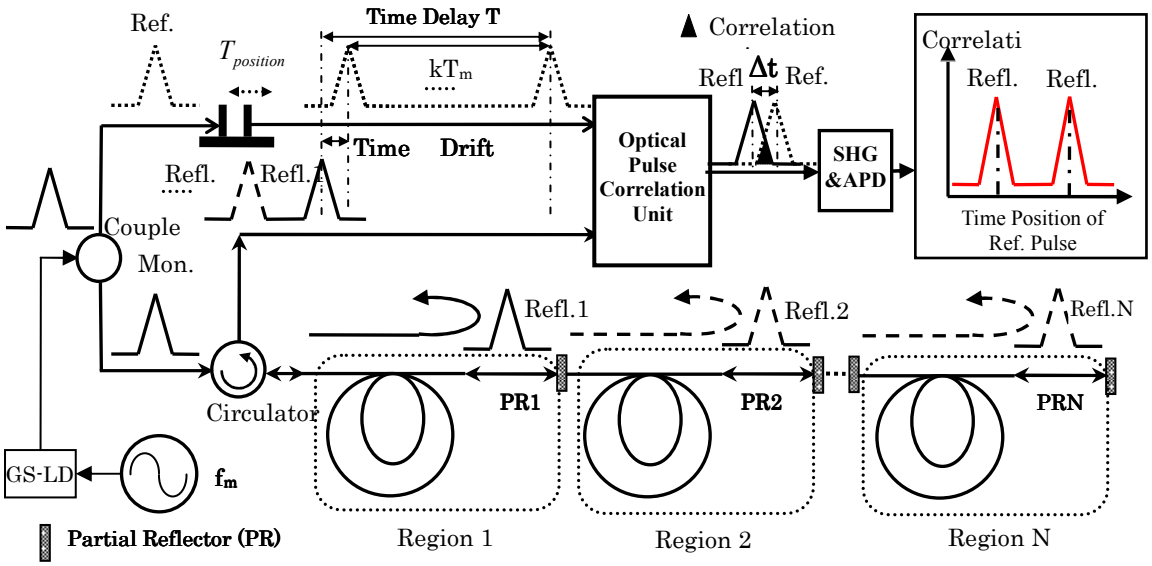


**Figure 5-3:** Scheme of multi-regions remote pulse-correlation-based sensing system

Single sensing region remote pulse-correlation-based sensing system already was showed in the previous paragraphs. However, for real application, the multiplex sensing regions are required. Therefore, a multi-regions remote pulse-correlation-based sensing system has developed by instead of the pulse source as follows.

The scheme of multi-regions remote pulse-correlation-based sensing system is shown in Figure 5-3. A repetition tunable GS-LD modulated by a synchronized source with frequency $f_m$ produces a low-time-jitter short optical pulse-train [6]. The optical pulse-train is split into a reference (Ref.) pulse and a monitoring (Mon.) pulse by a

coupler. The monitoring pulse accesses monitoring fibers in regions 1 and 2, through a circulator. Then, the monitoring pulse is reflected back by partial reflectors 1 and 2 (PR1 and PR2, are made with thin-file of metal, and are coated with the metal gold on the end of optical fiber by magnetron sputter method.), respectively, which becomes two regions' reflected pulses Refl.1 and Refl.2. The reflected pulses access to the monitoring fibers again and then input to an optical pulse correlation unit with the reference pulse in different ports. Thus, Refl.1 passes only through region 1 while Refl.2 passes through both region 1 and region 2. Using the optical pulse correlation unit to detect the time drifts between the reflected pulses Refl.1, Refl.2, and the reference pulse, the information on the strain changes in regions 1 and 2 can be received. This scheme can be easily upgraded to the region N.

There is a time position manipulation ΔT between the reflection and reference signals because of their different propagated paths ΔL .

$$\Delta T = \frac{n}{c}\Delta L \tag{5-1}$$

Where n is the refractive index, c is the velocity of light in a vacuum, and $\Delta L = 2\times(L_m - L_r)$ , where $L_m$ and $L_r$ indicate the reflection and reference signals respectively. When the strains of the monitoring fibers are changed, the propagated paths of the monitoring signal are changed due to the length wise expansion and contraction of the monitoring fiber.

Therefore, the differential propagation length ΔL between reflection and reference pulses is proportional to the strain or temperature change in the monitoring fiber. Because the optical pulse source is repetitional, the reflection pulse will be recombined with the adjacent reference pulse in the optical pulse correlation unit as shown in Fig. 5-3.

Therefore, the time drifts between the reflection pulses reflected by partial reflector 1, 2, ···, N (PR 1, PR 2, ···, PR N) and their adjacent reference pulses are given by

$$\Delta t_i = \frac{n}{c}\Delta L_i + T_{position} - k_i T_m \tag{5-2}$$

where subscript i = 1, 2,⋯, N, which indicate PR1, PR2, ⋯, PRN; $T_m$ is the period of modulated signal equal to $1/f_m$; $\Delta L_i (i = 1,2,\cdots,N)$ are the differential propagation lengths between the reflection pulses and the reference pulses; $k_i (i = 1,2,\cdots,N)$ are the constant integers standing for $\Delta t_i$ less than $T_m$; and $T_{position}$ is the time position of the optical delay line device. Equation (5-2) indicates that $\Delta L_i$ is proportional to $T_{position}$ when other parameters remain constant. Therefore, we can use a scanning of time position method to monitor the length change of different sensing regions.

## 5.3 Experimental Setups and Results

### 5.3.1 Single-Region Remote Pulse-Correlation-Based Sensing System

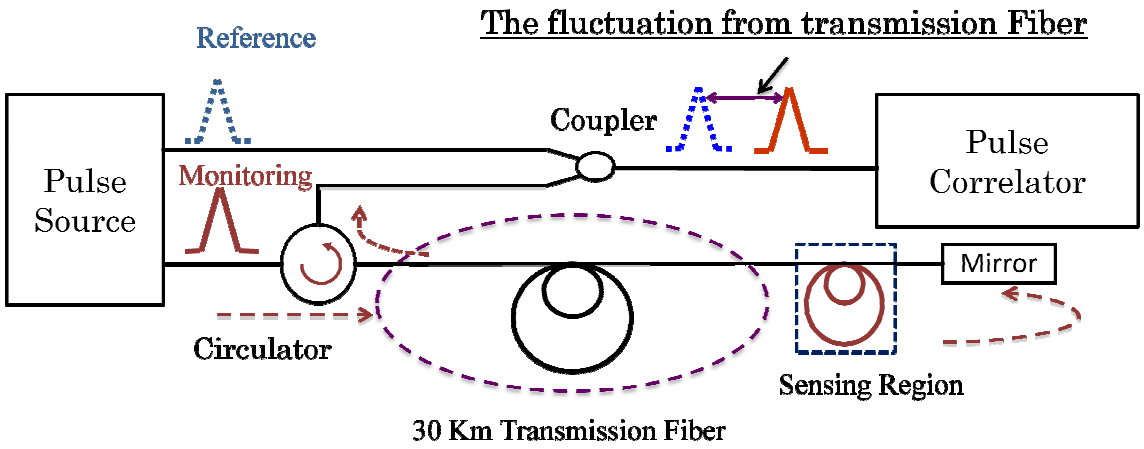


**Figure 5-4:** Long distance measurement in previous system

Optical pulse correlation sensor has high sensitivity, wide-dynamic-range and selectable-region characteristics as previous chapters shown, however, when employing the optical pulse correlation sensing system to measure long distance remote region, there are large noises during the propagation in the transmission fiber. When the pulse propagates in the transmission fiber, the fluctuation of transmission fiber length caused by environment changing will be added into the monitoring pulse fluctuation. That means noise is added into the sensing correlation value. If the transmission fiber is not so long, the noise is small and can be neglected. When the transmission fiber reaches to 30 km, the noise will become very large as show in Figure 5-4.

In order to investigate the noise of correlation sensor with the 30 Km long distance transmission fiber, noise experiments were set up. The optical time delay device was added in the sensing region and was used to simulate the strain change of sensing region. If the moving speed of delay line was very slow, the time of moving from 0 to 25 ps time position spent 5000 seconds. At that time, the output of optical pulse correlation senor was shown with solid line in Figure 5-5. There were large noises fluctuations from the environment change of the transmission fiber during the 5000 seconds. If the moving speed of delay line was very fast, the time of moving from 0 to 25 ps time position spent 50 second. At that time, the output was shown with dashes in Figure 5-5. There were few noise fluctuations; however, the shape of the dashes curve was greatly different from the normal output of original pulse correlation sensing system without transmission fiber. That means there were so large noise fluctuations from the long transmission fiber caused by its environment change.

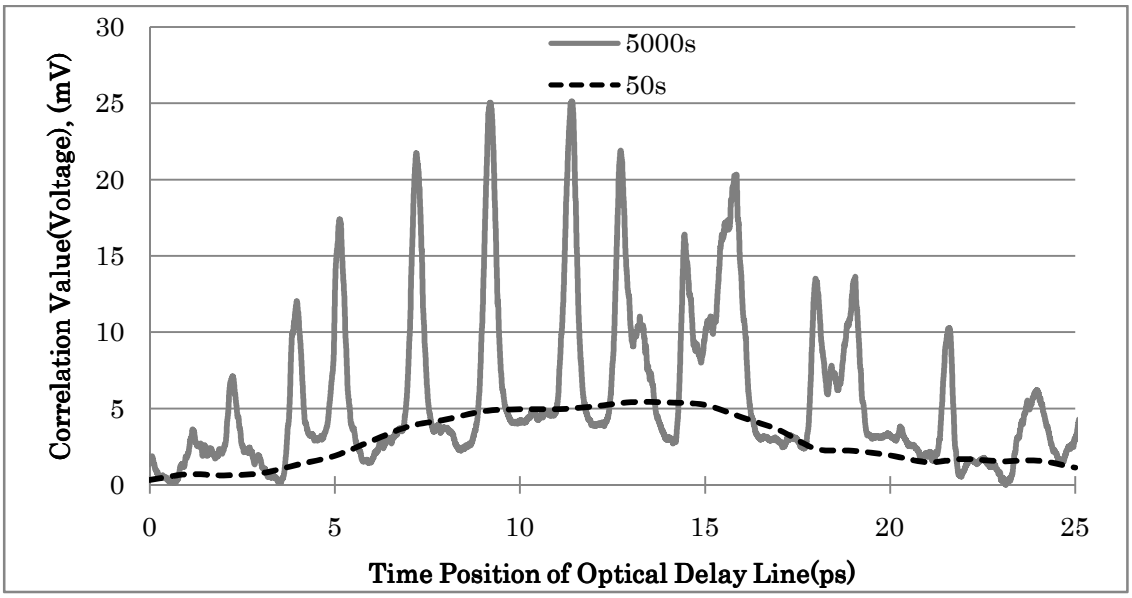


(a): Output data of optical pulse correlation sensor with 30 km transmission fiber

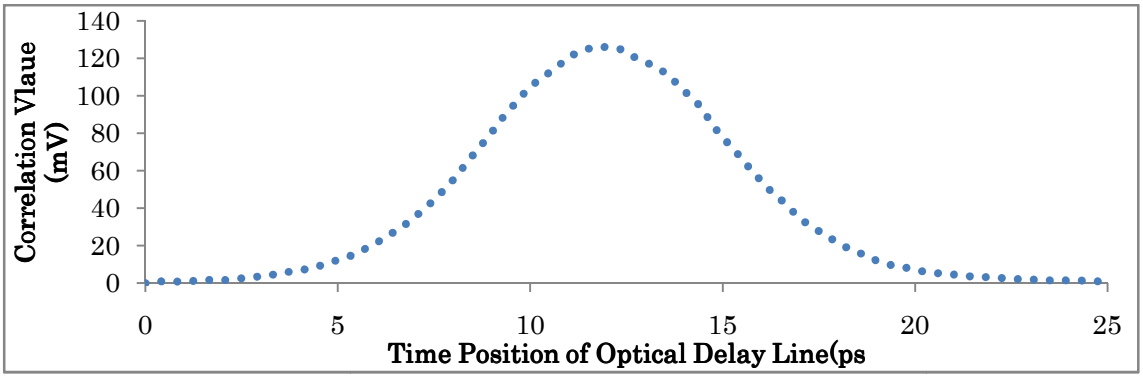


(b): Output data of optical pulse correlation sensor without transmission fiber

**Figure 5-5:** Output data of optical pulse correlation sensor with and without transmission fiber

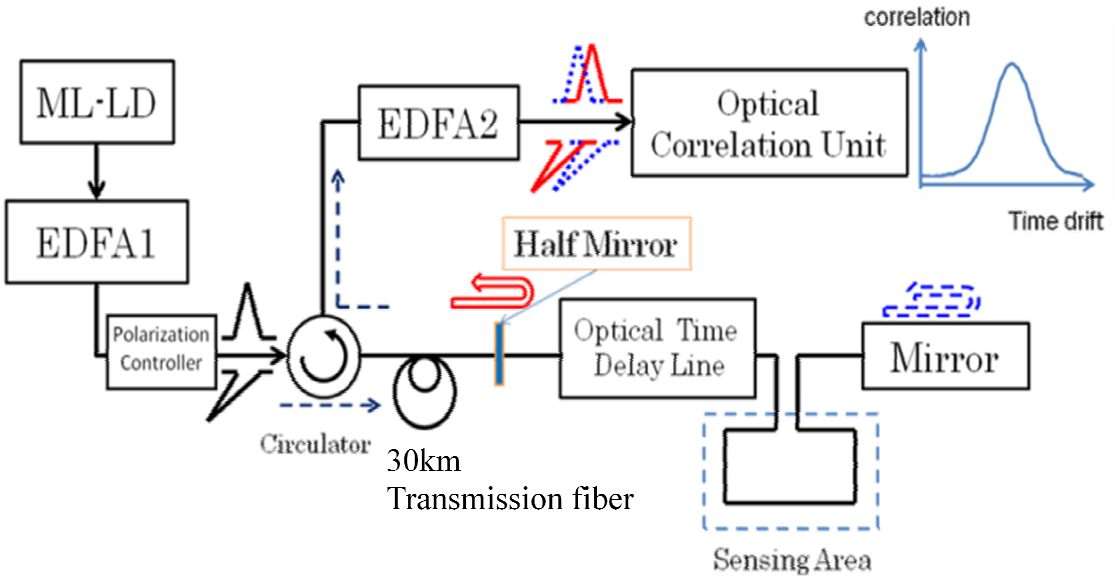


**Figure 5-6:** Experimental setup of single-region remote pulse-correlation-based sensing system with 30 km transmission fiber

For isolating the noise of transmission fiber, the single-region remote pulse-correlation-based sensing system setup was shown in Figure 5-6. ML-LD was modulated a frequency 20 GHz and produced pulse trains. The pulse train was amplified

by EDFA1, and was controlled by a polarization controller, through a circulator and 30 km transmission fiber, then was partially reflected by partial reflector (half mirror), and then input optical delay line and sensing area, finally reflected by mirror at the end of sensing area. Then the two reflected pulses were input the EDFA2 for amplifying. Thus, the optical correlation unit can detect the pulse correlation value.

Firstly, in order to investigate the noise of single-region remote correlation sensing system with the 30 Km long distance transmission fiber, noise experiments were set up. The optical time delay device was added in the sensing region and was used to simulate the strain change of sensing region. If the moving speed of delay line was very slow, the time of moving from 0 to 25 ps time position spent 5000 seconds. At that time, the output of optical pulse correlation senor was shown with solid line in Figure 5-7. There were small noises fluctuations from the environment change of the transmission fiber during the 5000 seconds. If the moving speed of delay line was very fast, the time of moving from 0 to 25 ps time position spent 50 second. At that time, the output was shown with dashes in Figure 5-7. There were also very smooth, and the shape of the dashes curve was greatly similar with the normal output of original pulse correlation sensing system. That means this system can isolate large fluctuations from the long transmission fiber caused by its environment change.

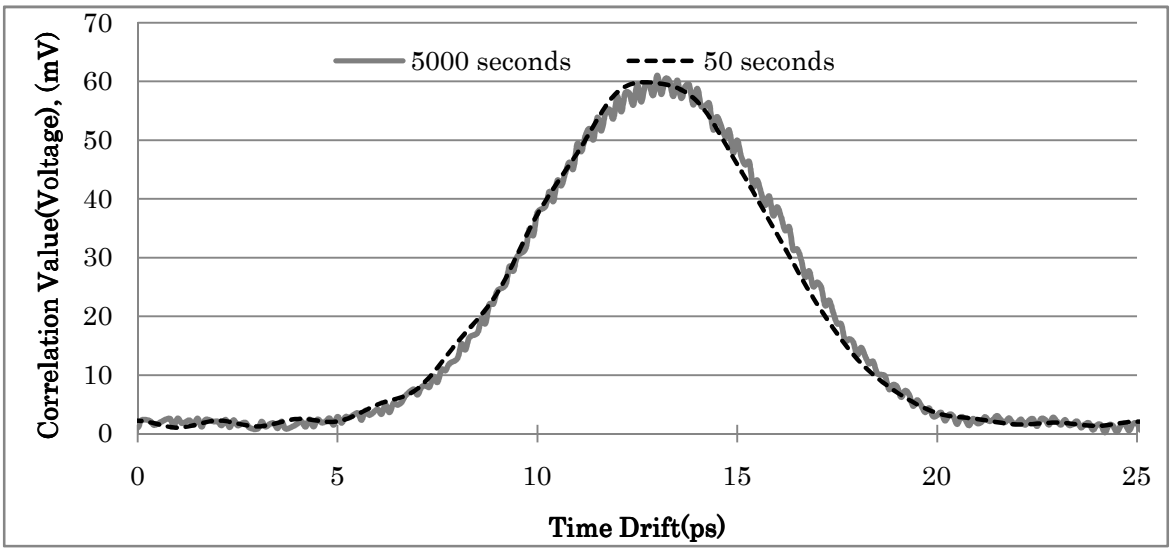


**Figure 5-7:** Experiment data of single-region remote sensor with 30 km transmission fiber

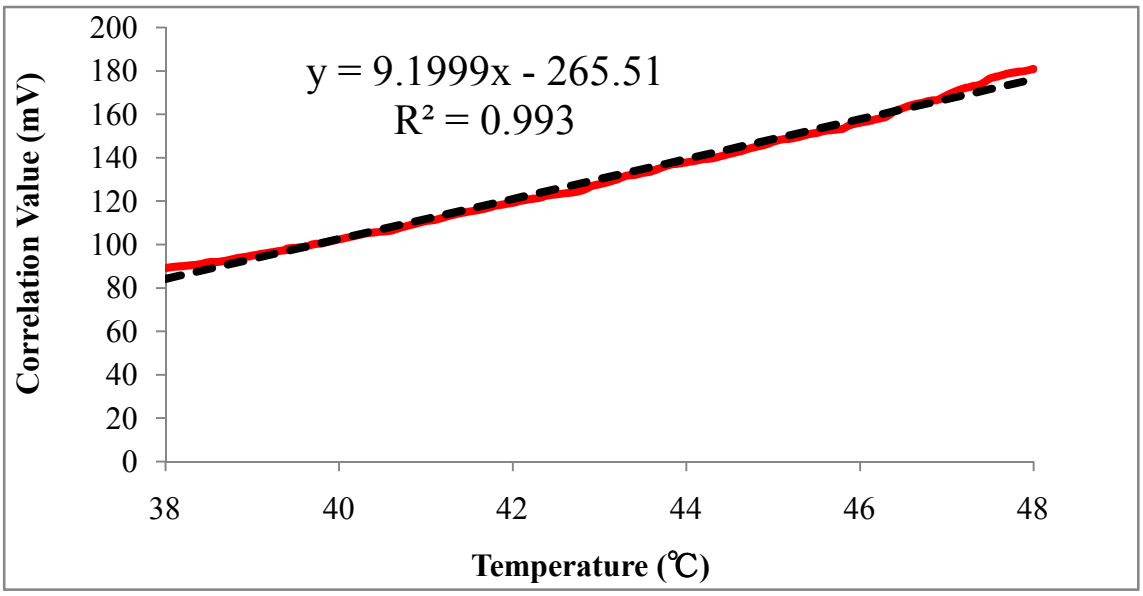


**Figure 5-8:** Temperature Experiment data of single-region remote sensor

Then, a temperature experiment was carried out by changing a 3 meter long sensing fiber temperature in the sensing region as Figure 5-6. Then changing the temperature of sensing fiber from 38 to 40 ℃ and measuring the correlation value were carried out. The linear relationship between correlation and temperature over the range from 38 to 48 ℃is plotted in Figure 5-8. It can be seen that the sensor has a linear response for temperature. The stability in the measurement was quite high; the fluctuation in the measurement was less than 1%. The calibration coefficient can be calculated as 0.11 ℃ /mV. Because the resolution of data acquisition is 1mV, the resolution of this system is 0.11 ℃.

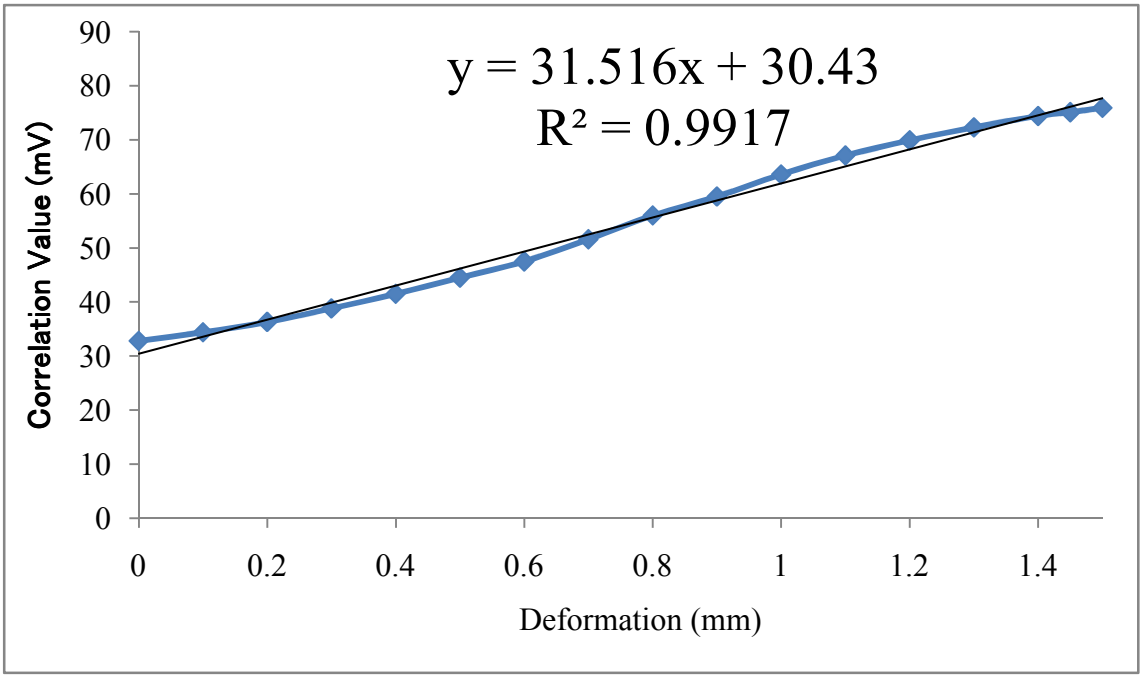


**Figure 5-9:** Deformation Experiment data of single-region remote sensor

Finally, a deformation experiment is carried out by deforming a 600 mm long sensing fiber for replacing the moving stages in the sensing area as shown Figure 5-6. Then changing the length of sensing fiber in 0.2 mm steps and measuring the correlation by scanning the data acquisition device. The linear relationship between the peak shift of correlation and deformation over the range from 0 to 1.5 mm is plotted in Figure 5-9. It can be seen that the sensor has a linear response. The stability in the measurement was quite high; the fluctuation in the measurement was less than 1%. The calibration coefficient can be calculated as 0.032 mm/mV. Because the resolution of data acquisition is 1mV, the deformation resolution of this system is 0.032 mm or 32 μm.

### 5.3.2 Multi-Regions Remote Pulse-Correlation-Based Sensing System

The experimental setup is shown in Figure 5-10. The GS-LD optical pulse source with 1555nm center wavelength was modulated a pulse generation of 2.08 GHz. The generated pulse width was about 40 ps with less than 1ps time jitter. The region 1 was 10 km single mode fiber; region 2 was a small moving stage. The two regions were

connected by partial reflector A and B. Then the electrical correlation value was detected and processed by DAC-card, the output signal of which was connected to a computer interfaced using Labview software. The optical time position control device in reference beam was ODL300 with 0.005ps min step and 0 to 350ps range. It was controlled by the computer through a serial port.

In order to demonstrate the applicability of high resolution of correlation OTDR, the experiments were carried out. The double region kept unchanged and with the help of scanning of time position method, the optical time position control device with 1ps step and 0 to 350 ps range were controlled to detect different measurement regions. As the special distance of A is 10000 m which is already known, it was easy to convert the horizontal axes of time position to distance. Thus the relationship of correlation vs. spatial distance was found shown in the solid line of Figure 5-11. The peak points of correlation value are marked for reflected point's measurement A and B. The A is at the 10000m point and B is at 10000.016m as shown in the solid line of Figure 5-11. Then moving the stage 2.6 mm from B to B', and scanning the time position of reference pulse again, the result was plotted in the dashes line of Figure 5-11. In Figure 5-11, the spatial distance from B to B' was also 2.6 mm. The experimental results show the possibility of high resolution of spatial measurement. The time resolution of the system was less than 1 ps during to the pulse source time jitter, and therefore the spatial resolution of the system was less than 0.2 mm. It should be noted that this OTDR can detect the real spatial distance of two reflected points when the distance between them is less than 500ps the period of reference pulse. Therefore, using flexible repetitional rate pulse source, the range for real spatial measurement is also flexible for any different application. Therefore, this multi-regions sensing system does not only detect the 10 km remote information of region 2, but also detect the 10 km transmission fiber information of region 1with out crosstalk.

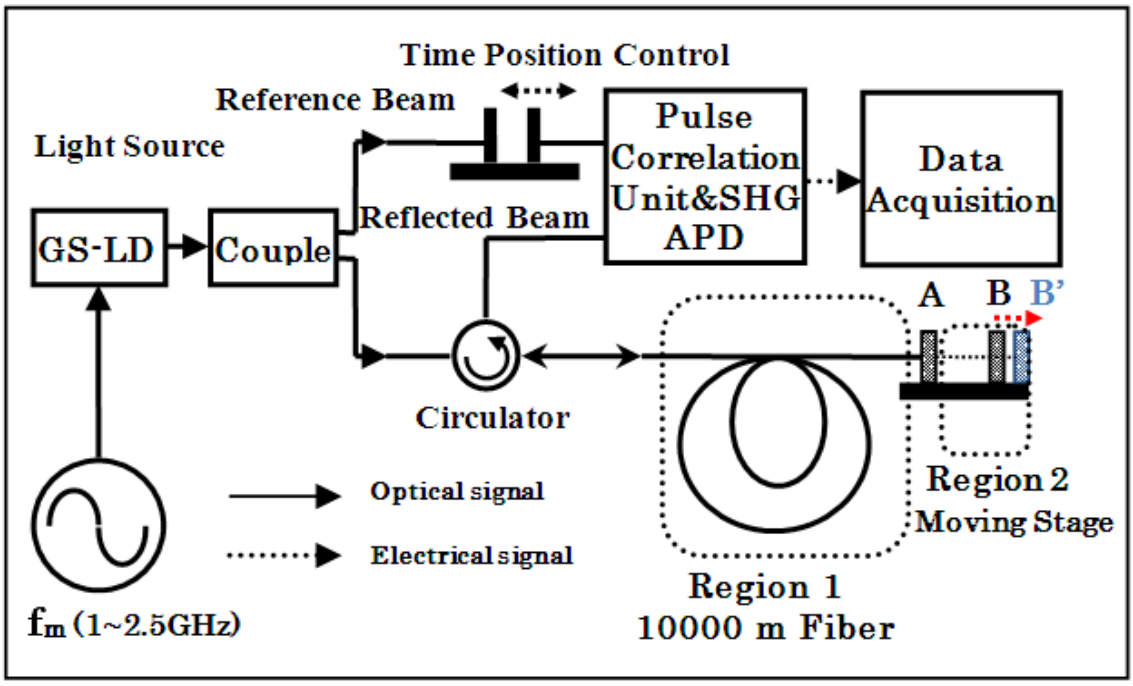


**Figure 5-10:** Experimental setup of multi-regions remote pulse-correlation-based sensing system with 10 km transmission fiber

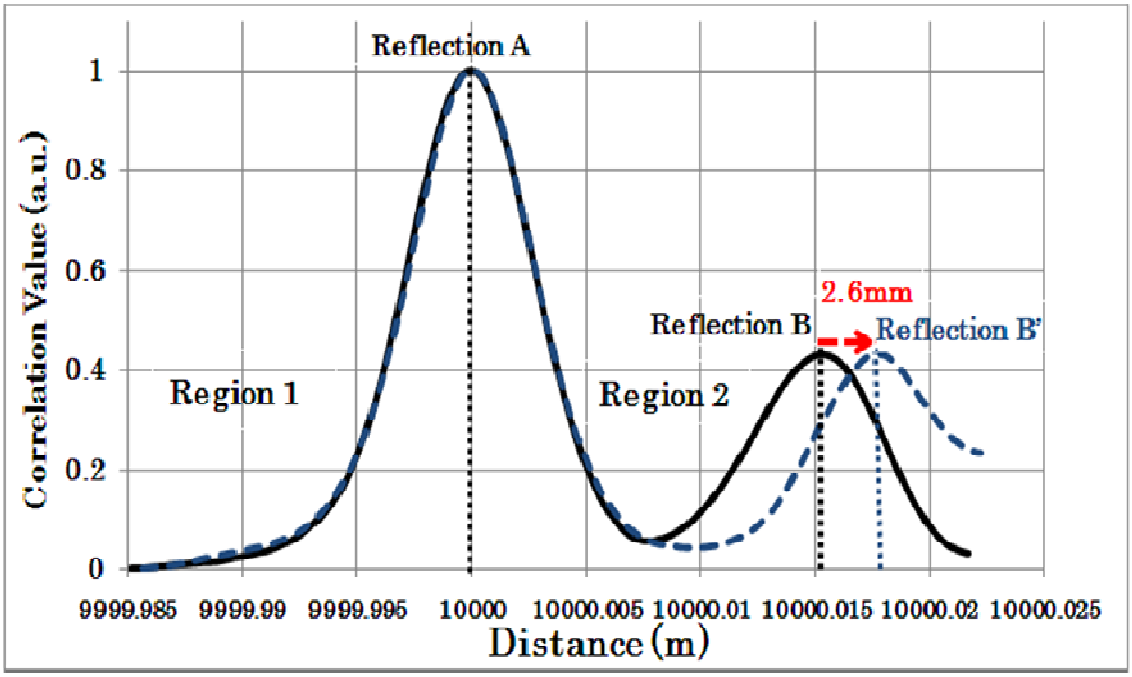


**Figure 5-11:** Two sensing regions experiment result of multi-regions remote pulse-correlation-based sensing system with 10 km remote distance

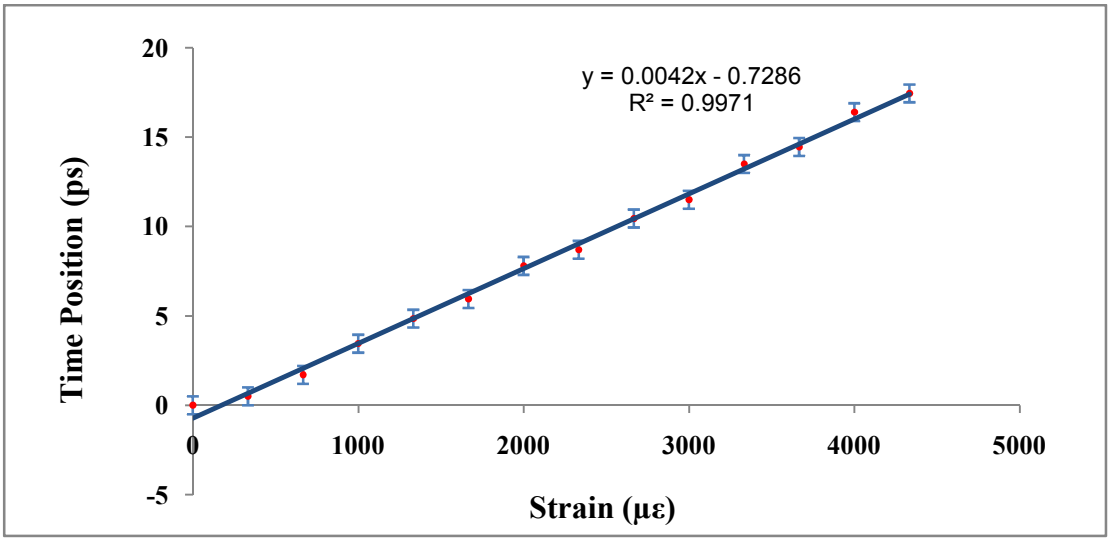


**Figure 5-12:** Strain experiment result of multi-regions remote pulse-correlation-based sensing system with 10 km transmission fiber

Because of the high spatial resolution, this system can be used to monitor the strain or temperature with 10km remote and multi-regions. Then, a strain experiment is carried out by deforming a 600 mm long sensing fiber for replacing the moving stages in the region 2. Then changing the length of sensing fiber in 0.2 mm steps (333.3 με for a fiber of 600 mm length) and measuring the time shift in the peak point of correlation by scanning the time position of the optical delay line device in the reference propagation path. The linear relationship between the peak shift of correlation and strain over the range from 0 to 4300 με is plotted in Figure 5-12. It can be seen that the sensor has a linear response. The stability in the measurement was quite high; the fluctuation in the measurement was less than 1%. The calibration coefficient can be calculated as 238 με/ps.

## 5.4 Discussion of Maximum Distance for Remote Sensing

For the long-distance remote fiber optic sensing system based on optical pulse correlation, the maximum distance of remote sensing mainly depends on the optical pulse signal propagation in the optical fiber.

According to the analysis of signal propagation in fibers from Ref [7-10], the basic optical pulse signal propagation equation inside a single-mode fiber is shown as

$$\frac{\partial A}{\partial z}+\beta_1\frac{\partial A}{\partial t}+\frac{i\beta_2}{2}\frac{\partial^2 A}{\partial t^2}-\frac{\beta_3}{6}\frac{\partial^3 A}{\partial t^3}=i\beta_{NL}A-\frac{\alpha}{2}A \tag{5-3}$$

Where, $z$ is the propagation distance along the fiber, $\beta_1$ is a dispersion parameter, which is inversely related to the group velocity $v_g$ of the pulse as $\beta_1=1/v_g$. $\beta_2$ and $\beta_3$ are known as the second- and third-order dispersion parameters and are responsible for pulse broadening in optical fibers. $\beta_2$ is related to the dispersion parameter D as

$$D=\frac{d}{d\lambda}\left(\frac{1}{v_g}\right)=-\frac{2\pi c}{\lambda^2}\beta_2 \tag{5-4}$$

This parameter is expressed in unit of ps/(km-nm). It varies with wavelength for the fiber and vanishes at a wavelength known as the zero-dispersion wavelength and denoted as $\lambda_{ZD}$. The parameter $\beta_3$ is dispersion slope $S$ as $S=(2\pi c/\lambda^2)^2\beta_3$. $\beta_{NL}$ is the nonlinear coefficient, which can be written as

$$\beta_{NL}=\gamma|A|^2,\gamma=\frac{2\pi n_2}{\lambda_0 A_{eff}} \tag{5-5}$$

the $\beta_1$ term simply corresponds to a constant delay experienced by the optical signal as it propagates through the fiber. Since this delay does not affect the signal quality in any way, it is useful to work in a reference frame moving with the signal. This can be accomplished by introducing the new variables *t'* and *z'* as

$$t'=t-\beta_1 z, z'=z \tag{5-6}$$

And rewriting Eq. (5-3) in terms of them as

$$\frac{\partial A}{\partial z'}+\frac{i\beta_2}{2}\frac{\partial^2 A}{\partial t'^2}-\frac{\beta_3}{6}\frac{\partial^3 A}{\partial t'^3}=i\gamma|A|^2A-\frac{\alpha}{2}A \tag{5-7}$$

Also the third-order dispersive effects are negligible in practice for single-mode fiber as long as $\beta_2$ is not too close to zero, or pulses are not short than 5 ps. Setting $\beta_3=0$, Eq.(5-7) reduces to

$$\frac{\partial A}{\partial z}+\frac{i\beta_2}{2}\frac{\partial^2 A}{\partial t^2}=i\gamma|A|^2A-\frac{\alpha}{2}A \tag{5-8}$$

This equation is known as the nonlinear Schrodinger (NLS) equation. The three parameters $\alpha$, $\beta_2$ and $\gamma$ refer to loss, dispersion and nonlinear effects, respectively. The next sections will discuss the effects of loss, dispersion and nonlinear, respectively.

### 5.4.1 Loss Effect

According to Ref. [7] , the loss parameter $\alpha$ reduces not only the signal power but it also weakens the strength of nonlinear effect. The nonlinear effect will be discussed in later section, this section will only discuss the loss effect of signal power. The power loss equation is written as

$$P(z)=P_0\exp(-\alpha z) \tag{5-9}$$

Where, $P_0$ is the injection power. As far as the power loss is concerned in the optical pulse correlation sensor, the remote sensing distance will be limited due to the conversion efficiency of SHG crystal which refers to the input signal power of SHG crystal as shown in Fig. 5-13. The insertion losses of related components are shown in Table 5-1. The minimum power at point G should be larger than 1 mW (0 dBm). The EDFA2 can amplify the signal more than 0.004 mW (-24 dBm) with 25 dB gain and over than 10 dB S/N. In the other word, the minimum power at point F should be larger than -24 dBm. Because the length of transmission fiber is much larger than the sensing fiber, the power loss of sensing fiber can be neglected.

In theory, when the reflected powers from PR1 and PR2 are same, the conversion efficiency of SHG crystal has maximum value (PR2 maximally reflects the optical

signal with $R_2 = 90\%$ reflection and $\beta_1 = 0.46dB$ insertion loss and the PR1 partially reflects the optical signal with $R_1$ reflection $\beta_2 = 0.46dB$ insertion loss). By using the equation 5-10 as follows,

$$R_1 = R_2(1-R_1)^2\beta_1^2\beta_2 \quad (5\text{-}10),$$

the reflection value $R_1$ can be calculated as 31.1%.

Therefore, if the transmission loss of fiber is taken as 0.2 dB/km and the length is *l*, the total loss from point A to F is

$$L_{total} = L_{A-B} + L_{B-C} + 2\times L_{trans.fiber} + L_{Sensing} + L_{C-F} \quad (5\text{-}11)$$

where, $L_{trans.fiber} = 0.2l(dB)$, $L_{Sensing}$ is the loss from the sensing fiber and PR1 and PR2. Because the length of transmission fiber is much larger than the sensing fiber, the power loss of sensing fiber can be neglected. And the reflected signals from PR1 and PR2 have same powers. Therefore the $L_{Sensing}$ is depended to the reflection value $R_1$ of PR1 and equals to 5.07dB.

Thus the relationship between the injection power and length of transmission fiber can be given as

$$10\log\left(\frac{P_{in}}{0.004}\right) = L_{A-B} + L_{B-C} + 2\times L_{trans.fiber} + L_{Sensing} + L_{C-F} \quad (5\text{-}12)$$

The numerical simulated in theory is shown in Fig. 5-14, when the effects of dispersion and nonlinear in optical fiber are not considered. However, since the effects of dispersion and nonlinear in long fiber, the injection power is limited within 10mw, which will be discussed in later section. When the maximum power at C point of Fig. 5-13 is set to 9 mW, the maximum transmission length is

$$l_{\max} = \frac{10\log\left(\frac{9}{0.004}\right) - 0.85 - 5.07}{2\times 0.2(dB/Km)} = 69.005Km \quad (5\text{-}13)$$

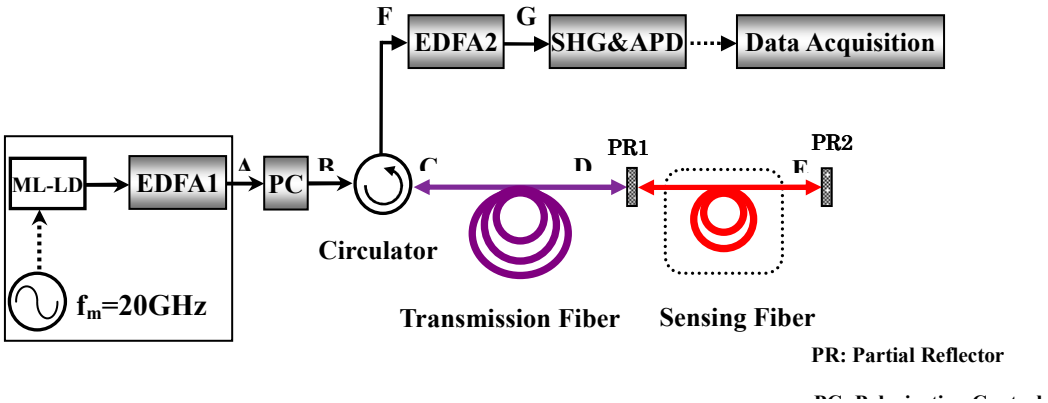


**Figure 5-13:** Configuration of long distance remote pulse correlation sensing system

**Table 5-1:** Typical insertion loss of each component

| Component | | Insertion loss(dB) |
|---|---|---|
| PC | (A→B) | 1.1 |
| Circulator | (B→C) | 0.84 |
| | (C→F) | 0.85 |
| PR1 | D | 0.46 |
| PR2 | E | 0.46 |

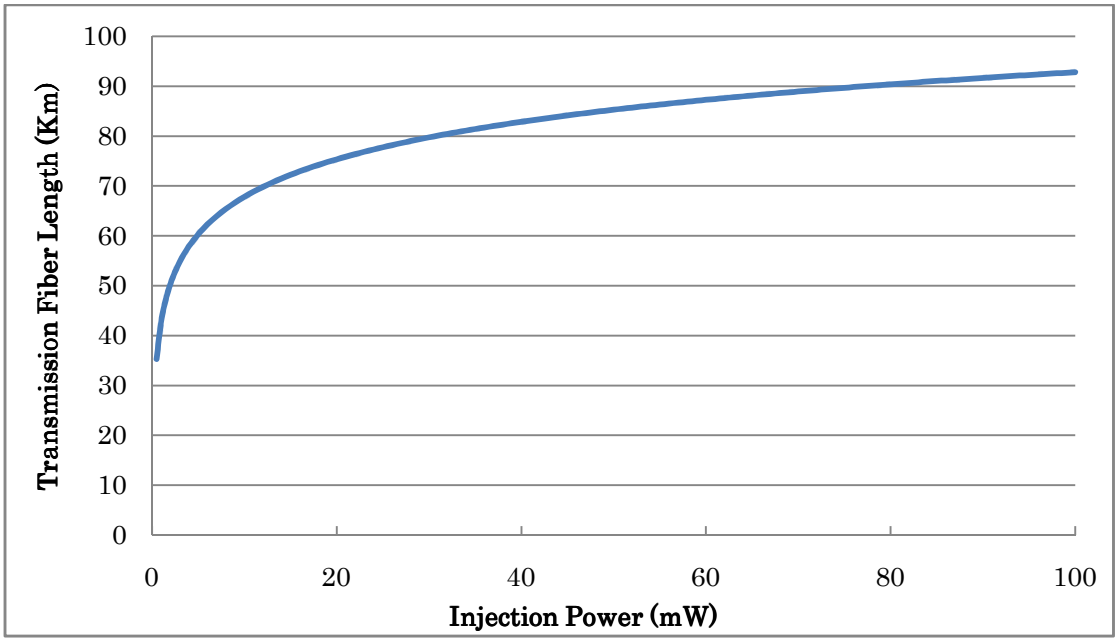


**Figure 5-14:** Transmission fiber length limited by injection power

### 5.4.2 Dispersion Effect

The dispersions include polarization-mode dispersion (PMD) and group-velocity dispersion (GVD). For the PMD, when using 100 km single mode fiber, the PMD –included broadening is less than 1 ps, which is much small [7, 8]. As the chapter 4 section 4.4.1 discussion, the PMD did not affect the shape of pulse so much in correlation sensing system by the experimental result. Therefore, PMD will not affect the performance of the correlation sensing system. For the GVD, the next part will discuss the effect in long distance fiber.

The GVD is characterized by the dispersion parameter $\beta_2$ as the effect of $\beta_3$ can be neglected [7]. Therefore, $\beta_2$ governs the strength of the dispersion of optical pulses propagation in the optical fiber. The dispersion parameter $\beta_2$ is easy to cause the broadening of the optical pulse. According to the analysis of the dispersion effect on optical pulse without chirp in ref. 7 and 8, the pulse broadening factor $b_f$ at distance $z$ is given as

$$b_f(z) = [1 + (z / L_D)^2]^{1/2} \tag{5-14}$$

Where, $L_D$ is defined as the dispersion length by $L_D = T_0^2 / |\beta_2|$. $T_0$ is the half-width of the pulse at $1/e$ power point, which is related to the full width at half-maximum (FWHM) of the input pulse by the relation $T_{FWHM} = 2\sqrt{\ln 2}T_0 \approx 1.665T_0$. The variation of broadening factor with the relative length is shown in Fig. 5-15.

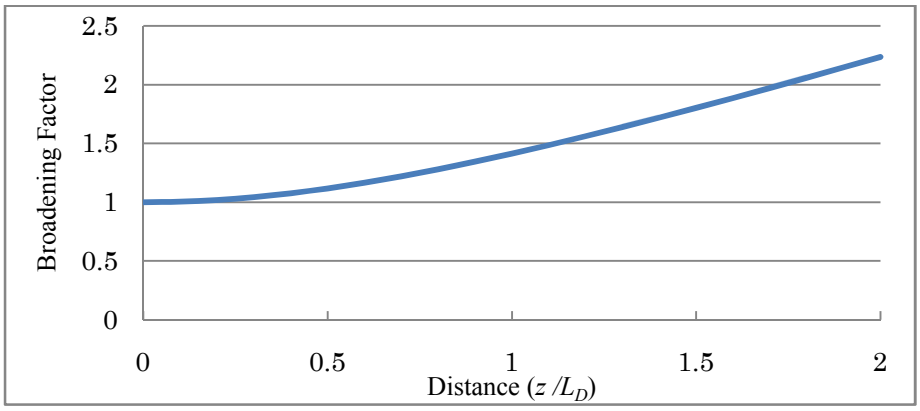


**Figure 5-15:** Broadening Factor

According to Fig. 5-15, it can been that there is a large broadening caused by the dispersion effect in a single mode fiber when the transmission length is larger than the dispersion length, which will limit the length of monitoring fiber in optical pulse correlation system. As far as the light source of the optical pulse correlation sensing system is concerned, the FWHM of the optical pulse launched into the dispersion-shifted fiber (DSF) is around 8.882 ps. The related typical parameters of DSF are shown in Figure 5-16. According to the related parameters of DSF and equation 5-14, the relationship between broadening factor and transmission fiber length is plotted in Figure 5-16. Therefore, the maximum length of DSF are limited within 58 km, the broadening factor is less than 1.5. It is very important to mention that the pulse width broadening is possible to be compensated by using dispersion compensated fiber. In that case, the dispersion effect will be degraded much.

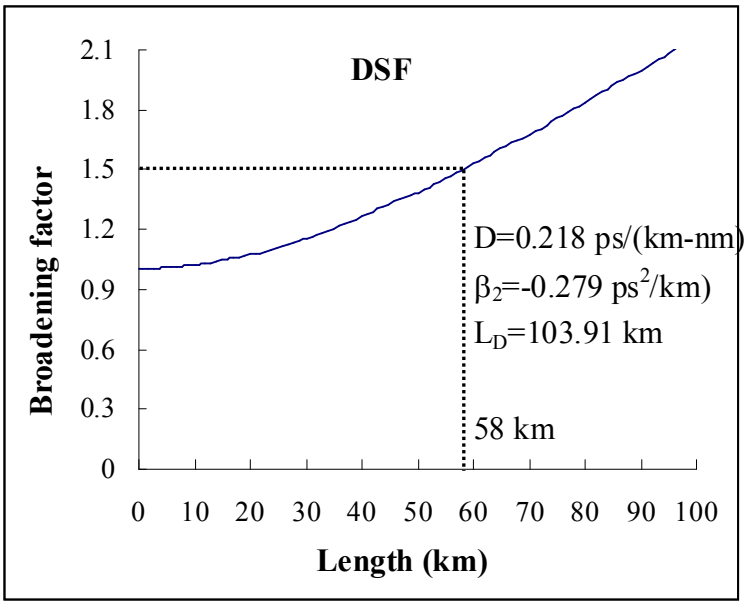


**Figure 5-16**: Broadening Factor vs. Length of Transmission Fiber

### 5.4.3 Nonlinear Effect

Nonlinear effect in long-haul communication systems includes self-phase modulation (SPM), cross-phase modulation (XPM), four-wave mixing (FWM), stimulated Raman

scattering (SRS) and stimulated Brillouin scattering (SBS). In this optical correlation sensing system, after being amplified, the average power of the light source is around 16.5 mW, which is potential to stimulate the nonlinear effect in the optical fiber. It is fortunate that such high power only transmit in the length around 1m in an optical circulator. For the launched power of long monitoring fiber, it is around 9 mW, which is a critical value for nonlinear effect in long-distance.

As there is only one signal propagated in the monitoring fiber, XPM and FWM will not depredate the monitoring signal. As far as SRS is concerned, there will be not much concern in the correlation sensing system as the average optical power of signal launched into the monitoring fiber is around 9 mW corresponding to a peak power of 51.3 mW, which is much less than the threshold power 450 mW for single-channel SRS [7, 8]. For the SBS, the threshold for the single-mode fiber is generally around 5 mW. However, since SBS will limit the transmission power of the optical fiber within 3 mW [7], but without interference on the pulse width of the optical signal. Moreover, it will reduce the SPM effect by limiting the transmission power in the optical fiber. Thus, just the effect of SPM should be considered.

SPM will affect the pulse width of the optical pulse through the frequency chirping due to the nonlinear phase shift resulted from the large optical power. However, the frequency chirp caused by the SPM will result in the broadening or compressing determined by the signal of $\beta_2$, that is for normal dispersion $\beta_2 > 0$, SPM causes the broadening and for the anomalous dispersion $\beta 2 < 0$, SPM leads to the pulse compressing.

According to the analysis of the SPM by simultaneously considering the dispersion effect in ref. [7, 8], the pulse width after transmitting a distance of $z$, can be given as

$$\sigma_p^2(z) = \sigma_L^2(z) + \gamma P_0 f_s \int_0^z \beta_2(z_1) \left[ \int_0^{z_1} p(z_2) dz_2 \right] dz_1 \tag{5-15}$$

Where $\sigma_L^2(z)$ is the RMS width expected in the linear case ($\gamma$=0), $P_0$ is the peak power of pulse 51.3 mW, $p(z) = e^{-\alpha z}$, $f_s$ is the parameter of input pulse shape. For a Gaussian pulse, $f_s \approx 0.7$ [7, 8].

Equation (5-15) makes clear the broadening or compressing effect of SPM. The total broadening of a DSF under the effect of dispersion and SPM are shown in Fig. 5-17. According to the simultaneous consideration of dispersion and SPM, for the DSF, since the dispersion is not so much which can be compensated by the SPM compression, for *l*=66 km. the broadening is less than 1.5. Therefore, for the DSF transmission fiber, the remote sensing length is mainly limited by the loss effect. Therefore, the possible length for the monitoring fiber is around 66 km by comprehensively considering the loss, dispersion and SPM.

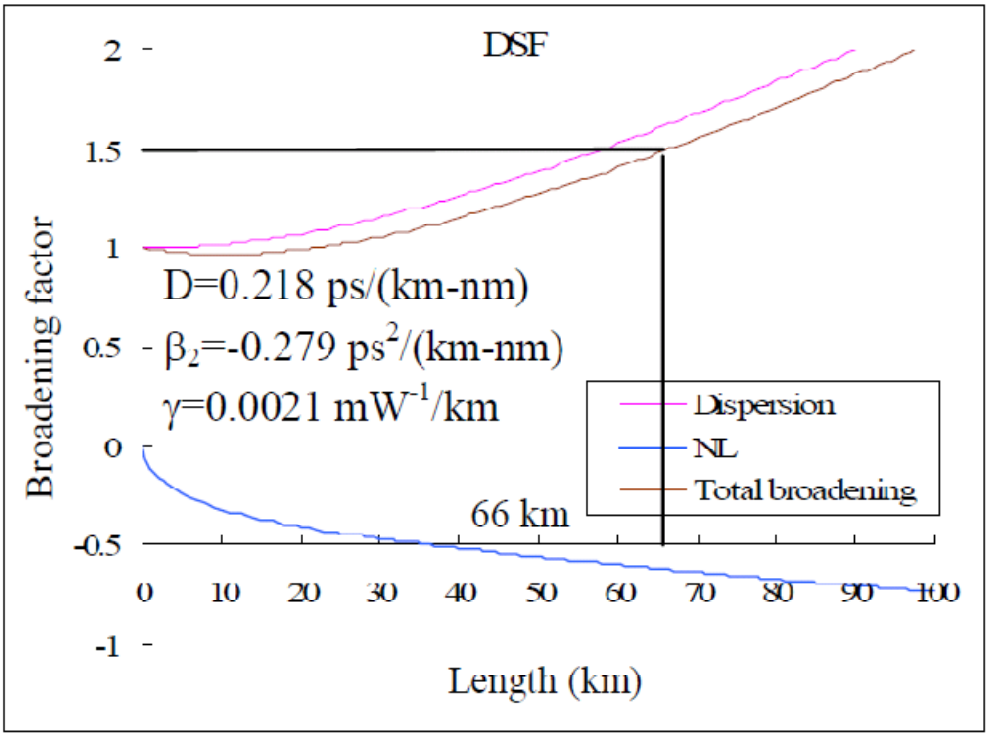


Figure 5-17 Broadening effect impacted by dispersion and SPM

According to the above analysis, it is very important to notice that:

1. The loss effect limits the length of transmission fiber within 69 km when the average injection power is limited at 9 mW and the peak power is 51.3 mW.

2. If there is no any dispersion compensation exerted to reduce the pulse broadening effect and just consider the dispersion effect of $\beta_2$ by neglecting the $\beta_3$, loss and nonlinearity. For DSF with typical parameters, the maximum length of the transmission fiber is 58 km.

3. For nonlinear effect, by simultaneously considering the dispersion and nonlinear effect, the possible monitoring length for a DSF is 66 km.

Therefore, the maximum length of monitoring fiber is estimated as long as 66 km in theory.

## 5.5 Summery

For long-distance remote monitoring, optical time domain reflectometry (OTDR) is a well-know method for the diagnostics and measurement of fiber optic systems. I proposed a novel reflectometry that detects the reflection point by measuring the optical pulse correlation using the overlap of reference and reflected pulses. The pulse overlap produces second harmonic signal in proportion to the intensity correlation of two pulses without using complicated high-speed electrical components. This pulse-correlation-based reflectometry can detect the reflectometry pulse with high time resolution better than 0.02 ps. In addition, comparing to the classical OTDR, all the system components are simple and low-cost. Replacing the short pulse with fixed light phase from a 20 GHz mode locked laser diode (ML-LD) to a low-time-jitter flexible repetition pulse source gain switching laser diode (GS-LD); we have shown the feasibility of pulse correlation OTDR measurement with very high time resolution 0.02 ps. A multi-region fiber sensing system with 30 km remote distance with high resolution is achieved. It means 4 με strain or 0.1 °C environmental changes per 1 meter sensing fiber can be detected within 30 km tele-monitoring in experiment and 66 km in theory. Using the pulse feedback and moving average technology, the noise factors of this system are suppressed.

## Reference


[1] http://www.fas.org/irp/doddir/usmc/mcwp2-15-1.pdf.

[2] T. Kurashima, M. Tateda, K. Shimizu, T. Horiguchi, and Y. Koyamada: “A high performance OTDR for measuring distributed strain and optical loss”, 22nd European Conf. on Optical Communication Norway, TuD.3.7, 1996.

[3] Y. Koyamada, M. Imahama, K. Kubota, and K.hogari: “Fiber-optic distributed strain and temperature sensing with very high measurand resolution over long range using coherent OTDR”, J. of Lightwave Technology, vol. 27, p. 1142, 2009.

[4] R. Goto, S. Matsuo, K. Himeno and K. Ohashi: “On-spool PMD estimation method for low PMD fibers with high repeatability by local DGD measurement using POTDR”, 31st European Conf. on Optical Communication UK, We2.5.6, 2005.

[5] M. Thollabandi, T. Kim, S. Hann, and C. Prak: “Tunable OTDR (TOTDR) based on direct modulation of self-injection locked RSOA for line monitoring of WDM-PON”, 34th European Conf. on Optical Communication Belgium, P.6.01, 2008.

[6] K. Nonaka, H. Mizuno, H. Song, N. Kitaoka, and A. Otani: “Low-time-jitter short-pulse generator using compact gain-switching laser diode module with optical feedback fiber line”, Jpn. J. Appl. Phys., vol. 47, p. 6754, 2008.

[7] Hongbin Song, “Development of High-Sensitivity Optical Fiber Sensor Based on Optical Pulse Correlation”, PhD. Thesis. Kochi University of Technology, 2008.

[8] G. P. Agrawal: “Signal propagation in fibers”, Light wave technology telecommunication systems, A JOHN WILEY and SONS, Inc., p. 66-104, 2005.

[9] G. P. Agrawal, Nonlinear Fiber Optics, 3rd ed., Academic Press, San Diego, CA, 2001.

[10] G. P. Agrawal, Applicatins of Nonlinear Fiber Optics, Academic Press, San Diego, CA, 2001.

# Chapter 6 Conclusions

To develop a high-sensitivity, wide-dynamic-range and selectable-regions fiber optic sensing system, this dissertation comprehensively investigates a potentials of time-based sensing's concept which means a basic optical pulse correlation sensing system configuration, a simple high-sensitive and wide-dynamic-range pulse-correlation-based sensing system, a selectable-region distributed pulse-correlation-based sensing system, and a long-distance remote monitoring pulse-correlation-based sensing system.

Optical pulse correlation sensor has been proposed and developed for past few years as a simple, useful and high resolution sensing mechanism for temperature, stress or strain measurement. Because of the high time resolution performance of this optical pulse correlation sensing system, this sensor concept can be used on many practical applications, such as wide-range ocean temperature monitoring, civil structure monitoring and long distance remote monitoring.

For industrial practical applications of ocean temperature monitoring, high-sensitive and wide-dynamic-range measurements are required. To resolve the requirement, in this study, I design and demonstrate a novel optical pulse correlation sensing system which is combined with short and long monitoring fibers by a time-division multiplexing (TDM) technique. This new approach differs from previously demonstrated measurement schemes in that only one monitoring fiber was used. In this new approach, the two different length monitoring fiber sensors are combined in one system. This outstanding increases the temperature sensitivity and maintains an acceptable measurable dynamic range simultanously. By using the optical time delay control component to change the measurable range, a wide dynamic measurable range is also available . By using the high speed optical switch to combine the correlation values of the short and long monitoring fibers, a high-sensitivity temperature measurement of 0.001 °C/mV with an approximately 20 °C measurable range is successfully carried out.

This system can be used in ocean water temperature measurements, oil tanks, power transformers, and high-resolution temperature controller applications owing to its high sensitivity and anti-electromagnetic interference characteristics. These were stated in Chapter 3.

For practical application of civil structure monitoring, distributed measurement is required function because the infrastructure's problem can be occurred in any unknown region. To monitor the damage and environmental condition on civil structures is becoming an important research field for civil engineers. It is very important to know the structural health and the degradation of these structures during their lifetime. Optical pulse correlation sensing system can inquire the total strain value of the monitoring fiber, but cannot identify in which region the strain is located. Therefore, I propose and demonstrate a compact and simple cascadable multi-regions distributed sensing system for wide region sensing. It is based on optical pulse correlation measurement with region separation techniques. The system uses inline-multiple monitoring fibers connected by wavelength partial reflectors or intensity partial reflectors for cascadable multi-regions responses sampling. Then, using wavelength scanning with wavelength selective reflectors (WSRs) by employing FBG or using time-position scanning with intensity partial reflectors (IPRs) by employing reflective index gap in fiber connectors, the system can successfully detect very short length changes in multiple regional monitoring fibers for temperature or strain measurement. These were stated in Chapter 4.

For long-distance remote monitoring, optical time domain reflectometry (OTDR) is a well-know method for the diagnostics and measurement of fiber optic systems. I proposed a novel reflectometry that detects the reflection point by measuring the optical pulse correlation using the overlap of reference and reflected pulses. The pulse overlap produces second harmonic signal in proportion to the intensity correlation of two pulses without using complicated high-speed electrical components. This pulse-correlation-based reflectometry can detect the reflectometry pulse with high time resolution better than 0.02 ps. In addition, comparing to the classical OTDR, all the system components are simple and low-cost. Replacing the short pulse with fixed light phase from a 20 GHz mode locked laser diode (ML-LD) to a low-time-jitter flexible

repetition pulse source gain switching laser diode (GS-LD); we have shown the feasibility of pulse correlation OTDR measurement with very high time resolution 0.02 ps. A multi-region fiber sensing system with 30 km remote distance with high resolution is achieved. It means 4 με strain or 0.1 °C environmental changes per 1 meter sensing fiber can be detected within 30 km tele-monitoring in experiment and 66 km in theory. Using the pulse feedback and moving average technology, the noise factors of this system are suppressed. These were stated in Chapter 5.

Therefore, the first main result is that using the TDM technique to combine long and short sensing fiber, the pulse-correlation-based fiber optic sensing system successfully reaches to a high-sensitivity temperature measurement of 0.001 °C/mV and wide dynamic range depended on the length of sensing fiber. The second main result is that using wavelength multiplexing or time multiplexing techniques, this system can successfully measure multi-regional strain or temperature. The max number of cascadable multi-region is estimated and can be enhanced by increasing the peak power of pulse source and decreasing the width of pulse source. The third main result is that this pulse-correlation-based fiber optic sensing system also can reach up to 30 Km long-distance remote measurement by using optical partial reflectors in experimental demonstration and 66 km in theory.

# Acknowledgement

The research work for this thesis was performed in the Nonaka Laboratory, Department of Electronic and Photonic System Engineering, Kochi University of Technology from October 2007 to October, 2010.

I would first like to deepest thank my supervisor, Professor Koji Nonaka, for supervising, encouraging and supporting me not only my research but also my life, and for his passion, honesty, faith, professional, wise and farsighted, warmhearted, and generous. I would like to thank him for support me to join international conferences and cooperation to get more help and information for this dissertation writing.

I would like to thank Prof. Masahiro Kimura, Prof. Katsushi Iwashita, Prof. Masayoshi Tachibana, and Prof. Hiroshi Furusawa as the members of my committee and for their helpful suggestions.

Especially I owe my thanks to Prof. Chaoyang Li, for her encouraging and helping my study and life in Japan. I also would like to thank Dr. Jiazheng Lu and Prof. Libo Yuan for their help in research and life.

I would like to thank all my colleagues and friends at the Nonaka group, especially Dr. Hongbin Song, Mr. Tsuduki Toshimasa, Mr. Shigeo Aria, Mr. Nishi Mura, Ms. Ziyuan Wang, for their kind help and support.

My sincerely thanks belong to my dear mother, father and younger brother for their love and support.

# Publications List

## (A) Journal papers

1. High Sensitivity fiber-optic temperature sensing system based on optical pulse correlation and time-division multiplex technique.

   **Xunjian Xu**, Koji Nonaka

   *Japanese Journal of Applied Physics*, **48**, 102403 (2009)

2. A regional selectable distributed fiber-optic sensing system based on pulse correlation and partial reflector.

   **Xunjian Xu**, Koji Nonaka

   *Measurement Science and Technology*, 21, 094018 (2010).

3. Fiber strain measurement for wide region quasidistributed sensing by optical correlation sensor with region separation techniques.

   **Xunjian Xu**, Koji Nonaka

   *Journal of Sensors*, **2010**, 839803 (2010).

4. Long-distance remote fiber optic sensing system based on pulse correlation and Partial Reflector.

   **Xunjian Xu**, Koji Nonaka,

   *Measurement Science and Technology* (will be submitted).

## (B) International conference

1. Fiber optic wide region temperature sensing system.

   **Xunjian Xu**, Koji Nonaka and Hongbin Song

   POEM2008, Wuhan, China 25/8/2008

2. High sensitivity and wide dynamic range fiber optic pulse correlation sensing system

   **Xunjian Xu**, Koji Nonaka

   APCC2009, Shanghai, China 10/10/2009

3. Regional selectable distributed sensor based on reflected optical pulse correlation measurement and low time-jitter gain-switch laser-diode

   **Xunjian Xu**, Koji Nonaka

   OFS-20, Edinburgh, UK, 8/10/2009

4. Quasi-distributed optical pulse correlation sensing system based on partial reflectors and mode-locked laser-diode

   **Xunjian Xu**, Koji Nonaka

   MOC'09, Tokyo, Japan, 26/10/2009

5. Multi-region fiber sensing system using high time resolution tunable pulse correlation OTDR technique.

   **Xunjian Xu**, Koji Nonaka

   **APCC2010**, Auckland, New Zealand, 2/11/2010

## (C) Domestic conferences in Japan

1. **Xunjian Xu**, Koji Nonaka: "Fiber Optic Wide Region Temperature Sensing System", 平成 20 年度電気関係学会四国支部連合大会, 徳島, (9-2008)
2. **Xunjian Xu**, Koji Nonaka: "High Resolution and Wide Dynamic Range Optic Fiber Temperature Sensing System Based on Correlation and Differential Technique", 電子情報通信学会光エレクトロニクス研究会, 东京 (3-2009)
3. **Xunjian Xu**, Koji Nonaka: "Cascadable Multi-region Fiber-Optic Temperature/Strain Sensing System Based on Optical Pulse Correlation Measurement and Partial Reflector", 第 44 回 光波センシング技術研究会講演会, 东京(10-2010)
4. **Xunjian Xu**, Koji Nonaka: "領域分割計測法を付与した光パルス相関センサを用いたファイバ歪み計測による準分布型広域センシング", 札幌(2-2010)